RESEARCH IN SUPPORT OF MOTOR TRUCK BRAKE SYSTEMS DESIGN AND DEVELOPMENT

Paul Fancher
Research Engineer
Highway Safety Research Institute

Industrial Development Division
Institute of Science and Technology
The University of Michigan

RESEARCH IN SUPPORT OF MOTOR TRUCK BRAKE SYSTEMS DESIGN AND DEVELOPMENT

Paul Fancher
Research Engineer
Highway Safety Research Institute

Industrial Development Division
Institute of Science and Technology
The University of Michigan

August 1980

TABLE OF CONTENTS

		Page
PREFACE		iii
Chapter		
1	INTRODUCTION	1
	A Methodology for Predicting and Evaluating the Response of Commercial Vehicles to Braking Inputs	1
2	THE FORM OF A COMPUTER SIMULATION FOR ANALYZING THE PROPERTIES OF THE DECELERATING COMMERCIAL VEHICLE	7
	Overview of the Mathematical Model	10
	Detailed Descriptions of the Operation of Subsystems of the Vehicle Model	16
3	DEVICES FOR MEASURING THE PROPERTIES OF VEHICLE COMPONENTS	78
	A Device for Measuring the Braking Traction of Truck and Bus Tires	79
	Brake-Testing Devices	92
	Measurement of the Properties of Air Control Systems	100
	Devices for Measuring Suspension Properties	109
	A Pitch-Plane Inertial Properties Facility	117
4	PREDICTING BRAKING PERFORMANCE	120
5	CONCLUDING STATEMENTS	132
REFERENCES		135

PREFACE

The author's knowledge of motortruck braking has been derived from research studies supported by grants from the Motor Vehicle Manufacturers Association of the United States, Inc. The members of the Physical Factors Division of the Highway Safety Research Institute (HSRI) of The University of Michigan have been instrumental in developing the computer simulations and the parameter measurement techniques described in this monograph. With assistance from the Industrial Development Division of the Institute of Science and Technology, the work of the HSRI researchers referenced herein has been organized into a single account of research pertaining to motor truck braking performance.

This account is intended to be of interest to persons, involved in studying, improving, or evaluating the dynamic performance of commercial vehicles and their components. It is hoped that executives and planners of engineering and scientific research will find the material presented here to be useful and stimulating to engineers, scientists, and computer analysts concerned with brakes, antilock systems, tires, suspensions, and overall braking performance.

CHAPTER 1

INTRODUCTION

A Methodology for Predicting and Evaluating the Response of Commercial Vehicles to Braking Inputs

This monograph describes the results of research performed in support of a national effort to improve the stopping capability of commercial vehicles. The results of this research are (1) new knowledge concerning the properties of pertinent vehicle components, (2) computer tools for analyzing system performance, and (3) a methodology for predicting and evaluating the response of commercial vehicles to driver-initiated braking inputs.

In the interest of enhanced highway safety, the National Highway Traffic Safety Administration (NHTSA) of the U.S. Department of Transportation has tried to promulgate an acceptable Federal Motor Vehicle Safety Standard for commercial vehicles with air-actuated braking systems. Since 1970, when such a standard was first considered, brake, brake component, and vehicle manufacturers have conducted extensive development efforts directed at creating braking systems suitable for meeting government regulations. The problems associated with developing improved braking systems have been much more difficult than expected by government officials, vehicle manufacturers, and component suppliers.[1] The requirements of the

government standard (FMVSS121)[2] have been changed repeatedly in attempts to obtain regulations that are both stringent and achievable using current technology. Nevertheless, court decisions have ruled parts of the standard invalid.[3] After nearly ten years of effort, many technical (as well as philosophical) issues remain unresolved.

The introduction of government safety standards has added an emphasis on stopping distance capability to the traditional requirement for a commercial vehicle's brakes to be able to absorb large amounts of energy. Engineers and scientists have made the friction brake into a remarkable device for converting into heat the kinetic energy possessed by a moving vehicle. As demonstrated in service, typical brakes can reliably perform their energy-conversion function many times without failure or inordinate wear. They can withstand high temperatures (such as those developed while maintaining velocity in a mountain descent) without fading excessively or failing entirely. Yet a braking system design that minimizes wear and optimizes performance in mountain descents is not necessarily the best arrangement for minimizing stopping distance capability in sudden (emergency or accident-avoidance) stops on good road surfaces.

Designing to improve stopping distance performance is a total vehicle problem. The force decelerating the vehicle is almost entirely generated at the tire-road interface. Given adequate torque from the installed brakes, the maximum braking force available is limited by tire characteristics,

the instantaneous loading of each tire, and the condition of the road surface (slippery or dry). In turn, the loading of each tire depends upon the deceleration of the vehicle, suspension properties, and the arrangement and size of the load carried by the vehicle. Not only the characteristics of the brakes themselves, but many other vehicle properties must be considered in striving for improved stopping distance.

The design of braking systems for commercial vehicles is complicated by the wide range of operating conditions encountered in service. Ideally, efficient utilization of the available tire-road friction is obtained by proportioning the braking effort at each axle in accordance with the instantaneous vertical load carried by each axle. However, due to the goods-carrying function of most commercial vehicles, the load carried by the various tires differs greatly between the fully-laden and the empty state of the vehicle. Further difficulty in suitably proportioning the braking effort derives from the desire to stop efficiently both on good, dry roads at relatively high rates of deceleration with an attendant large aft-to-fore load transfer, as well as on wet, slippery roads allowing only low deceleration with little load transfer. The problems of designing for changes in vertical load and tire-road friction are sufficiently demanding that so-called "advanced braking systems," such as antilock systems and variable proportioning schemes, have been tried in various parts of the world.

The braking regulations proposed and eventually enacted in the United States led to the adoption of antilock systems by American vehicle manufacturers. The antilock systems were intended to provide good stopping performance under all operating conditions. In addition, the prevention of wheel lockup, the main function of antilock systems, was expected to improve directional stability and controllability during braking. However, even though the suppliers of antilock systems generated high hopes within industry and government for improved braking performance, the experience of the last few years has demonstrated unforeseen difficulties in reliably achieving the short stopping distances believed to be possible.

An improved understanding of some of the problems involved in antilock braking has been obtained by an analysis of the vehicle as a dynamic system.[4] The methodology developed for analyzing vehicle dynamics and predicting braking performance necessarily involved incorporating detailed knowledge of the performance of the components of the vehicle (including the antilock system) into a computerized mathematical model of the vehicle system.

The research approach used in developing computer tools for predicting how trucks and tractor-semitrailer vehicles respond to steering and braking inputs forms the basis for the methodology described in this monograph. Three research tasks were addressed in developing the desired methodology. The first task consisted of generating mathematical descriptions of the physics involved in motortruck systems and

programming the resulting equations into computer simulations of heavy vehicles. The second task involved creating laboratory devices and test methods for measuring the properties of the components used in modern trucks. In the third task, comparisons between test results for the complete truck and calculations of performance were made to assure that the developed simulations were valid. Within this general framework, the research proceeded from a basic vehicle model to addressing the problems associated with complex motortruck systems. Figure 1 illustrates the interactive nature of the three tasks, described above, and the "closed-loops" in the diagram emphasize the iterative form of the methodology. In essence, the overall task has been to perfect the state of the art in predicting the braking performance of motortrucks in order to make the engineering design and test process as efficient as possible.

In summary, this report describes a "simulation methodology" which has been developed to aid in addressing the technical issues facing engineers responsible for vehicle braking performance. Key elements of this methodology are (1) new devices and test procedures for measuring the mechanical properties of the components of the motortruck (specifically, tires, brakes, suspensions, and antilock systems) and (2) computer simulation programs for analyzing the braking performance of total vehicle systems. The material presented hereinafter discusses computer tools, testing equipment, and bases for engineering judgment not available ten years ago.

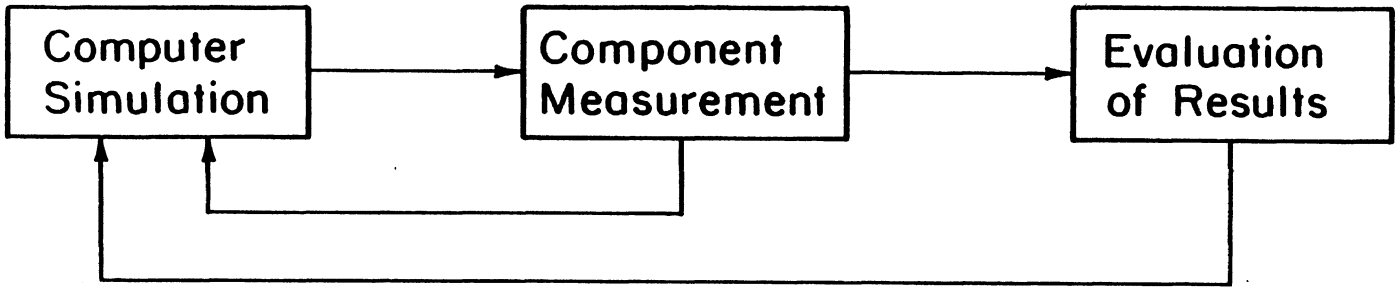

Figure 1. Elements of a methodology for predicting and evaluating the braking performance of commercial vehicles.

CHAPTER 2

THE FORM OF A COMPUTER SIMULATION FOR ANALYZING THE PROPERTIES OF THE DECELERATING COMMERCIAL VEHICLE

A mathematical model is a logically reasonable starting point for a systematic approach to analyzing the braking performance of a commercial vehicle. The process of modeling a vehicle system may be characterized as attempting to describe the system in quantitative terms using the methods of physics, mathematics, and engineering technology. A carefully conceived model is an expression of what is known and understood about the pertinent properties of the vehicle. In this sense a model serves as a summary of the state of the art in a particular area of vehicle technology.

The process of developing a model for analyzing the performance of a system usually illuminates gaps in existing knowledge. At the beginning of this research the need for a better understanding of tire shear-force characteristics, brake-system operation, and tandem-axle dynamics was apparent. As the modeling progressed, requirements developed for obtaining detailed data describing the mechanical properties of the vehicle and its components. The needed data for exercising the model did not exist at the beginning of this work and, furthermore, devices for measuring inertial parameters, tire shear-force characteristics, and suspension properties of heavy trucks were not available.

As noted elsewhere,[5] a common pattern of activities in vehicle dynamics studies consists of deriving complex models, implementing the models using computer simulation, and then searching for parametric values to insert into the equations constituting the model. Often, to the surprise of the model developer, the search for parametric data proves to be the most difficult, costly, and time-consuming part of the vehicle dynamics study. The study of commercial vehicle dynamics is no exception to this pattern; the development of devices for measuring the mechanical properties of heavy-vehicle components may be the most valuable contribution of this research. Nevertheless, a description here of the mathematical model employed will provide a foundation for later discussions of test equipment and analytic procedures.

Because of the complexity and difficulty of solving the system of relationships describing the vehicle, the mathematical model (in the form of equations and tabular functions) is implemented in a computer simulation, thereby permitting analyses of vehicle response to be performed. The computer simulation is an analytic tool; it is used to compute the response of the vehicle--that is, the output of the vehicle system--for a prescribed time-history of braking inputs. The simulation does not solve synthesis problems directly. Rather, the synthesis or design of vehicles must be approached by "trial-change-retrial" techniques analogous to the methods used in modifying actual vehicles and then testing them to evaluate new designs or the use of new components.

The simulation process might be thought of as experimenting with models. During the model development activity, the simulation can be exercised to challenge preconceived ideas concerning the vehicle system. Once data from component tests are available, the new information can be incorporated in the simulation (as previously indicated in Figure 1) to improve the description of the vehicle's components. Similarly, the model can be refined and the simulation improved as a better understanding of the vehicle system is obtained through comparisons between measured and calculated results for vehicles whose mechanical properties have been carefully determined. After experimenting with the model to build confidence in the validity of the results and to understand the limitations of the model, the simulation can be used to predict what would happen in a particular braking situation if a baseline vehicle were to be changed in a specified manner.

The model, whose form will be described next, has undergone the development and experimentation process just described.[6] In addition, it has been used in studies dealing with the performance of vehicles equipped with antilock braking systems.[7,8] Computer codes corresponding to this general type of model have been delivered to motor vehicle manufacturers, agencies of the federal government, and other research groups. However, the simulation should be viewed as a flexible entity in which changes in the model are still being made as new insights are gained and new components or systems are introduced.

2.1 Overview of the Mathematical Model

The system to be described and the mathematical model to be discussed are portrayed in general in Figure 2. In the system diagram of Figure 2, the vehicle is represented as an assembly of interconnected subsystems that respond to braking commands from the driver. To initiate a stop, the truck driver moves the treadle valve to allow compressed air to flow into the brake chambers, thereby raising the chamber pressures, moving the actuation mechanisms, and causing each brake to produce torque as the shoes are forced against the drum. In service, the driver may alter braking commands based on perceived vehicle motion. However, the driver's actions in closing the control loop are not the focus of this study. Rather, open-loop braking commands are used as inputs to the analysis. The analysis then predicts how the subsystems interact in decelerating the vehicle.

To represent the effect of moving the treadle valve, the model employs a predetermined function of time corresponding to the air pressure that would be measured at the treadle valve during a braking maneuver. In the model the air delivery system responds to treadle pressure. The instantaneous pressure at the treadle valve is used to compute the pressure at each brake chamber unless the action of an antilock system or some sort of automatic proportioning device intervenes.

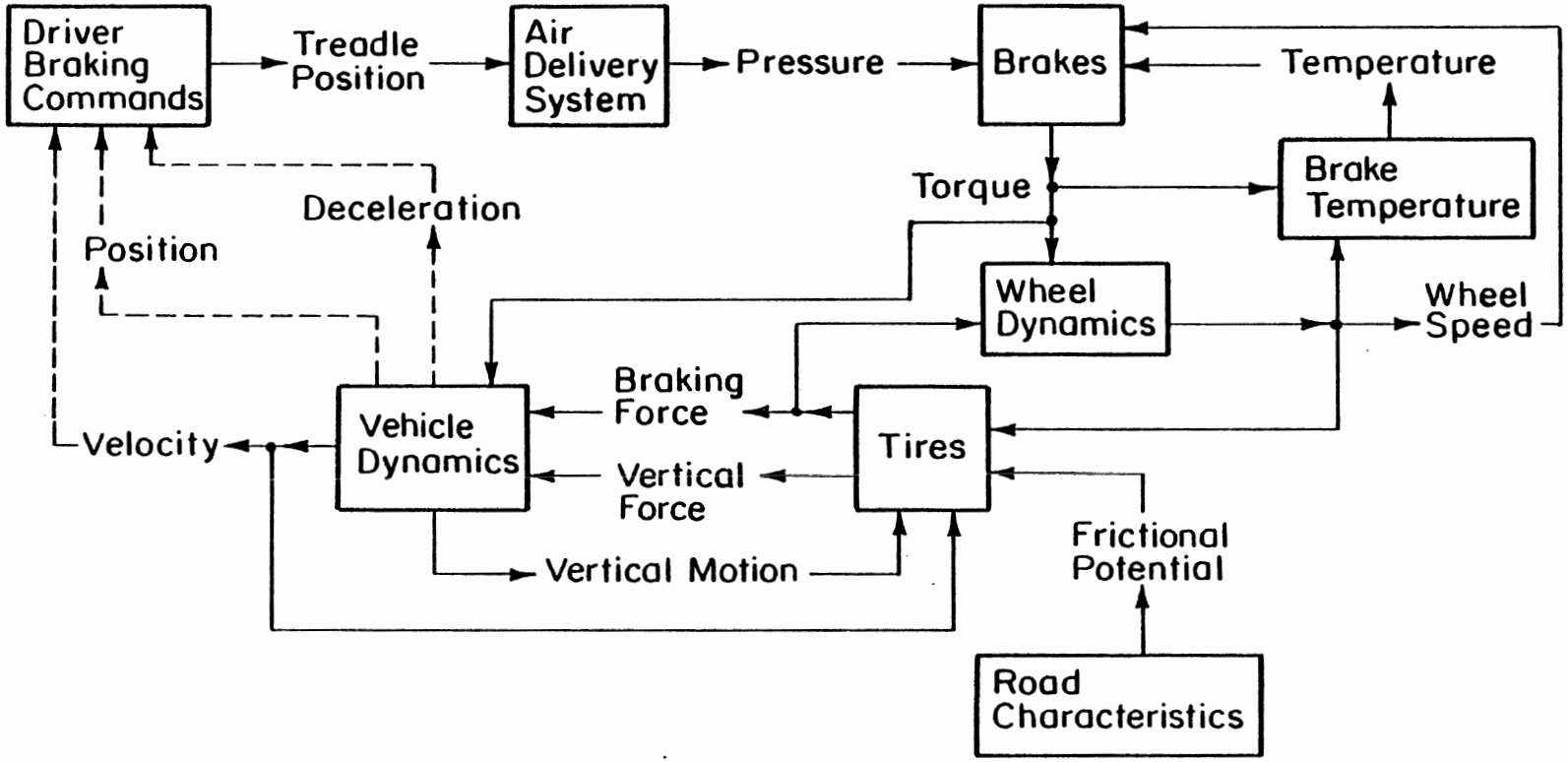

Figure 2. System Diagram For A Braking Commercial Vehicle

The brakes are represented as devices whose torque characteristics are primarily a function of brake-chamber pressure, but these torque characteristics are modified during a stop by changes in the rotational speed of the brake drum and the temperature of the brake shoes and drum at their interface. The temperature distribution in the brake is altered through the process of converting mechanical power (the product of brake torque and wheel speed) into heat flow. In the simulation an idealized thermal model computes the instantaneous temperature at the rubbing surface of the drum. Hence, the model includes what might be called an "in-stop fade and recovery cycle" (see Figure 2).

The rotational speed of each wheel (or dual wheel) depends upon the applied brake torque and the moment of the braking force acting at the tire-road interface. The equations of motion for each wheel are included in the model and they are solved for wheel speed in the simulation.

The force-producing properties of the tires are influenced by wheel speed, forward velocity, road characteristics, and the vertical motions of the wheel centers. As illustrated in Figure 2, nearly every motion of the vehicle system has an effect on the braking force produced by the tires.

Clearly, the accurate prediction of stopping distance requires an accurate representation of the shear force properties of the installed tires on the road surface in question. The pneumatic tire, however, is a complicated structure whose shear force characteristics are not readily

modeled from (1) detailed theoretical principles, (2) known properties of the tire's composite materials, and (3) the texture, composition, and contamination of the road surface. (In fact, tire models of greater complexity than the entire vehicle model described here have been developed.[9,10] Obviously, tire models for commercial vehicles--with from 10 tires for a straight truck to 18 tires for a typical tractor-semitrailer to 42 tires for a Michigan double tanker--must be carefully selected. Instead of utilizing primarily theoretical models, semi-empirical models or tables of directly measured tire data are implemented in the simulation.

Besides being influenced by nearly all vehicle motions, the tire forces are obviously the primary causes for changes in vehicle motion. Vehicle motion is analyzed in the model by treating the main masses of the vehicle as a system of interconnected rigid bodies, with the tires providing external forces. The tire forces act on the so-called "unsprung masses" consisting of axles and their associated wheels, brakes, and mounting hardware. The unsprung masses are connected to the "sprung masses" through suspension springs, dampers (if used), and constraining links. In articulated vehicles, the main masses are connected by hitches such as the typical fifth wheel employed in tractor-semitrailer rigs. The dynamic motions of the system of rigid bodies selected for modeling a commercial vehicle are computed by numerically integrating conventional equations of motion

that have been formulated using principles of Newtonian mechanics.

The motions of the sprung and unsprung masses could be computed in a straightforward manner if it were not for the properties of the tandem suspensions and the "springs" used in many commercial vehicle suspensions. In the model special attention is given to the effect of brake torque on the interaxle load transfer taking place in tandem suspensions. The "springs" commonly employed in commercial vehicles are actually complicated force-producing mechanisms containing varying amounts of energy loss (nonlinear damping or hysteresis) in a deflection cycle. The models of both tandem suspensions and commercial vehicle springs are examples of representations of vehicle components that have been refined as new knowledge has been acquired from component and vehicle tests.

Although the scope of this monograph does not include directional response, it should be emphasized that braking has an important influence on directional control and stability. Furthermore, computer simulations for making detailed studies of vehicle response to braking and/or steering inputs have been developed as companion efforts to the braking research described herein.[11]

It is generally well known and frequently observed that disastrous skids and spins may occur when wheels lock up on highway vehicles. For example, if the steered wheels lock up while the other wheels continue to roll, the vehicle tends

to proceed straight ahead without steering control. When wheels other than the front wheels lock up, an assortment of jackknifing and trailer-swinging phenomena may occur due to the articulation joints in commercial vehicles. Obviously, an important safety consideration in the development of braking systems is an attempt to arrange the proportioning of braking effort at each axle so as to achieve high utilization of the available tire-road friction prior to locking any wheels. Historically, braking requirements or specifications have been stated in terms of the deceleration (or stopping distance) achievable prior to wheel lock in order to give proper consideration to the influence of braking on directional control and stability.

In attempts to shorten wheels-unlocked stopping distances, special brake control devices such as antilock systems and load-sensing proportioning valves have been installed on commercial vehicles.[1] By their very nature, these control devices make vehicle performance extremely sensitive to their inputs and outputs.

The use of automatic devices for controlling braking requires that certain details of the vehicle system be modeled very precisely. For example, with regard to antilock systems, the model contains a flexible method for including (1) control laws and logical rules typifying the operational properties of currently available control units, (2) dynamic properties of the wheel-speed sensors employed in the control system, and (3) characteristics of the pressure modulators used to change

brake-chamber pressure in accordance with commands from the control units. In addition, as already mentioned, the model contains means for determining instantaneous wheel speed. Accurate representation of wheel speed (that is, the variable that the control system senses) is a necessity if control actions are to be predicted realistically. Furthermore, any property of the brake causing delays in responding to braking commands should be represented, because these delays may upset the desired performance of the system. In this research, findings obtained from a process of comparing calculated with measured wheel-speed and brake-torque signals indicated the need for including in the model (1) hysteresis in the brake mechanism, (2) side-to-side torque imbalance in the brakes installed on each axle, and (3) time lags in the increase of brake torque due to delays in refilling the brake chambers if the chamber pressure drops below the pushout pressure of the brake.[13, 7, 6]

2.2 Detailed Descriptions of the Operation of Subsystems of the Vehicle Model

The previous section provided an overall description of how the vehicle has been modeled as a system. It also presented some of the rationale used in determining what would be included in the model. This section presents models of specific aspects of the performance of individual components or subsystems of commercial vehicles. Emphasis is placed on describing features that are unique to the components of heavy vehicles.

Specialized devices used in measuring component characteristics will be described in Chapter 3.

The details of implementing the subsystem models into a computer simulation are presented with only enough information to provide a general understanding. Detailed descriptions of this type of simulation and its use are presented in reference [6].

Air Delivery System

An important operational characteristic of the air delivery system is the length of time between the application of pressure at the treadle valve and the achievement of a corresponding pressure in each of the brake chambers. This response time depends upon the "plumbing" of the air system, which is a fairly complicated arrangement of air lines, connectors, relay valves, check valves, and other specialized devices. The response times depend upon the lengths of the air lines, the sizes of the orifices, and the volumes to be filled. As with most vehicle components, a very complicated model could be constructed to study the operation of the air system in detail. Rather than developing a detailed model with the burden of representing a wide variety of air system components, judgment and experience indicate that the input/output characteristics of the air delivery system can be satisfactorily represented using a relatively simple model.

In the simple model, the response times of the brakes are determined by two parameters per axle, namely, a time

delay, T_d, and a rise time, T_r. Using these parameters, the air transmission process for both of the brakes installed on a particular axle is modeled as a pure time delay followed by a linear first-order system. In mathematical terms, the model is expressed by the following pair of equations:

$$P_{td}(t) = P_t\ (t-T_d) \qquad (1)$$

where

t = time,

T_d is the time delay parameter,

$P_t(.)$ is the function selected to describe the treadle pressure during a braking maneuver of interest, and

$P_{td}(t)$ is an auxiliary variable used in the model (this variable is the delayed version of P_t)

and

$$T_r \frac{d}{dt} P_a(t) + P_a(t) = P_{td}(t) \qquad (2)$$

Clearly this model represents the operation of the air system and not the hardware used in it. It is a semi-empirical model in which the parameters to be used must be determined experimentally (or possibly analytically if a detailed model of the air delivery system were to be developed).

A qualitative idea of the agreement between measured and simulated responses of a typical air system may be obtained by examining Figures 3a and 3b. (In this case, the simulated response could be improved if necessary by adjusting the value of T_r chosen for the tractor's rear axle.)

Equation 2 could be solved by an appropriate numerical integration method. A convenient method is to consider the continuous input signal, $P_{td}(t)$, as adequately represented by a staircase function with a step occurring at each time step of the digital computer, as shown in Figure 4. Then equations 1 and 2 can be solved analytically prior to programming the simulation. In this approach, the value of pressure at axle A at the time t_i, that is, $P_a(t_i)$, is calculated using (1) $P_a(t_{i-1})$ (the value of P_a at the last time step) as the initial condition and (2) the stair-step approximation to the delayed version of the treadle pressure as the forcing function:

$$P_a(t_i) = [P_a(t_{i-1}) - P_t(t_i - T_d)]\, e^{-\Delta t/T_r} + P_t(t_i - T_d) \quad (3)$$

where i is the index of the i^{th} time step and Δt is the integration step size

As illustrated in Figure 4, the approximating stair-step function leads the continuous signal in time; however, the time step is very small in the simulation and, accordingly, the difference between the signals is unimportant in practical calculations. Furthermore, in practice, the value of T_d is chosen to get a good fit to the test data, using equation 3.

Hence, equation 3 becomes, in effect, an empirical digital model of the functional characteristics of the air delivery system.

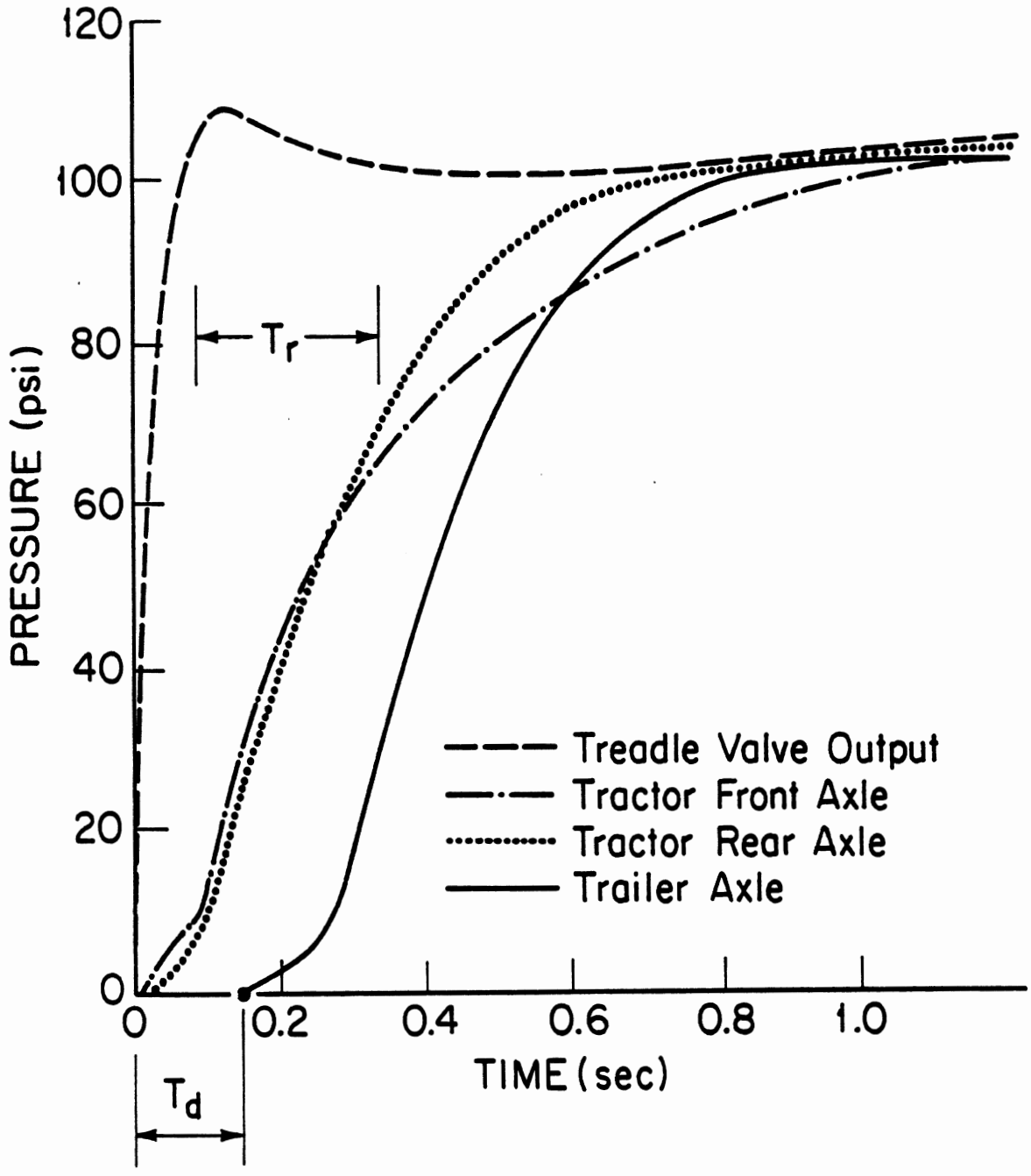

Figure 3a. Measured brake-pressure response curves.

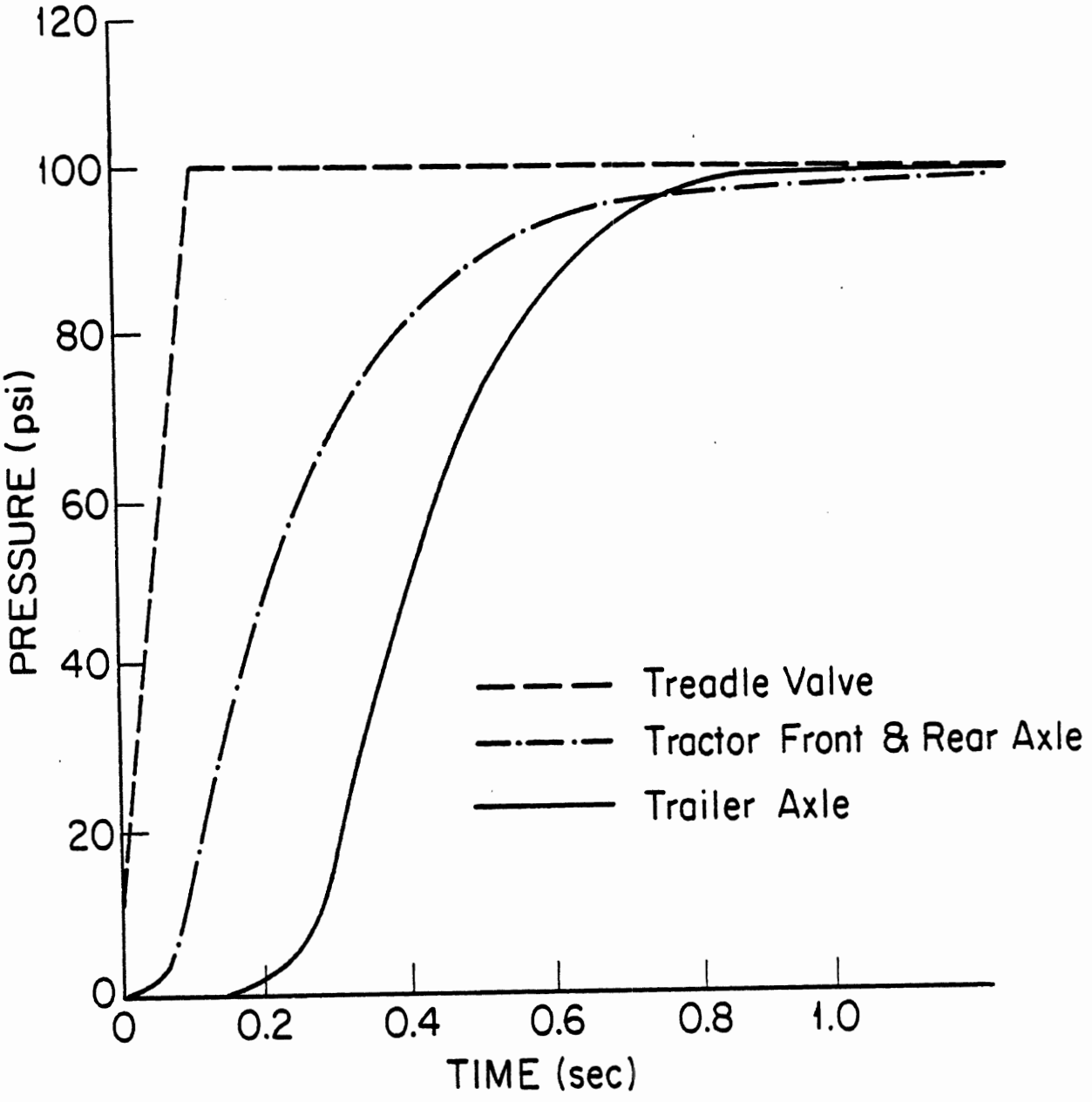

Figure 3b. Simulated brake-pressure response curves.

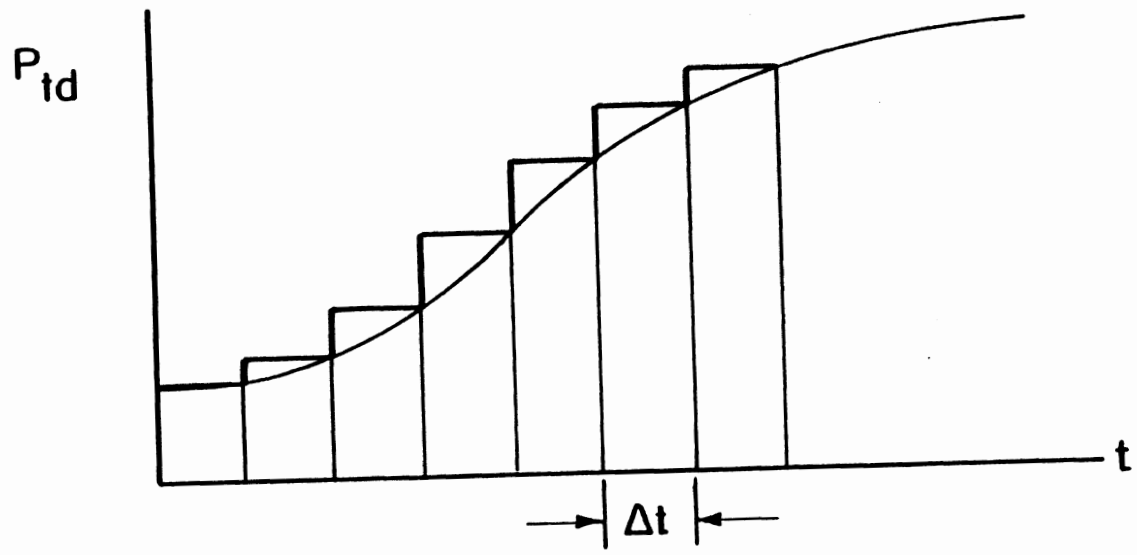

Figure 4. Stair step approximation.

Brakes

This discussion pertains to the torque-producing characteristics of commercial vehicle brakes. Methods for calculating temperatures within the brake will be presented later.

The brake has been a very difficult component to model accurately. First, the frictional properties of linings vary considerably from one sample to the next for the same kind of lining.[14] For certain types of brake mechanisms the torque-to-actuation pressure gain is high and quite sensitive to lining friction, thereby accentuating the influence of variability in lining properties. Secondly, the torque characteristics of commercial vehicle brakes are highly dependent upon their past usage, that is, their "work history." Standard test procedures call for exercising a brake through many burnishing applications in order to arrive at a well-conditioned state which can be achieved repeatedly. However, even a burnished brake may change its characteristics with further use or testing. Finally brake torque is influenced by mounting conditions and brake adjustment.[15] The net effect of these factors is to cause uncertainty concerning the braking performance of a vehicle equipped with a particular kind of brake.

For research purposes, measurements of the brake torques and brake-chamber pressures occurring during stopping tests are often needed to obtain suitable information for a detailed analysis of vehicle performance in a particular stop.

The variability in brake characteristics might seem to limit the utility of computer predictions. However, this variability pervades test results (both brake alone and total vehicle). It makes the design of efficient proportioning or brake control systems subject to error. This variability of currently available brakes needs to be taken into account in evaluating braking systems and predicting how they will perform. Accordingly, a computer simulation can be a valuable tool for studying the influence of variations in brake characteristics on vehicle stopping performance.

Two basic types of approaches have been used to simulate brakes. In one approach, a model of the brake and its actuation mechanism is formulated using the geometry of the brake layout and a value of lining-to-drum friction. Since there are various brake types (for example, S cam and dual-wedge brakes), different mathematical models are required for each type of brake being simulated. In the other approach, brake torque is calculated by using tables or empirical functions derived to match test data. Both the physical model and the empirical representation are useful approaches--the physical model for cases in which test data are not available, and the empirical representation when they are.

Using the physical modeling approach, the torque "attempted" by a brake is calculated by an expression of the following form:

$$T_i = PB_i \cdot Q_i \cdot BF_i \qquad (4)$$

where

T_i is the torque attempted by the i^{th} brake (since the brake is a friction device, the torque produced under locked wheel conditions is just enough to keep the wheel locked regardless of the air pressure so long as the pressure is large enough to produce the needed torque);

PB_i is the brake chamber pressure minus the pushout pressure; Q_i is a brake system gain factor depending upon drum radius, brake chamber area, and actuation mechanism properties; and

BF_i is the brake factor, defined as the ratio of drum drag to the actuating force applied to the brake shoes.

The gain factor Q_i depends upon the type of actuation mechanism employed. The gain factor for "S-cam brakes" is a function of the cam radius and the length of the slack adjuster arm; for "wedge brakes" the gain factor depends upon the wedge angle. The brake factor is influenced by the geometry of the brake layout, how the shoes are pivoted or mounted, and the coefficient of friction between the lining and the drum. Specific equations for commonly used types of brakes are given in reference [6]. The physical modeling approach has not been relied upon exclusively in vehicle simulation exercises because useful brake-test data are generally available, owing to the requirements for dynamometer tests in FMVSS 121.

In a simplified analysis, the brake may be represented as a tabulated function of torque versus chamber pressure.

However, test results indicate that brake torque is a function of chamber pressure, sliding velocity, interface temperature, and possibly other variables. Furthermore, the variability in brake test results, as already mentioned, confounds the problem of determining appropriate empirical functions for representing the brakes. Semi-empirical models, based on an understanding of the mechanics, thermodynamics, and chemistry of the braking process, have not been developed. The current state-of-the-art is either to apply "correction factors" to a simple torque versus pressure relationship[6] or to derive a multinominal fit to test results using regression techniques.[16]

A type of correction factor that has been used with moderate success in the studies underlying this monograph is based on a calculation of interface temperature, θ. In this case a so-called "fade factor," θ_f, is used to determine the influence of lining-drum interface temperature on brake torque. A commonly used form for computing the influence of temperature on brake torque is as follows:

$$T = T_i\left(1 - \frac{\theta(t)}{\theta_f}\right) \qquad (5)$$

or

$$T = T_i\ (1 - \theta(t)/\theta_f)$$

where

T is the brake torque;

T_i is called the "unfaded brake torque" and corresponds to the torque which would have been obtained without any "fade";

$\theta(t)$ is the calculated temperature;

θ_f is the fade factor; and

t is time.

The unfaded torque T_i can be computed either from equation 4 or from tables (T_i versus pressure) selected to produce a good match between the brake torque T and available test data.

Experience has shown that for typical inertia dynamometer data of the form illustrated in Figure 5,[6] the fade factor approach may work well when suitable values of T_i and θ_f can be found for initial velocities and inertial loads corresponding approximately to conditions of interest in predicting vehicle performance. As can be seen by examining the torque data and the computed-temperature curve presented in Figure 5, the torque decreases as the temperature increases, and then the torque increases as the temperature decreases at the end of the stop. These trends are typical of brakes with linings that decrease in frictional potential as temperature increases. Nonetheless, certain linings may exhibit the opposite trends at normal operating temperatures. Accordingly, the fade factor approach will not always work unless the form of equation 5 is adjusted to account for the idiosyncrasies of the particular linings under study.

Obviously, the data-fitting procedures just described are not straightforward and efficient to use, nor are they scientifically and aesthetically satisfying. Their main virtue is that they have been made to work as a matter of necessity.

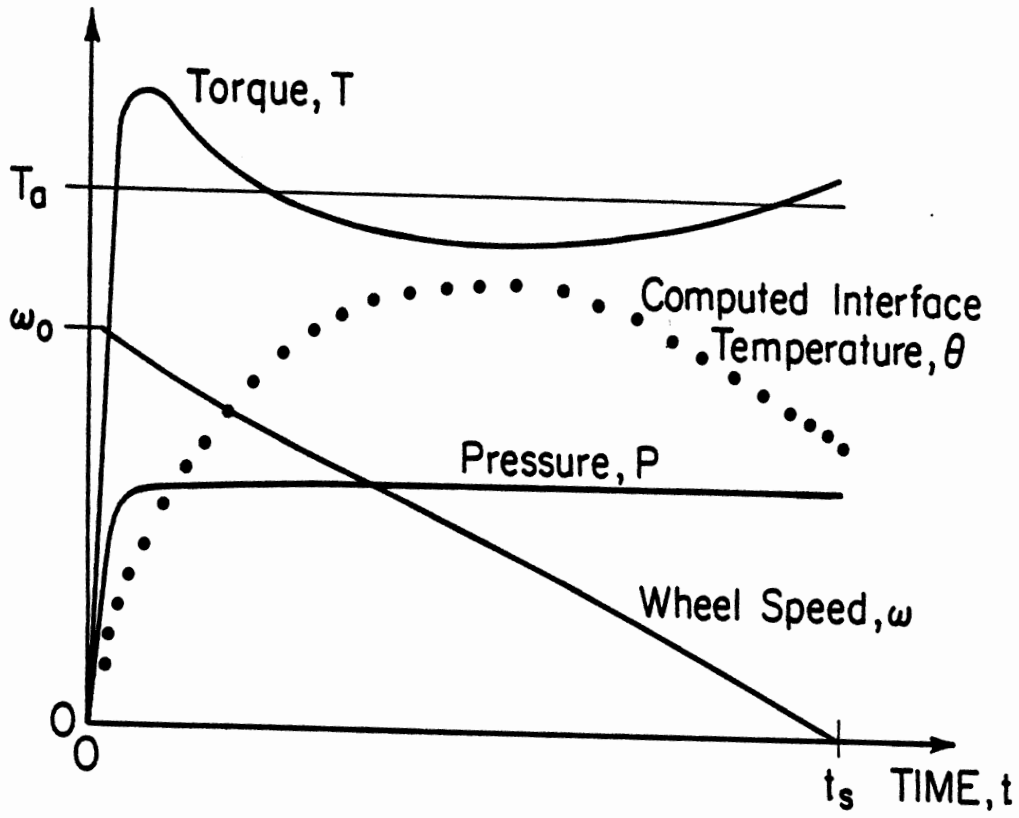

Figure 5. Data from a spin-down dynamometer test.

Accordingly, recent research efforts have addressed the development of an improved method for processing data from tests of commercial vehicle brakes.[16] In these efforts an "effectiveness" function relating torque to actuation effort, velocity, temperature, and work history is sought.

At this time an appropriate method for including work history in a functional relationship for effectiveness is not known. Instead, effectiveness data gathered at various stages of a specified test program (for example, a postburnish effectiveness and a final effectiveness from the sequence of tests called for in FMVSS 121) can be used to characterize the performance of the brake as it experiences a well-defined work history.

In work performed recently,[16] effectiveness functions for S-cam and dual-wedge brakes have been derived from test data. For an S-cam brake, the effectiveness, e, is calculated as

$$e = \frac{T}{F_{AC}\ell - S_c} \tag{6}$$

where

T is the brake torque,

F_{AC} is the force produced by the air chamber (i.e., chamber pressure times the effective area of the diaphragm in the brake chamber),

ℓ is the length of the slack adjuster arm (F_{AC} is the torque applied to the cam used to force the brake shoes against the drum), and

S_c is the torque required to overcome the return springs.

For a dual-wedge brake

$$e = \frac{T}{\left(\frac{F_{AC_1} + F_{AC_2}}{2} - S_w\right) 1/2 \cot \frac{\alpha}{2}} \tag{7}$$

where

$F_{AC1,2}$ denotes the force produced by the two air chambers,

S_w denotes the force required to overcome the return springs, and

α denotes the included angle of the wedge.

The effectiveness function is determined from data obtained during brake applications over appropriate ranges of temperatures, sliding speeds, and actuation forces. During a single stop (dynamometer test), effectiveness can be calculated as a function of time, with each instant in time corresponding to a set of values for temperature, sliding speed, and actuation force. Figure 6 illustrates the procedure used for calculating effectiveness from dynamometer data. (Clearly, time histories of the variables involved in the test are needed because temperature, sliding speed, and torque are changing continuously during a brake application at constant chamber pressure.)

Note that a calculated temperature is used in determining the effectiveness function. The reasons for this are:

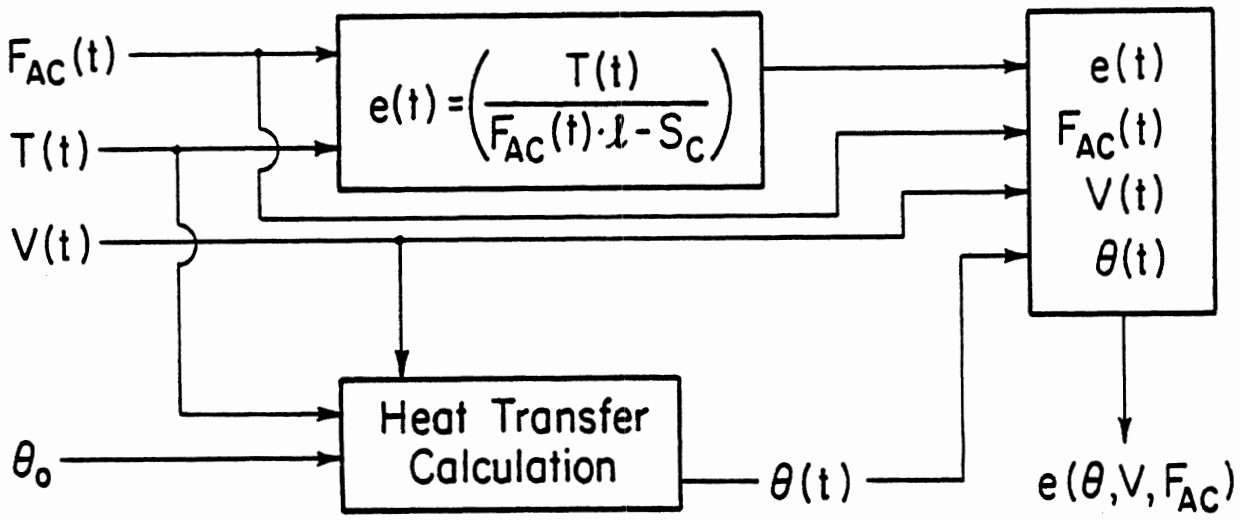

V = Sliding velocity ($V = \omega r$ where ω = drum rotational speed and r is the drum radius)

θ_0 = Initial brake temperature

$\theta(t)$ = Calculated interface temperature

Figure 6. Flow diagram for calculating values of effectiveness from dynamometer data.

(1) the interface temperature is extremely difficult to measure, (2) measured temperatures can vary greatly from stop to stop even when stops are made from seemingly identical conditions, and (3) temperatures can vary markedly across the width of the lining. The measured temperature of the drum at the time the brake is first applied is used as an initial condition for the calculation. The rate at which heat is generated (i.e., the heat flow into the brake) is proportional to the product of brake torque and rotational speed (both measured quantities). The temperature, calculated from the initial drum temperature and the heat flow into the drum, represents the average temperature across the width of the lining.

The effectiveness data obtained from the process illustrated in Figure 6 could be implemented in a computer simulation in tabular form. In the past, however, it has been frustrating to try to construct meaningful tables because of variability in the test data, a lack of data repeatability due to work history effects, and inadequate temperature information. Although some of these past difficulties have been reduced or alleviated as a better understanding of the brake has been acquired, the current approach is to develop a mathematical equation describing the data.

The effectiveness data are fitted by a least-squares procedure using a multinominal of the following form

$$e = \sum_{i=1}^{n_i} \sum_{j=1}^{n_j} \sum_{k=1}^{n_k} a_{ijk}\, \theta^{i-1}\, V^{j-1}\, F^{k-1}$$

where n_i, n_j, and n_k are picked so that the data are adequately described with the simplest equation. Two numerics, the coefficient of determination, r^2, and the standard error, S_e, are computed using a statistical analysis package. These numerics are useful in selecting appropriate values for n_i, n_j, and n_k. The value of r^2 represents the fraction of the behavior (variation) of the data which the curve fit describes, and the standard error can be used to estimate the range of torques a brake might produce under identical operating conditions.[16] Hence, the least-squares procedure provides a numerical indication of the quality of the fit and the uncertainty in the brake torque.

The use of the approach just described for fitting dynamometer data is only practical if automatic data-handling capabilities are added to existing brake dynamometers. The need to process great quantities of time-history information necessitates the use of computerized data-processing methods. Fortunately, at least one brake manufacturer is planning to store dynamometer data in digital files. Given digitized time-history information, the calculations needed to make a "curve-fit" model of the brake can be performed in a straightforward manner using the techniques and programs developed in

this research effort. Whether empirical models determined by regression techniques become a practical means for representing brakes in vehicle simulations depends upon the development of a suitable base of dynamometer data for, at least, the standard types of brakes employed on commercial vehicles.

In addition to effectiveness matters, hysteresis and side-to-side imbalance should be modeled for use in studies including automatic control devices such as antilock systems.

Due to hysteresis a reduction in brake-chamber pressure is not accompanied by as large a reduction in brake torque as would be expected from data gathered during tests made with increasing pressure. The forms of typical pressure-torque cycles observed in brake and vehicle tests are illustrated in Figure 7. A representation of hysteresis suitable for simulating the types of results shown in Figure 7 is included in the mathematical model described in [6, pp. 78-83].

In a straight-line braking model, side-to-side brake imbalance is considered because of its influence on brake system operation, not because of its influence on directional response. In the straight-line braking case, it is assumed that the driver steers to correct for any yaw movement created by brake imbalance. Brake imbalance influences the operation of currently available antilock systems because these systems use a "worst wheel" strategy to control the air pressure to both brakes on an axle. The "worst wheel" is defined as the wheel closest to lockup, and the rotational speed and deceleration of this wheel determine when brake pressure will be

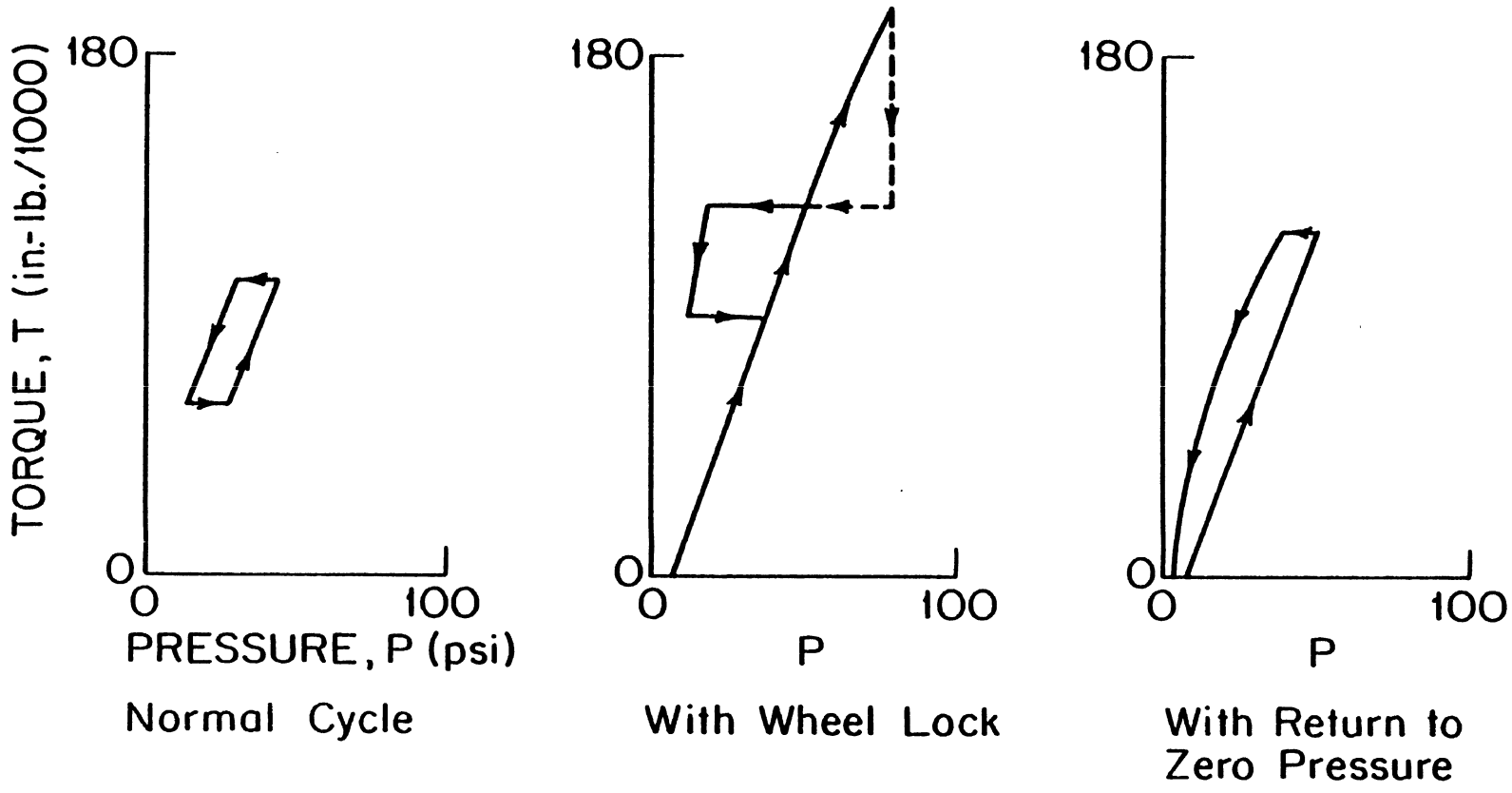

Figure 7. Forms of brake hysteresis.

decreased to prevent wheel lock. However, if the brake associated with the other wheel (the "best wheel") is considerably less effective than the worst wheel's brake, then the best wheel may not be producing anywhere near its maximum braking force when its brake pressure is decreased. In this way brake imbalance can significantly reduce the efficiency of antilock braking.

The model described in [6] contains a means for studying the influence of brake imbalance. In [6] both brakes on an axle are assumed to be of the same type with a specified baseline torque, but an imbalance parameter designates the percentage deviation above the baseline torque for one of the brakes and below the baseline torque for the other.

To summarize the discussion of brake modeling the following observations are in order: (1) Brake modeling is a highly empirical art, (2) Experience has shown the need for developing a method for dealing with the variability of brake data, and (3) Brake characteristics (imperfections) such as hysteresis and imbalance can degrade the performance of antilock systems. It is no wonder that acceptable antilock systems have been difficult to design, given that the changeable performance of a basic device in the system (that is, the brake) is not well understood.

Brake Temperature

A model of the heat flow processes taking place in the brake drum has been included in braking analyses. The purpose

of the heat-flow model is to provide a means of calculating temperature changes during a stop and thereby to allow study of the phenomenon referred to as "in-stop fade and recovery." Empirical methods for treating in-stop fade and recovery constituted the primary emphasis of the previous discussion on the representation of brake torque as a function of actuation effort (pressure), sliding speed, and interface temperature.

In the research studies performed in support of brake system development, two types of temperature analysis have been used. For use in simulation studies, classical heat flow equations have been applied to a simplified model of the drum.[6] For use in analyzing and processing brake data, a finite-element model of the drum has been developed.[16] Both models have worked successfully in their intended applications.

The reasons for the different models seem to be a matter of the investigators' preferences and experience. Nevertheless, since both models now exist in practical form, they could be compared with respect to their cost and ease of use, range of applicability, etc. To date, a detailed comparison has not been made, probably because the study of brake temperature is of modest significance in relation to the overall vehicle-modeling task. However, both models are of interest in their own right and they will be described.

In a systems sense, the input to the drum is the heat flow generated by the braking process. The time history of the heat being put into a unit area of the rubbing surface of the drum is defined by:

$$f = \frac{BT\omega}{A} \tag{9}$$

where

B is the fraction of the generated heat entering the drum (B = 0.95 for brakes having organic linings and cast-iron drums),

T is the instantaneous torque,

ω is the instantaneous wheel speed (drum speed), and

A is the swept area.

The initial temperature of the drum and the rate of heat input, f, are the starting points for both temperature models of the drum. The desired output from these models is the interface temperature at the inside (rubbing) surface of the drum.

For use in a vehicle simulation, the calculation of the temperature at the drum-lining interface is facilitated by developing an idealized model in which the drum is treated as a flat strip. The conceptual notions involved in transforming the drum into a flat strip are illustrated in Figure 8. Specifically, the following assumptions are made:

(1) Since brake drums have radii which are large compared with the drum thickness, the drum may be modeled as a flat strip.

(2) Since no appreciable heat loss occurs during a single brake application, the outer drum surface is assumed to be insulated.

(3) The rate of energy input per unit area at the drum-lining interface is constant over the rubbing area of the drum.

(4) A constant proportion of the heat generated at the drum-lining interface is assumed to flow into the drum.

Under these four assumptions, which have been previously used in the analysis of the temperature in brake drums,[17] the heat flow equation is:

$$\frac{\partial \theta}{\partial t}(x,t) = k \frac{\partial^2 \theta}{\partial x^2}(x,t) \qquad 0 \leq x \leq L \qquad t>0 \tag{10}$$

under boundary conditions

$$\frac{\partial \theta}{\partial t}(0,t) = \frac{-BT\omega}{\alpha A} \tag{11}$$

$$\frac{\partial \theta}{\partial x}(L,t) = 0 \tag{12}$$

and initial temperature profile θ (x, 0) = θ_o(x)

where

θ = drum temperature,

t = time,

x = distance (x = 0 at drum-lining interface, x = L at the outside of the drum),

α = conductivity of the drum, and

k = diffusivity of the drum.

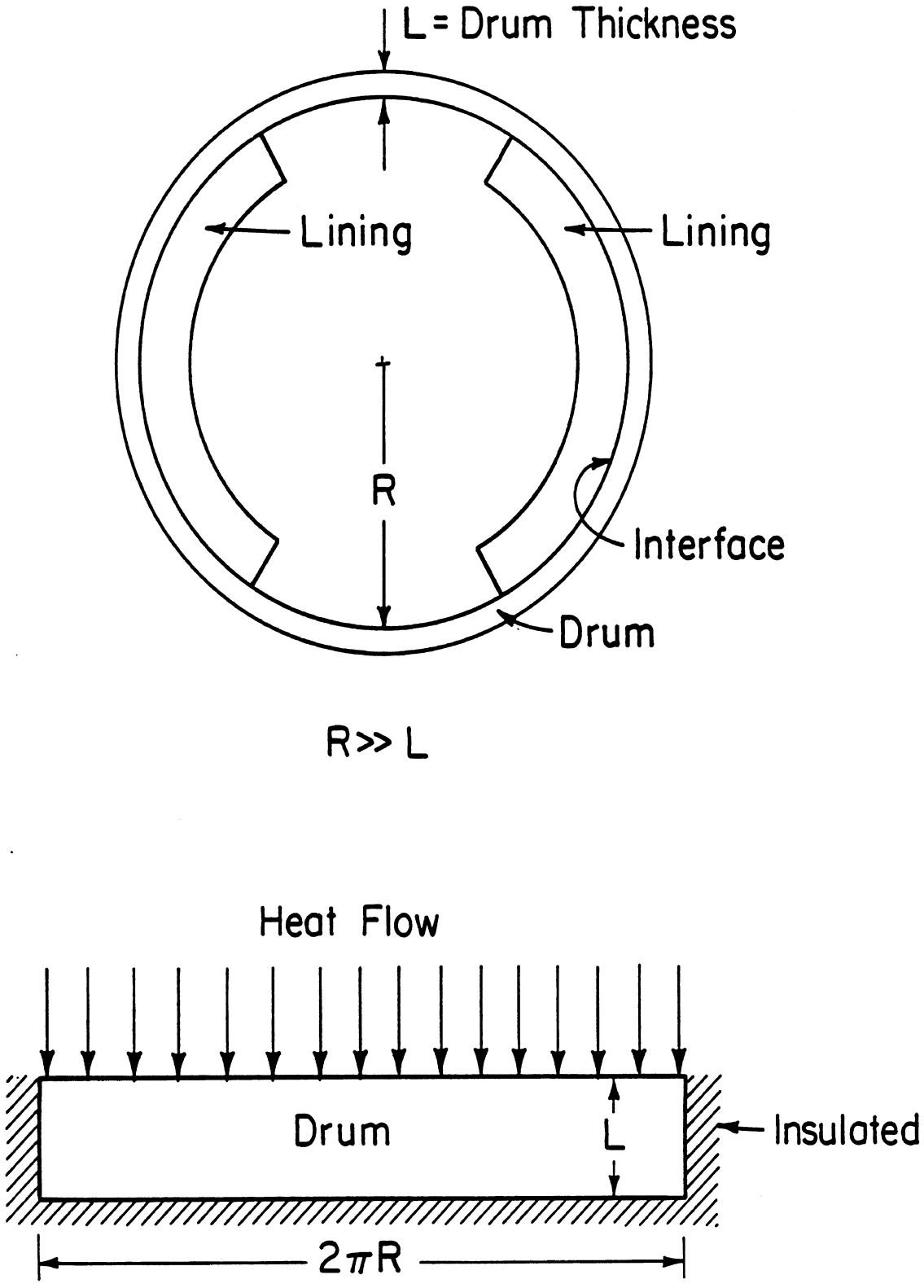

Figure 8. Schematic diagram-brake drum and lining.

Equation 10 is solved analytically using well-known (albeit elegant) techniques involving separation of variables, eigen values and functions, Fourier series, and integration by parts. This process leads to a set of ordinary differential equations to be solved for the coefficients in the Fourier series representing the solution to the heat flow problem.

These differential equations could be solved directly by numerical integration, but in the interest of reducing computational costs, special numerical solution techniques have been developed. These techniques are based on ideas similar to those used in the simulation of the air delivery system. The input (heat flow) is approximated by a stair-step representation, with steps corresponding to the time steps of the digital simulation. Specifically, for a single time step starting at time t_o and lasting Δt seconds, the temperature at the drum-lining interface at the end of the time step (i.e., at $t = t_o + \Delta t$) is given by the following equation:

$$\theta(x,t) = A_o(t) + \sum_{1}^{\infty} A_n(t) \cos\lambda_n x \qquad (13)$$

where $\lambda_n = \frac{n\pi}{L}$

$$A_o(t) = A_o(t_o) + \frac{k}{\alpha L} f(t_o)\Delta t, \text{ and}$$

$$A_n(t) = \frac{2f(t_o)L}{\alpha\pi^2 n^2} + \left(A_n(t_o) - \frac{2f(t_o)L}{\alpha\pi^2 n^2}\right)e^{-k\lambda_n^2\Delta t}$$

in which

$$f(t_o) = \frac{BT(t_o)\omega(t_o)}{A}$$

For use in practical calculations, equation 13, as shown in reference [6], can be reduced to the following form for the temperature at the drum-lining interface:

$$\theta(0,t) = A_o(t) + \frac{f(t_o)L}{3\alpha} + \sum_{n=1}^{3}\left(A_n(t_o) - \frac{2f(t_o)L}{\alpha\pi^2 n^2}\right)e^{-k\lambda_n^2\Delta t} \quad (14)$$

Only the first three terms of the summation in equation 13 are needed in equation 14 to obtain numerical results virtually identical to exact solutions [6]. Accordingly, the interface temperature may be found with sufficient accuracy for simulation purposes by updating t_o, $f(t_o)$, $A_o(t_o)$, and $A_n(t_o)$ ($n = 1, 2, 3$) at the end of each step and then reapplying equation 14 in the next time step.

In contrast to the flat-plate idealization, the finite element approach uses the geometry of the drum in formulating the model. Figure 9 from [16] illustrates the finite element nodes used in the analysis of a typical 16½" x 7" brake drum. In this analysis heat is assumed to flow in the radial and axial directions but not in the circumferential direction.

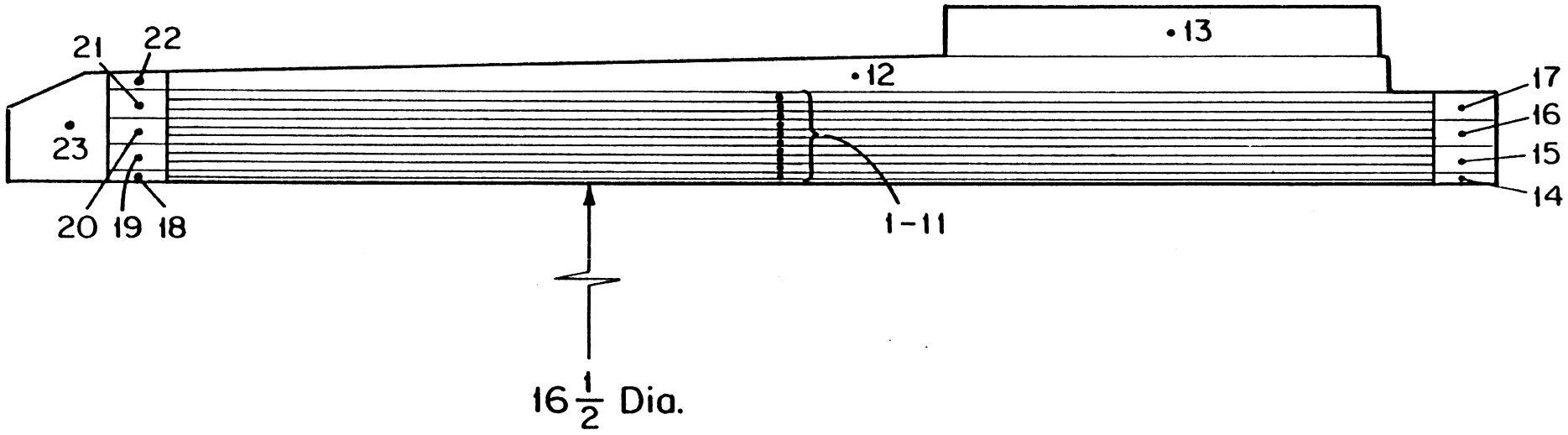

Figure 9. Cross section through 16 1/2" x 7" brake drum showing the finite element nodes.

Heat flow into the mounting flanges is ignored. The heat flow input per unit area is assumed to be uniform over the rubbing surface ("hot spots" are neglected). The thermal conductivity and diffusivity of the drum material are used to determine the resistance to heat flow between nodes and the thermal capacity of each finite element. The thermal model includes convective heat transfer at the periphery of the drum. Using these assumptions, reasonable agreement between calculated and measured temperatures has been obtained (see [16], pp. 39 and 40).

The finite-element model is more general than the flat-plate model because convective heat transfer is allowed, thereby making the study of fade during mountain descents (or repeated snubs) possible with the finite-element model. (Incidentally, calculations using this model show that convective heat transfer at the periphery of the drum is unimportant in a single stop and, therefore, the assumption of an insulated outside boundary in the flat-plate model will not lead to inaccurate temperature predictions during a single rapid stop.)

Wheel Dynamics

The basic form of the equation of motion used to describe the rotational dynamics of each wheel is

$$I\dot{\omega} = -T - F_x R \tag{15}$$

where I is the polar moment of inertia of the rotating parts,

$\dot{\omega}$ is the wheel angular acceleration,

T is the applied brake torque,

F_x is the longitudinal force at the tire-road interface ($F_x < 0$ for braking),

and R is the effective tire radius (the distance from the wheel center to the ground).

The angular acceleration, $\dot{\omega}$ as expressed in equation 15, is integrated with respect to time to obtain the wheel speed (rotational velocity), ω.

Equation 15 contains only the basic factors determining wheel speed. For drive axles connected by transmission components, the equations for the speed of the associated wheels are coupled to each other through the shared inertia of the rotating parts in the transmission (and by engine characteristics unless the engine is declutched). In addition, equation 15 omits small terms due to rolling resistance moments and the angular acceleration of the unsprung mass to which the wheel is attached. In some detailed studies the influence of the omitted terms could be of interest; however, they are ordinarily neglected unless specifically asked for.

The direct solution of equation 15 by numerical integration can be costly because of the high frequencies involved due to the "stiffness" of the tire in producing longitudinal force. To alleviate this cost burden, equation 15 can be solved numerically using a linearized version of the functional characteristics representing the tire.[18]

Experimental results show that tire braking force F_x depends primarily upon wheel speed, vertical load, and forward velocity. Since vertical load and forward velocity are changing relatively slowly compared to wheel speed, the braking force during a time step may be approximated as follows:

$$F_x(\omega,F_z,V) \doteq F_x(\omega_o,F_{zo},V_o) + \frac{\partial F_x}{\partial \omega}\Big|_{\omega_o,F_{zo},V_o} (\omega - \omega_o)$$

noting that $\frac{d}{dt}(\omega - \omega_o) = \dot{\omega}$

$$I\dot{\omega} \doteq -T - RF_x(\omega_o,F_{zo},V_o) + \frac{\partial F_x}{\partial \omega}\Big|_{\omega_o,F_{zo},V_o} (\omega - \omega_o) \qquad (16)$$

Equation 16 can be solved analytically to obtain the following numerical expression for the wheel speed at the end of the i^{th} time step based on the wheel speed at the beginning of the time step:

$$\omega(t_i) = [\omega(t_{i-1}) - F_\omega(t_{i-1})]e^{-\Delta t/\tau_\omega} + F_\omega(t_{i-1}) \qquad (17)$$

where Δt is the length of the time step,

$$\tau_\omega = \left(\frac{I}{R\frac{\partial F_x}{\partial \omega}\Big|_{t_{i-1}}}\right)$$

and $$F_\omega = \left(\frac{-T - R(F_x - \frac{\partial F_x}{\partial \omega})\omega}{R\frac{\partial F_x}{\partial \omega}}\right)\Big| \quad \text{evaluated at } t_{i-1}$$

A more sophisticated version of equation 17, using longitudinal slip s, (where $s = 1 - R\omega/V$) rather than wheel speed

ω_4 has been used in both truck[6] and passenger car simulations[19] with considerable savings in computational costs compared to direct numerical integration of the equations of motion.

Tires

The tire performs many functions. It supports a load, envelops bumps, and generates braking force.

For braking studies the development of a method for representing the longitudinal force properties of tires is clearly most important. Prior to the availability of data from an over-the-road truck-tire dynamometer, a semi-empirical model was developed and used. The semi-empirical model consists of a phenomenological description of the deflection and shear force characteristics of the tire. Empirical data or estimated tire shear-force characteristics are needed to evaluate the parameters used in this type of model. The values of the parameters are selected so that the forces predicted by the model match test results or a desired set of tire properties.

In this type of model[2] a quasistatic analysis of the rotating tire is made. The tread is envisioned as a continuum of elastic elements which touch the ground in the contact patch. Even though the wheel is rotating, some tread element is assumed to be deflected by a determinable amount at each point in the contact patch. The following sketches (Figures

10 and 11) and the subsequent analysis are intended to clarify the form of the tire model.

As shown in Figure 10, tread elements are assumed to become elongated longitudinally as they pass through the contact patch. For an arbitrary element at a distance x from the front of the contact patch (see Figure 11), the deflection δ of that element may be determined from the longitudinal slip, using the following reasoning. For an element entering the contact patch Δt_x seconds ago, the carcass end of the element has traveled a distance equal to $R\omega\,\Delta t_x$. The road-contact end of this element has travelled a distance equal to $V\Delta t_x$ if this end of the element adheres to the road. (The case of sliding friction between tire elements and the road will be treated later.) Hence, the deflection of the element at point x in the carcass is given by:

$$\delta(x) = (V - R\omega)\Delta t_x$$

By noting that $x = R_\omega \Delta t_x$, it is possible to express the deflection as a function of slip;

$$\frac{\delta(x)}{x} = \frac{(V - R\omega)\Delta t_x}{R\omega\Delta t_x} x = \frac{V}{R\omega}\left(1 - \frac{R\omega}{V}\right)$$

or, since $s = \left(1 - \frac{R\omega}{V}\right)$

$$\delta(x) = \frac{xs}{1-s} \qquad (18)$$

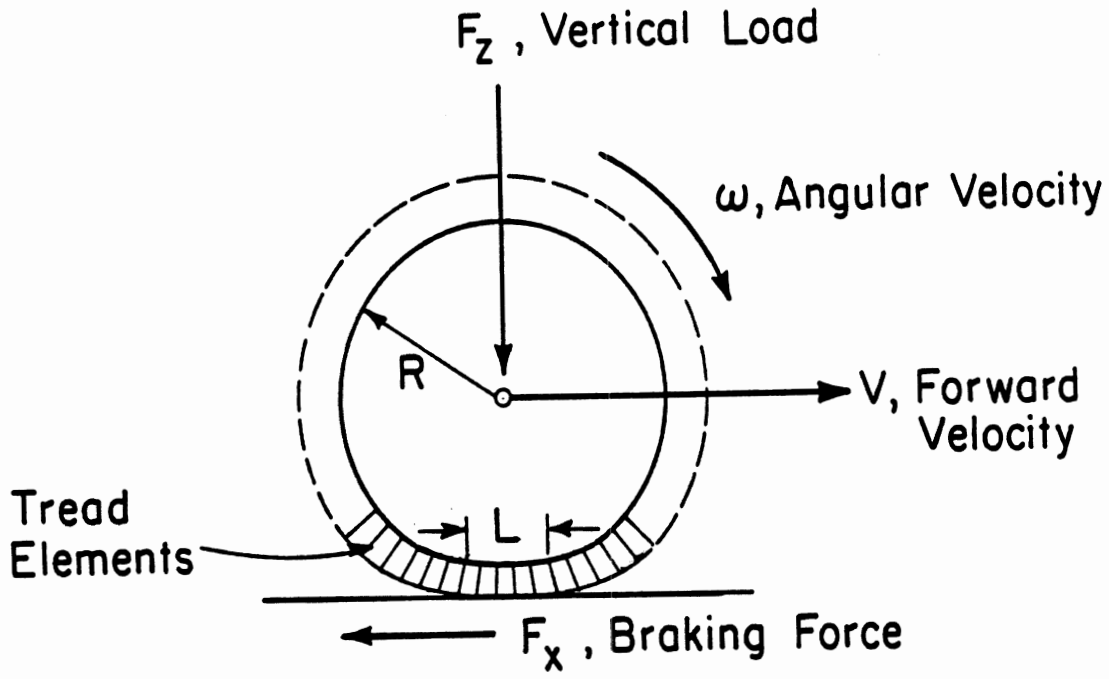

Figure 10. Sketch of an idealized tire.

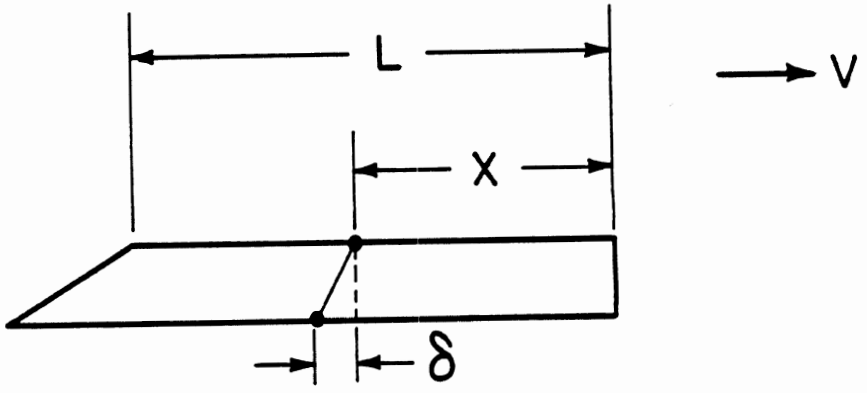

Figure 11. The longitudinal deflection δ of a tread element at location x in the contact patch.

Figure 12 illustrates the predicted form of the deflection pattern along the length of the contact patch for a situation in which no elements are sliding with respect to the road.

For simplicity, lateral variations over the width, w, of the contact patch are neglected and the deflection pattern in Figure 12 may be thought of as an average over the lateral direction.

To compute the total shear force due to the deflection pattern, the tire is assumed to be characterized by a stiffness per unit area of the contact patch. This stiffness parameter, K_x, will be replaced by an empirically determined longitudinal stiffness parameter, C_s, in the final form of the brake-force model. Nevertheless, K_x serves as a means for converting deflection into shear force; specifically, the following integral defines the braking force, F_x, when no sliding occurs:

$$F_x = \int_{x=0}^{L} \delta(x) k_x w dx$$

or, substituting for $\delta(x)$ from 18 and evaluating the integral above,

$$F_x = \left(\frac{k_x L^2 w}{2} \right) \left(\frac{s}{1-s} \right) = \frac{C_s s}{1-s} \qquad (19)$$

The quantity $\frac{k_x L^2 w}{2}$ in equation 19 is equal to the $\left.\frac{\partial F_x}{\partial s}\right|_{s=0}$ and it is defined as the longitudinal stiffness parameter, C_s. Furthermore, C_s may be evaluated empirically from the slope of test data for F_x versus s without knowing K_x or the dimensions of the contact patch.

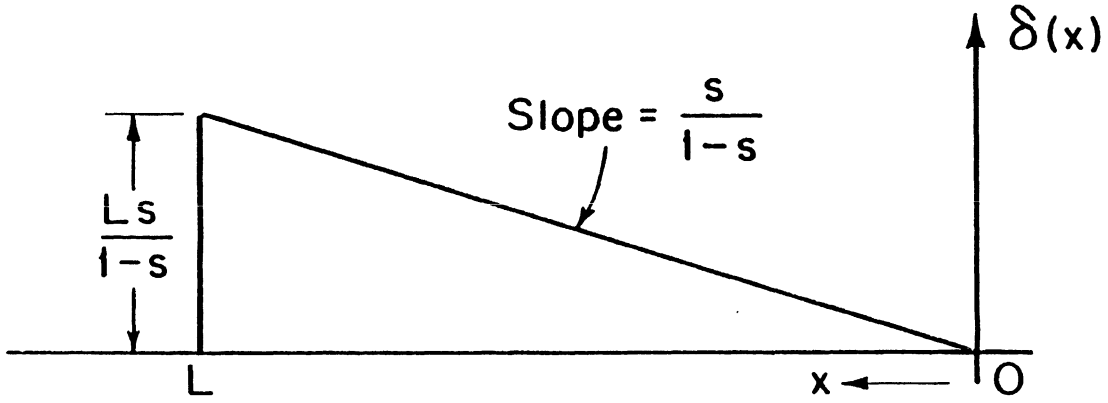

Figure 12. Tire deflection pattern, no sliding.

Sliding starts to occur in the contact patch at the point where the frictional potential per unit area can not support any more deflection. That is, sliding starts when

$$\frac{\mu F_z}{A} = \frac{k_x x_s s}{1-s} \tag{20}$$

where μ is the tire-road friction coefficient,

A is the area of the contact patch ($A = Lw$),

F_z is the vertical load (A uniform pressure distribution of magnitude F_z/A is assumed in developing the simplest model.),

and x_s is the value of x at which sliding starts.

Figure 13 illustrates the estimated form of a deflection pattern with sliding at the rear of the contact patch.

For the deflection pattern shown in Figure 13 the longitudinal shear force, F_x, is given by

$$F_x = \int_{x=0}^{x_s} \delta(x) k_x w dx + \frac{\mu F_z}{A} w(L - x_s)$$

$$\text{or} \quad F_x = \frac{k_x x^2 w}{2} \left(\frac{s}{1-s}\right) + \mu F_z \left(1 - \frac{x_s}{L}\right) \tag{21}$$

It is convenient to re-express 21 in terms of C_s, the longitudinal stiffness, and x_s/L, the fraction of the contact patch which is not sliding. From equation 20

$$\frac{x_s}{L} = \frac{\mu F_z}{k_x AL\left(\frac{s}{1-s}\right)} = \frac{\mu F_z (1-s)}{2c_s s} \tag{22}$$

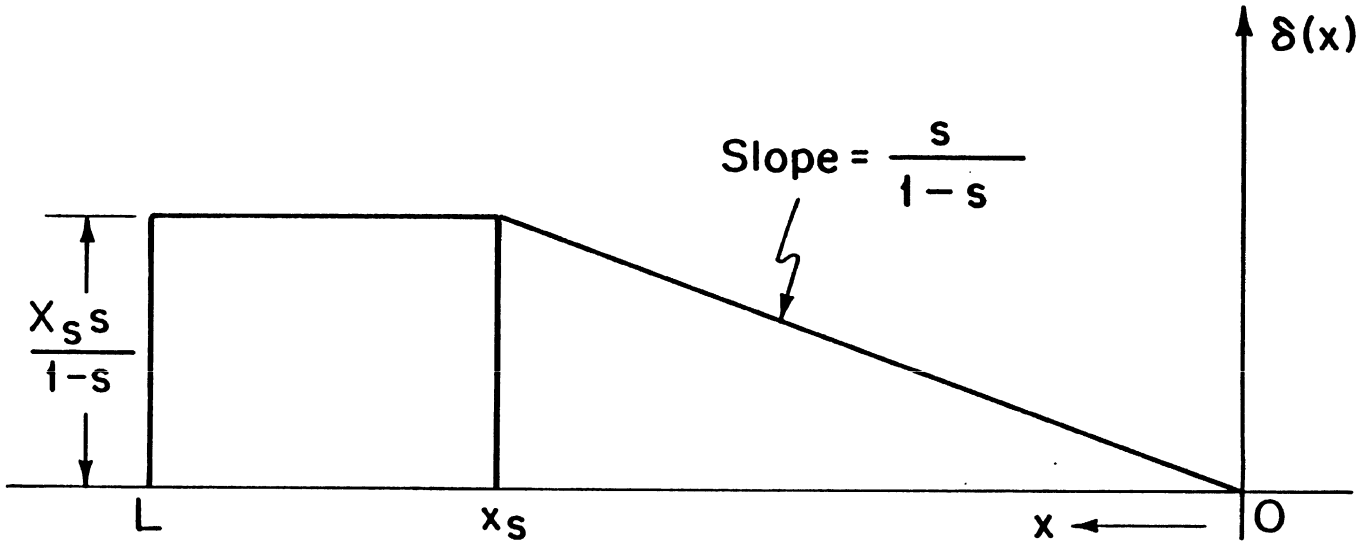

Figure 13. Tire deflection pattern, with sliding.

and, using equations 22 and 21

$$F_x = \frac{(\mu F_z)^2}{4c_s}\left(\frac{1-s}{s}\right) + \mu F_z\left(1 - \frac{x_s}{L}\right) \qquad (23)$$

In numerical computations x_s/L is evaluated from equation 22 if $s > 0$. If x_s/L is greater than 1.0, then no sliding takes place in the contact patch and F_x is calculated from equation 19. If x_s/L is less than 1.0, then F_x is evaluated using equation 23. Note that for a locked wheel (i.e., $s = 1.0$), all of the contact patch is sliding ($x_s/L = 0$), and F_x is determined by tire-road friction (i.e., $F_x = \mu F_z$).

If the friction coefficient μ is treated as a constant, then the model will predict that the maximum braking force occurs at locked wheel conditions. However, in practice, μ is not constant and the braking force reaches a maximum at some intermediate value of slip, usually around $s = 0.2$. Experiments with pieces of tire tread indicate that above a very low velocity, tire-road friction tends to decrease with sliding velocity. A simple method for including this phenomenon in the model is to make μ a function of sliding velocity,

$$\mu = \mu_o - f_a V_s \qquad (24)$$

where μ_o is the maximum value of friction at low velocity,

f_a is a parameter chosen to represent the decrease in friction with sliding velocity,

and V_s is the sliding velocity of a tread element with respect to the ground (i.e., $V_s = V \cdot s$)

Clearly, equations 19, 22, 23, and 24 represent a very simplified model of highly complicated elastic and frictional processes between the tire, which is a complex structure, and the road, which may have random characteristics due to dirt, liquid contamination, variable composition, and nonuniform texture from one contact patch area to another. Nevertheless, this model has proven to be quite accurate for simulating passenger car tires and, when combined with lateral slip (slip angle) effects, it has been very useful in studying combined braking and steering maneuvers.[21]

The semi-empirical model has been less successful in representing truck tires than in representing passenger car tires. Figure 14 illustrates the type of difficulty that can occur if a simplified model of the friction process is used in treating truck tires. In Figure 14 the solid line indicates that the model does a very good job of fitting test data obtained at 40 mph. However, if the values of $_{o}$ and f_a employed for matching the 40 mph data are used to predict longitudinal force at 30 or 55 mph, the match between results predicted by the model and data measured for a particular tire on a good, dry road can be in substantial disagreement at high values of slip as shown in Figure 14.

In addition, the friction between tire and road has been found to be significantly dependent upon vertical load.[22] Accordingly, an improved semi-empirical model requires a better understanding and representation of the frictional processes between the tire and pavement than that expressed by equation 24.

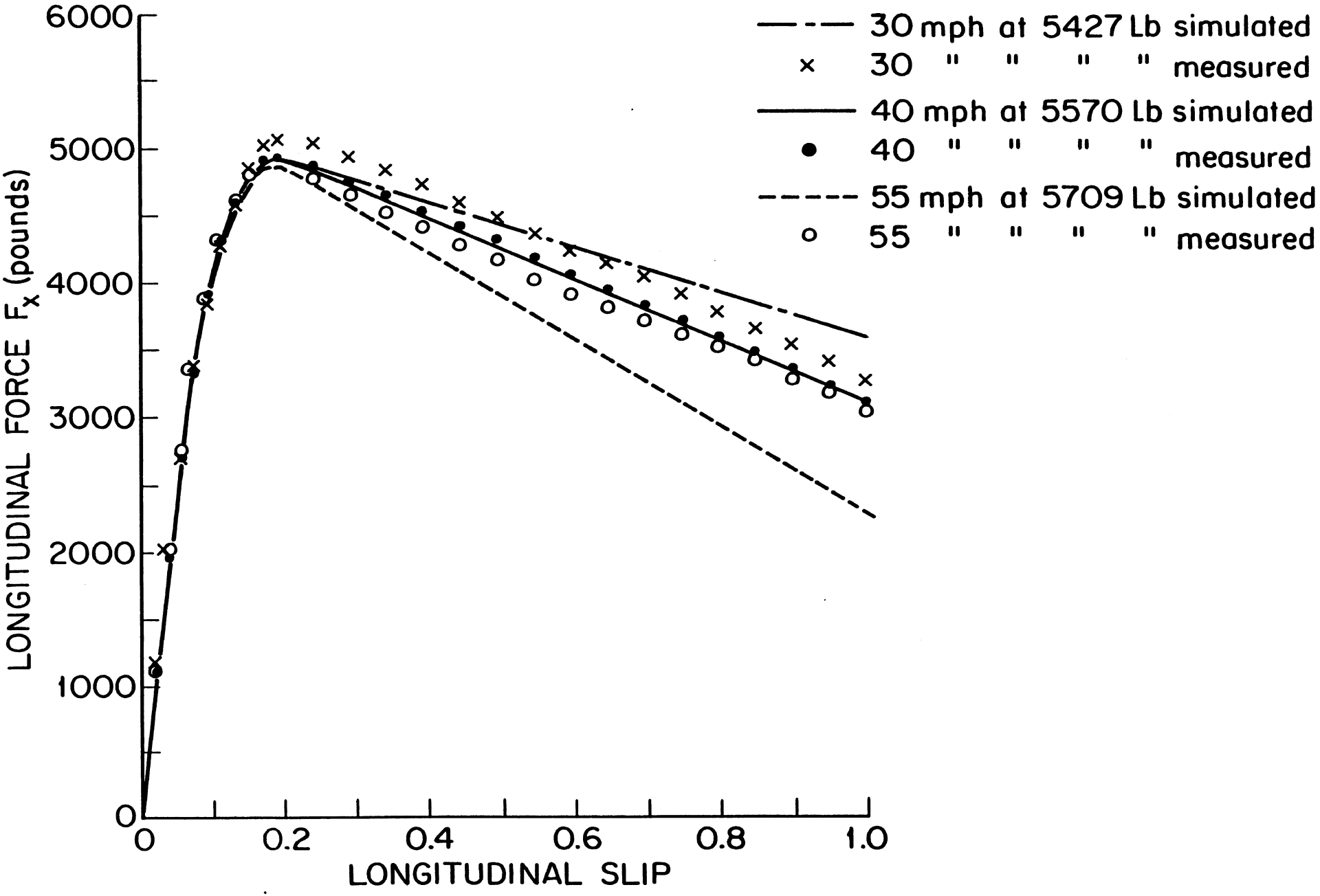

Figure 14. Effect of speed on force vs. slip curve for Firestone Transport 1 (10.00 x 20/F).

For braking studies of particular vehicles, the current trend has been to use measured tire data rather than a semi-empirical model. In some cases, special tire tests on a specific surface are performed using the mobile dynamometer described in Chapter 3. In other studies, measured data from (1) test programs devoted to studying tire properties[22, 23] or (2) previous vehicle dynamic studies[24] are employed. Typically, measured tire data are entered into simulations using tabular functions of longitudinal force at three velocities and three vertical loads for five values of slip. (Of course, more data points could be used to provide greater fidelity.)

The choice of using a model or test data for representing tires is an example of a classical situation that often occurs in simulation studies. A model provides more insight into the basic phenomenon than that provided by tables of data. If the model is not overly complex, it requires a limited number of parameters, thereby facilitating parameter-sensitivity studies. On the other hand, empirical data (if carefully obtained under controlled conditions) accurately describe a particular tire-road combination of interest. Emphasis on demonstrating compliance with vehicle performance standards makes imperative the use of an accurate representation of the tires to be installed on a particular vehicle. To provide flexibility, the simulation described in [6] has options for selecting either a semi-empirical tire model or tables of user-entered tire data.

In addition to the longitudinal force characteristics of the tires, the vertical force versus deflection characteristics of the tires are included in the model. In the simulation the locations and velocities of the wheel centers are computed, and these quantities are used to determine the vertical forces between the tire and the road and the "equal but opposite" forces accelerating the unsprung masses. The vertical force versus deflection property of the tire is represented by a spring constant measured under rolling conditions. A small amount of viscous damping (approximately 35 lbs sec/in for a 10 x 20 truck tire) is included, thereby providing a relatively small, dissipative force opposing wheel-hop motions. This small amount of tire damping is included to prevent the prediction of transient wheel hop oscillations in response to rapid changes in vertical motion. Experimental results from tire tests under conditions of varying vertical load as well as the examination of vehicle test data from antilock braking studies indicate that a certain amount of damping is present in the tire. (The mechanism by which the energy is dissipated in the vertical motion of a rolling tire is not entirely clear, but somehow it does not appear to make a substantial contribution to the rolling resistance of the tire.)

This discussion of tire representation has emphasized a largely empirical approach in determining longitudinal and vertical force characteristics of truck tires. The development of suitable tire-testing devices makes this a viable

approach to use in simulation studies of heavy-vehicle braking. The development of vehicle simulations including detailed tire models based upon fundamental principles will require (1) advanced methods for analyzing the structure of tires, (2) a comprehensive and possibly new theory of tire-road friction, and (3) powerful computers with low computational costs. In the near future, an empirical approach to tire representation appears to be the most reliable and practical approach to pursue.

Vehicle Dynamics (Including Suspension Properties)

The vehicle is modeled as a system of rigid bodies consisting of sprung and unsprung masses. The equations of motion for these bodies may be derived using basic principles of dynamics once the degrees of freedom to be included in the model are determined. Well-known numerical integration algorithms are used in the simulation to solve the equations describing the motions of the rigid bodies constituting the vehicle model.

The modeling and simulation of the rigid body motions are relatively straightforward tasks. The difficult and unique parts of the simulation concern the representation of vehicle components. Accordingly, after discussing the degrees of freedom included in the model, certain details of representing commercial vehicle suspensions are described in this section.

The degrees of freedom considered are:

- longitudinal motion of the entire vehicle
- pitch and bounce of each sprung mass
- vertical motion of the front axle (and any other single-axle suspension)
- two degrees of freedom for the vertical and pitch motions of each set of tandem axles
- rotational degrees of freedom for each wheel set (the rotational degrees of freedom for the wheels were discussed in the section on wheel dynamics).

For a tractor-semitrailer vehicle with tandem suspensions on both the tractor and the semitrailer, 20 degrees of freedom (including 10 wheel rotational degrees of freedom) are ordinarily included in the model.

Two methods for representing the coupling provided by the fifth wheel hitch have been used. In both methods, the fifth wheel is assumed to be (1) rigid in the longitudinal direction and (2) unable to transmit pitch moments between the tractor and the semitrailer. In one method, the fifth wheel is represented as a spring and damper in the vertical direction. In the other method, the vertical connection is treated as a rigid connection, thereby eliminating a degree of freedom. Similar results have been obtained using either approach,[6] and the choice of method appears to depend upon the ease of implementation.

Several degrees of freedom which are important in certain specialized studies have not been included. For the

study of braking-induced axle-tramp, relative longitudinal motions between the sprung and unsprung masses and axle wrap-up are needed.[25] Since most currently available suspension systems include mechanisms for preventing axle hop or tramp during braking, the longitudinal and wrap-up degrees of freedom are not included in the model. In addition, if the model were to be extended for use in studies of ride motions, a representation of the first frame-beaming mode would be required to predict accelerations in the 7 to 10 Hz range. Nonetheless, the degrees of freedom included in the model have proven to be adequate for braking studies.

The parameters needed for describing the sprung masses are items such as standard dimensions, weights, and moments of inertia. Due to the variety of commercial vehicle configurations in use, separate computer codes have been written for straight trucks, tractor-semitrailers, and doubles combinations.[6] Figure 15 from [6] illustrates a typical set of geometric and inertial parameters needed for simulating the sprung masses of a tractor-semitrailer vehicle. The symbols used in Figure 15 are defined in Table 1.

The only unusual items contained in Figure 15 are the "suspension reference points." In the model, the internal vertical and longitudinal forces between the sprung and unsprung masses act at the suspension reference points. The use of suspension reference points allows the sprung mass model to be used with a variety of suspension models in the simulation.

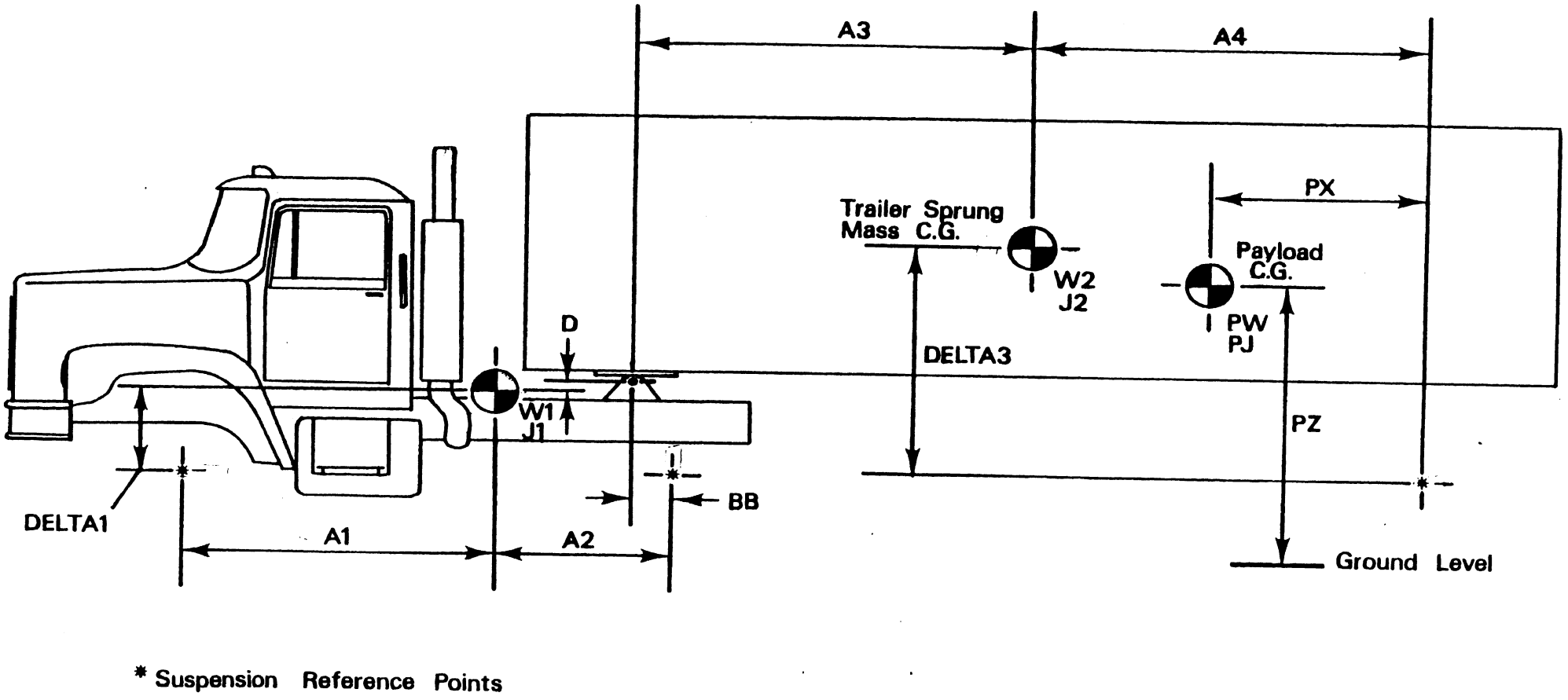

Figure 15. The sprung masses of the tractor-trailer.

TABLE 1

TRACTOR-TRAILER SPRUNG-MASS DATA

Sprung Mass:		
A1	Horizontal Distance from Tractor CG to Reference Point of Tractor Front Suspension (IN)	35.90
A2	Horizontal Distance from Tractor CG to Reference Point of Tractor Rear Suspension (IN)	106.10
A3	Horizontal Distance from Trailer CG to 5th Wheel (IN)	222.00
A4	Horizontal Distance from Trailer CG to Reference Point of Trailer Suspension (IN)	144.00
BB	Horizontal Distance from 5th Wheel to Reference Point of Tractor Rear Suspension (IN)	0.0
D	Vertical Distance from 5th Wheel Connection Down to Tractor CG (IN)	-4.50
DELTA1	Static Vertical Distance, Tractor CG to Tractor Front Axle (IN)	33.30
DELTA3	Static Vertical Distance, Trailer CG to Trailer Axle(s) (IN)	49.50
J1	Tractor Polar Moment (IN-LB-SEC**2)	53374.00
J2	Trailer Polar Moment of Inertia (IN-LB-SEC**2)	607200.00
PW	Weight of Payload (lbs)	0.0
W1	Sprung Weight of Tractor (lbs)	9245.00
W2	Sprung Weight of Trailer (lbs)	8120.00
PW	Weight of Payload (lbs)	
PJ	Polar Moment of Inertia of Payload	
PX	Horizontal Distance from Center of Rear Suspension to Payload CG	
PZ	Vertical Distance from Ground to Payload CG	

The simulation contains subprograms for treating several types of commonly employed tandem suspensions such as walking beam, air, and four-spring suspensions with various load leveler and torque rod arrangements. Options for choosing the desired types of suspensions for a particular vehicle are available in the input data for the simulation.[6] To accomplish the interaction of a variety of suspension subprograms with the sprung mass program, each suspension subprogram computes resultant longitudinal and vertical forces acting on the sprung mass at the suspension reference point plus a pitch moment. The suspension reference point concept allows a variety of suspensions to be included as options in the simulation without rewriting the computer code. Furthermore, additional suspension subprograms can be readily incorporated into the simulation.

In tandem suspensions, the load-leveling mechanism, used to equalize the loads carried by each axle, may react to brake torque. For example, brake torque tends to increase the load on the foremost axle of a walking-beam (Hendrixson) suspension; while for other designs such as the four-spring suspension, the application of brake torque tends to increase the load on the rearmost axle. These interaxle load-transfer characteristics are of importance in braking studies because they determine which wheels will lock up first. Although the influence of locking wheels on one axle of a tandem pair does not present the same magnitude of directional stability problem as locking all wheels on a given suspension, braking standards

typically specify stopping distances or decelerations without locking both wheels on any axle. Accordingly, a useful model should predict interaxle load transfer.

Two approaches have been used in modeling suspensions so as to include interaxle load transfer in the simulation. The initial approach consisted of developing models of the suspensions from free-body diagrams, using basic dimensional parameters and assumptions about frictional connections at various slippers and other sliding contacts.[6] More recently,[26] interaxle load transfer has been represented by a parameter called "percent" which determines the percentage of the brake torque that is reacted on the sprung mass, the remainder of the brake torque acting on the unsprung masses to alter the load carried by the individual axles of a tandem pair. In the more recent approach, the polarity of the percent parameter is used to determine whether the load on the foremost or the rearmost axle will be increased. Using the "percent" concept, separate models for various types of suspensions are not required.

In the last few months, a laboratory device suitable for measuring tandem suspension properties has been completed. The data from this device can be used to determine a value of percent for particular suspensions. Before the availability of this test equipment, special vehicle tests were used to estimate percent.

Undoubtedly, studies using the new suspension measurement device will lead to a better understanding of the properties of commercial vehicle suspensions. For example, preliminary test results indicate the need for extending the models of four-spring suspensions to include the influence of frame-rail pitch angle on the loads carried by each axle. The process of measuring components, discovering new effects, and revising the models has occurred for every vehicle component, and the suspensions are proving to be no exception.

Laboratory tests show that the leaf springs used in commercial vehicle suspensions are actually complicated force-producing mechanisms. Illustrative test results for a walking-beam suspension are presented in Figure 16. The hysteresis loops in the data indicate that the leaf springs provide a considerable amount of damping (energy loss per cycle). This damping has a significant influence on the pitching and bouncing motions which take place during severe braking, especially if the brake torque is modulated by the driver or an anti-lock system.

The internal friction mechanisms which account for energy dissipation in leaf springs are difficult to model directly. For use in digital simulations, a mathematical technique for representing spring data has been developed. In this technique the spring is characterized by two envelopes, one for compression of the spring and the other for extension of the spring. The force versus deflection characteristics for deflection cycles between the envelopes are represented by exponential

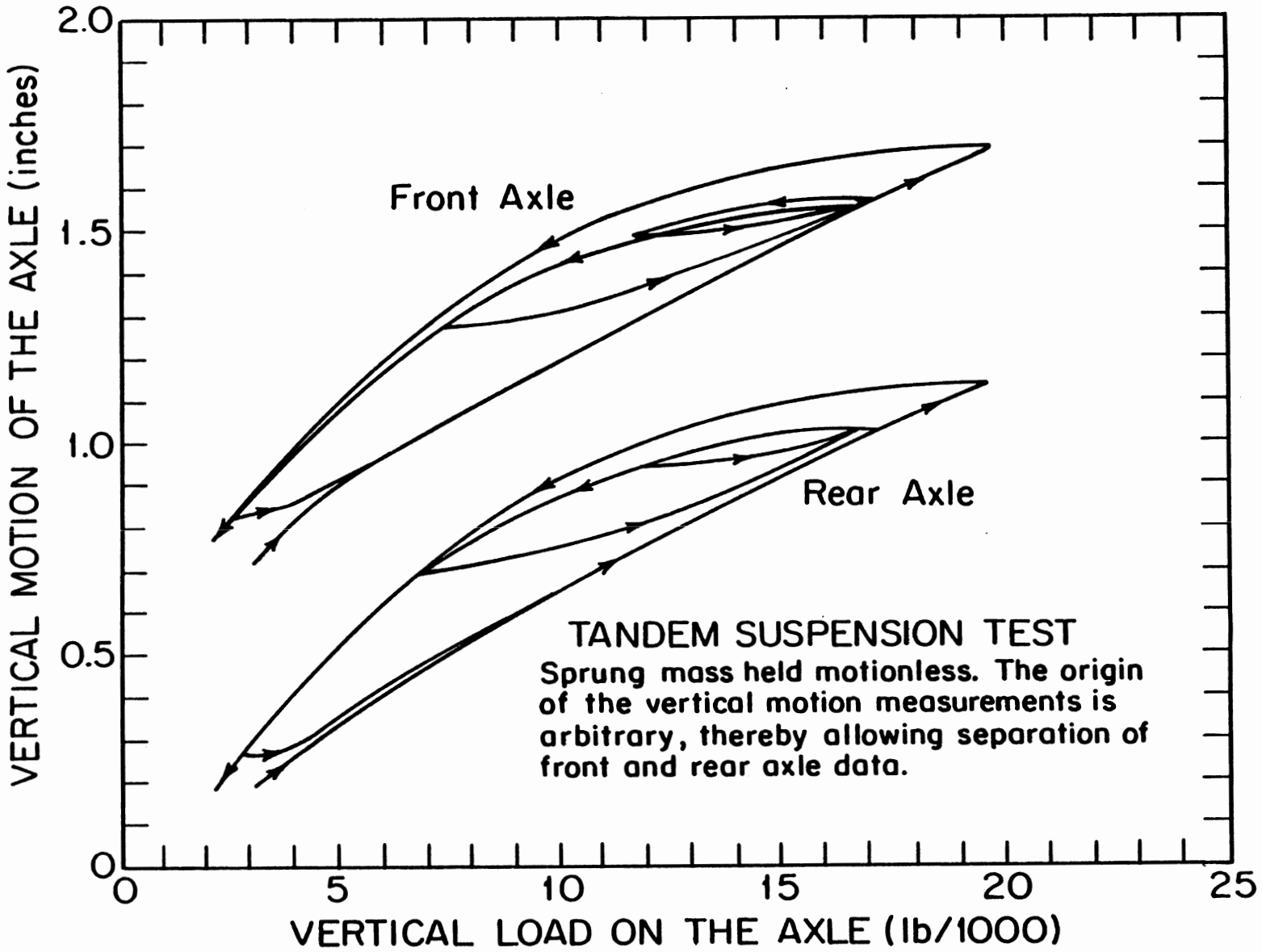

Figure 16. Leaf spring test results.

functions. To be more explicit, the force at time t_{i+1} is a function of (1) whether the deflection at time t_{i+1} is larger than the deflection at time t_i, (2) the force at time t_i, and (3) the value of the appropriate envelope function at time t_{i+1}. In mathematical terms, if

$$\delta(t_{i+1}) > \delta(t_i)$$

where δ is the compression of the spring (in the digital calculation procedure, a time step of length Δt occurs between t_i and t_{i+1}), then

$$F(t_{i+1}) = F_u(\delta t_{i+1}))\ (1 - e^{-|\Delta\delta|k_u}) + F(t_i)e^{-|\Delta\delta|k_u} \qquad (25)$$

where

F is the spring force,

$F_u(\cdot)$ is a table representing the upper envelope of the spring force data,

$\Delta\delta = \delta(t_{i+1}) - \delta(t_i)$, and

K_u = a spring parameter describing the exponential increase in spring force toward the upper envelope.

If

$$\delta(t_{i+1}) > \delta(t_i)$$

then

$$F(t_i+1) = F_\ell(\delta(t_{i+1}))\ (1 - e^{-|\Delta\delta|k_\ell}) + F(t_i)e^{-|\Delta\delta|k_\ell} \qquad (26)$$

where

$F_\ell(.)$ is a table representing the lower envelope, and

K_ℓ describes the exponential decrease toward the lower envelope.

(It is worth noting that equations 25 and 26 simply represent the step-function response of a first-order system. The technique of imbedding this type of calculation within the digital computation procedure has been used before in connection with the air system and wheel rotational dynamics. In this case, the independent variable is the deflection, δ, rather than time, even though δ is a function of time.)

The use of equations 25 and 26 provides an accurate description of the force characteristics of leaf springs. This type of representation has been employed in the simulation of severe pitching and bouncing motions excited by antilock braking.[8] These techniques should be useful for predicting and explaining some of the ride vibrations experienced by heavy trucks, although they have not previously been applied in that context. Clearly, the leaf-spring considerations just discussed are an example of a situation in which the state of the simulation art depends upon the state of the art of parameter measurement.

Automatic Braking Control (Antilock Systems)

The vehicle model and computer simulation were developed during the period of time in which vehicle manufacturers were equipping their products with antilock systems in order to

comply with government safety standards. In 1977 and 1978, nearly all newly produced commercial vehicles were equipped with antilock braking systems. Accordingly, a meaningful simulation during that time had to include models of appropriate antilock systems.

Various component manufacturers (primarily companies supplying brakes) developed antilock systems for commercial vehicles. These systems have differences in control logic and pressure modulation characteristics. To represent the operational characteristics of these diverse systems, a general-purpose model was developed.

The basic elements of antilock braking systems are illustrated in Figure 17. Separate models have been developed for representing the functions of the wheel sensors, control logic, and pressure modulators included in current systems.

In the simulation, the wheel-speed signal, ω, from the wheel dynamics sections of the main program is the input to the wheel-speed sensor, which produces a delayed version of the wheel-speed signal, ω_d. The wheel-speed signal is approximately differentiated to provide a measure of the angular acceleration of the wheel, $\dot{\omega}_d$. These signals (ω_d and $\dot{\omega}_d$) are inputs to the control logic section of the antilock system.

In some antilock systems other vehicle motion signals are transduced and used in controlling wheel speed. For example, one system employs a measured value of vehicle deceleration in its control laws. In addition, a feedback

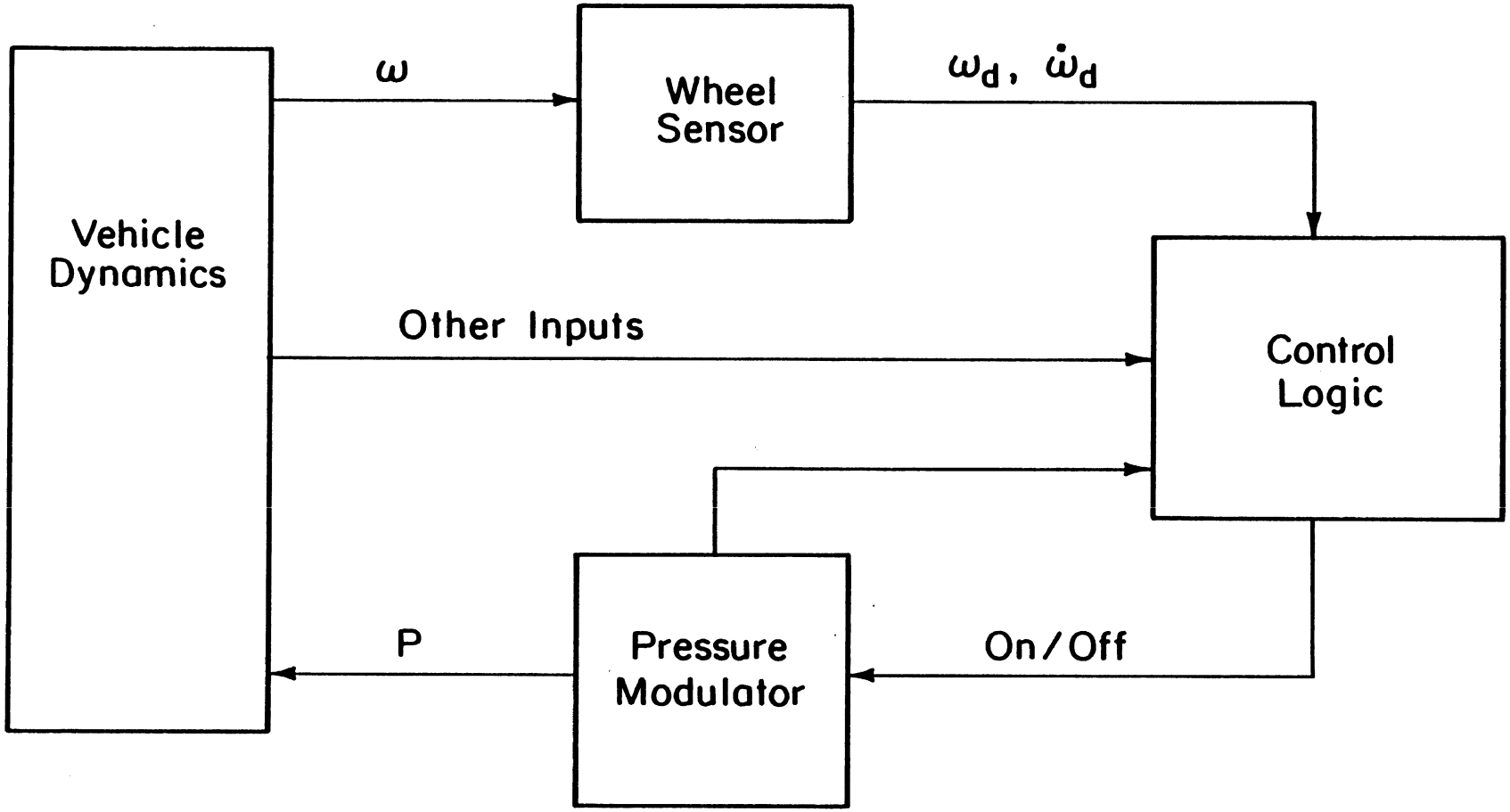

Figure 17. Antilock system diagram.

signal from the pressure modulator may be input to the control logic module if needed for representing a particular design. The control logic module sends an on/off signal to the solenoid in the pressure modulator. (If more than one solenoid is employed, the appropriate number of on/off signals is generated.) The pressure modulator returns pressure commands to the brake model in the main simulation.

Although there are fundamental differences in the control laws and pressure modulation methods used in various systems, all of the currently available systems use measured wheel speed as the primary variable for controlling braking. The main effect of the wheel sensor is similar to a phase shift between the actual wheel rate and the measured wheel rate. This phase shift is adequately represented by a transfer function of the form $(1/(\tau_{\omega}p+1))$ where τ_{ω} is the time constant of the first-order system and p is an operator denoting differentiation with respect to time.

To obtain an estimate of the angular acceleration of the wheel, further electronic processing of the measured wheel speed, ω_d, is performed. The transfer function $(p/(\tau_{\omega d}p+1))$ approximates the relationship between ω_d and $\dot{\omega}_d$. These relationships are summarized in Figure 18.

Several factors contributed to the decision to adopt a generalized approach for representing the control laws, logic, and modulation properties of antilock systems. First, a variety of differing systems is commercially available. Second, descriptions of these systems suitable for including in vehicle

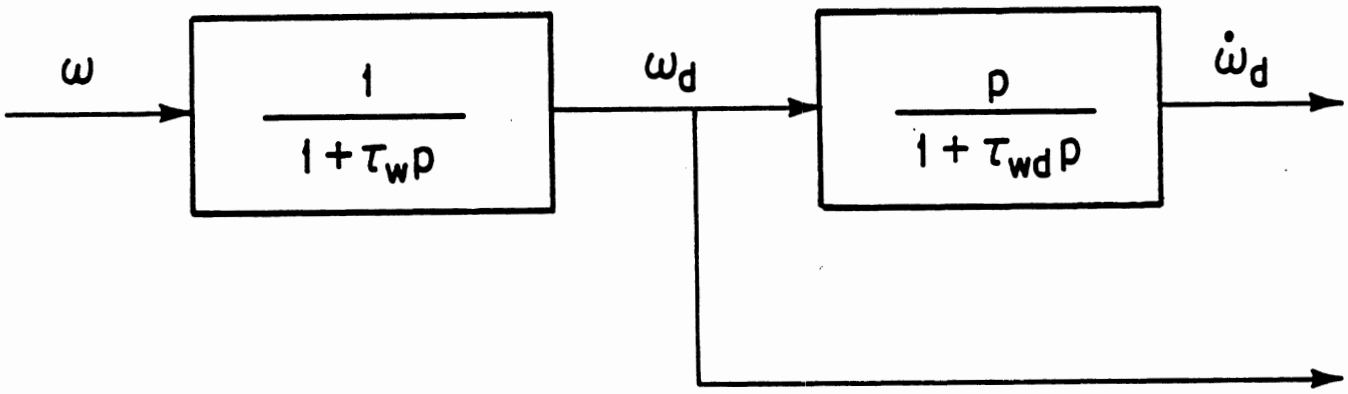

Figure 18. Wheel sensor module.

simulations are not easily obtained. And, finally, the original systems were subject to modification or major change as improved versions and new designs were developed. Consequently, the simulation model may be viewed as a tool for designing antilock systems. Nevertheless, the model has not been used to design a system; it has been used to develop functional representations of existing systems.

The "model" of the control module consists of (1) a "dictionary" of variables that can be used in representing various systems, (2) general algebraic expressions (inequalities) that can be programmed to represent a particular system, (3) logical operators that generate signals based on the status of the programmed inequalities, (4) adaptive coefficients for adjusting the values of the parameters in the inequalities, and (5) an assortment of schemes for representing time-ramps and sequential logic.

Figure 19 contains some examples of the types of quantities which might be used in the control logic. Pertinent values from the time histories of wheel speed, acceleration, and brake line pressure are indicated in the figure. Signals corresponding to the timing of certain events are illustrated by the quantities, TON2 and TON1. The dictionary contains a listing of approximately 60 pertinent variables and quantities providing the user of the simulation a means for programming the control relationships representing a specific type of antilock system. See reference [6] (pp. 108-175 and Appendix E) for detailed information on the general-

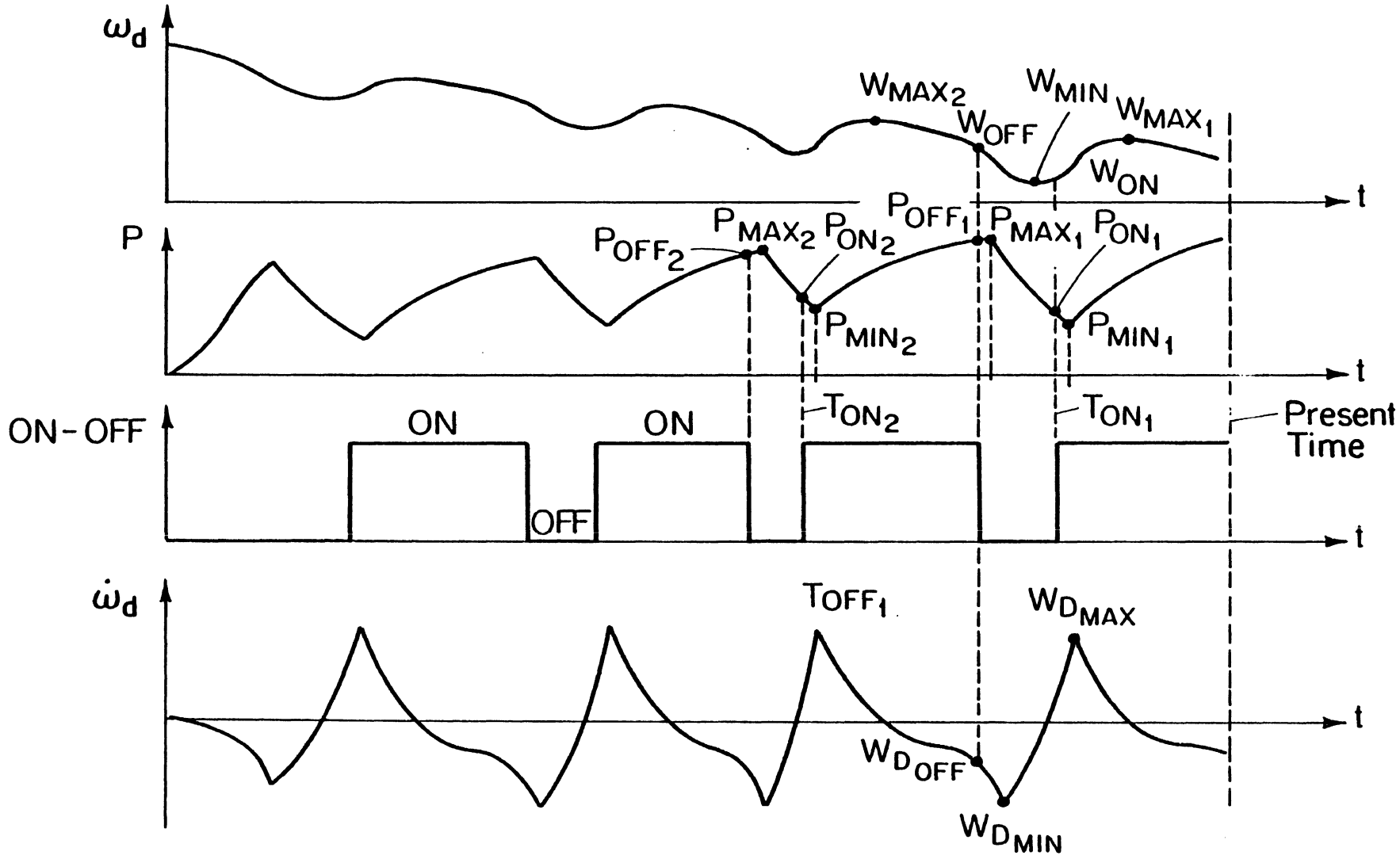

Figure 19. Examples of quantities included in the dictionary.

purpose model. An example of a set of control laws derived from laboratory tests of a particular system is given in Chapter 3.

Some of the early antilock systems used relatively simple valves for modulating pressure. In these systems the brake pressure increased at nearly an exponential rate with a time constant typical of a first-order system. The pressure (when "dumped" to prevent wheel lock) decreased at a much faster rate than it increased. Other systems were based on (1) more complicated valves, (2) means for modulating the action of the solenoid, or (3) more than one solenoid in the pressure modulator. Pneumatic logic was employed in later systems.

The features of the various types of pressure modulators have been included in the general-purpose model using the same techniques as those employed in representing the control laws. The user of the simulation can select parameters representing (1) time lags between the time an "ON" or "OFF" is generated and when the pressure begins to change, (2) programmable exponential and/or linear pressure rise-and-fall characteristics, and (3) relatively complex pressure-modulator activity, including designs involving pneumatic logic or pulse-width modulation.

Clearly, the inclusion of antilock systems increased the difficulty and complexity of the simulation task. More importantly, the timing of various events took on significance in controlling braking effort. Time lags on the order of one or two hundredths of a second became important in predicting vehicle braking performance.

Footnotes to Chapter 2

[1]Recent court rulings[3] have resulted in the withdrawal of government regulations requiring the use of antilock systems to meet the requirements of the rules until the reliability of the antilock system is demonstrated.[12]

[2]The mathematical form of the semi-empirical model developed for generating braking force as a function of vertical load, longitudinal slip, and forward velocity is similar to semi-empirical models developed for analyzing lateral force except that longitudinal slip is used in place of the slip angle of the tire.[20]

CHAPTER 3

DEVICES FOR MEASURING THE PROPERTIES OF VEHICLE COMPONENTS

The discussion of the computerized model presented in Chapter 2 indicates that specialized devices have been developed for measuring the mechanical properties of the brakes, tires, suspensions, and antilock systems used on heavy vehicles. The computerized model cannot be successfully employed in simulating a particular vehicle unless the pertinent mechanical properties of that vehicle are accurately represented. Obviously, development of a useful simulation methodology requires the development of practical means for acquiring the needed parametric data.

Moreover, many vehicle problems can be diagnosed and corrected on the basis of parametric or component measurements alone. Given knowledge of how particular components perform and how these components contribute to overall stopping performance, the direction for improvement in component design may be apparent without performing simulation exercises. Under the circumstances just described, simulation can be used to make quantitative estimates of the improvement in stopping performance obtainable through proposed changes in the mechanical properties of the vehicle. In this way, empirical data on vehicle components and systems provide the

foundation for evaluating future improvements in vehicle performance.

3.1 A Device for Measuring the Braking Traction of Truck and Bus Tires

An over-the-road dynamometer for measuring the shear force properties of truck tires has been developed at HSRI.[27] As illustrated in Figure 20, this device consists of a tractor pulling a unique semitrailer constructed from pipe and plate sections. The test wheel used in making longitudinal force measurements is situated on the centerline of the trailer, approximately at the longitudinal location of the center of gravity of the trailer.

Figure 21 shows the arrangement of (1) the parallel arm suspension employed to keep the test tire vertical, (2) the load cell utilized for measuring longitudinal force, vertical load, and braking torque, and (3) the air spring used for applying vertical load. The parallelogram linkage suspension provides kinematic isolation between (a) the vertical load and braking torque applied to the test wheel, and (b) the resulting shear forces and moments reacted by the suspension. The load cell is a serial element in mounting the wheel. The mounting configuration and flexure design of the load cell have been given special consideration so that this cantilevered multi-component transducer provides universally interpretable outputs. The air spring, in conjunction with a precision regulator, provides a straightforward means for selecting vertical load. In addition, the air spring is a

relatively "soft," virtually frictionless device that enhances the quality of the vertical load condition by partially isolating the vibrations of the foundation vehicle from the test wheel. The test fixture, including a 10 x 20 truck tire and a 20 x 7.50 disc wheel rim, has a tare weight of 1850 lbs. This design provides data of more than adequate quality while meeting the obvious needs of strength, stiffness, and economy of construction.

Additional features of the test trailer include limit stops for safety in case of a blowout of the test tire and a hydraulic lift system to aid in mounting tires. Nominal pitch and bounce trim of the test wheel is maintained through the use of self-leveling air suspensions on both the trailer and the tractor rear tandem.

The test trailer can mount any tire in the 20-inch rim size or above, which is less than 46 inches in free diameter and 18 inches in maximum section width. The trailer can apply a maximum load of 20,000 lbs. to the test tire, although brake torque limitations prevent the lock-up of tires on high friction surfaces at loads exceeding approximately 15,500 lbs.

For longitudinal force measurements, the tractor is strictly a support vehicle. (For lateral force measurements, outboard wheels are mounted near the center of the tractor. See Figure 20.) The tractor/service vehicle provides the following specific capabilities.

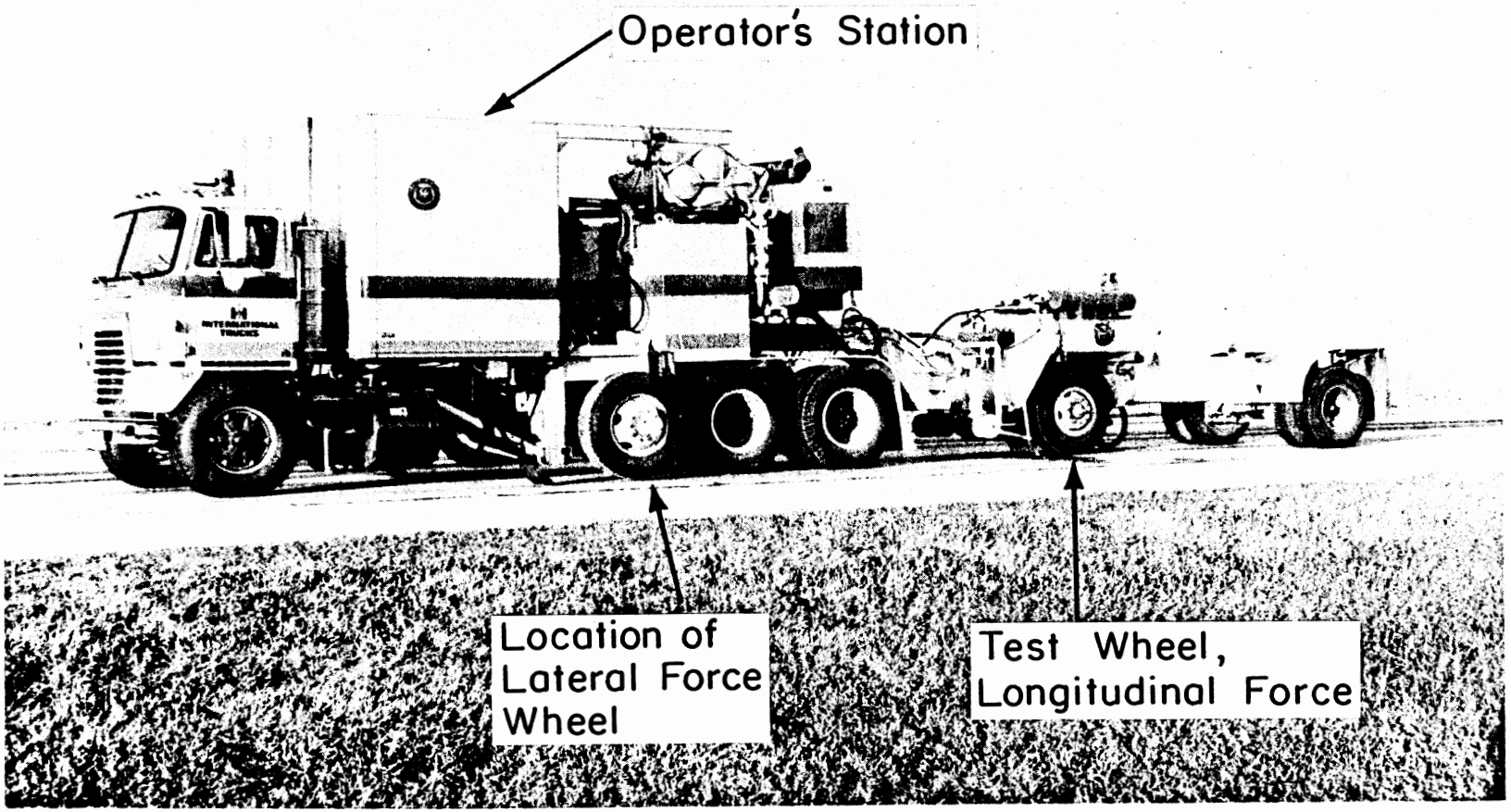

Figure 20. The HSRI Mobile Truck Tire Dynamometer, consisting of service tractor and longitudinal traction measurement trailer.

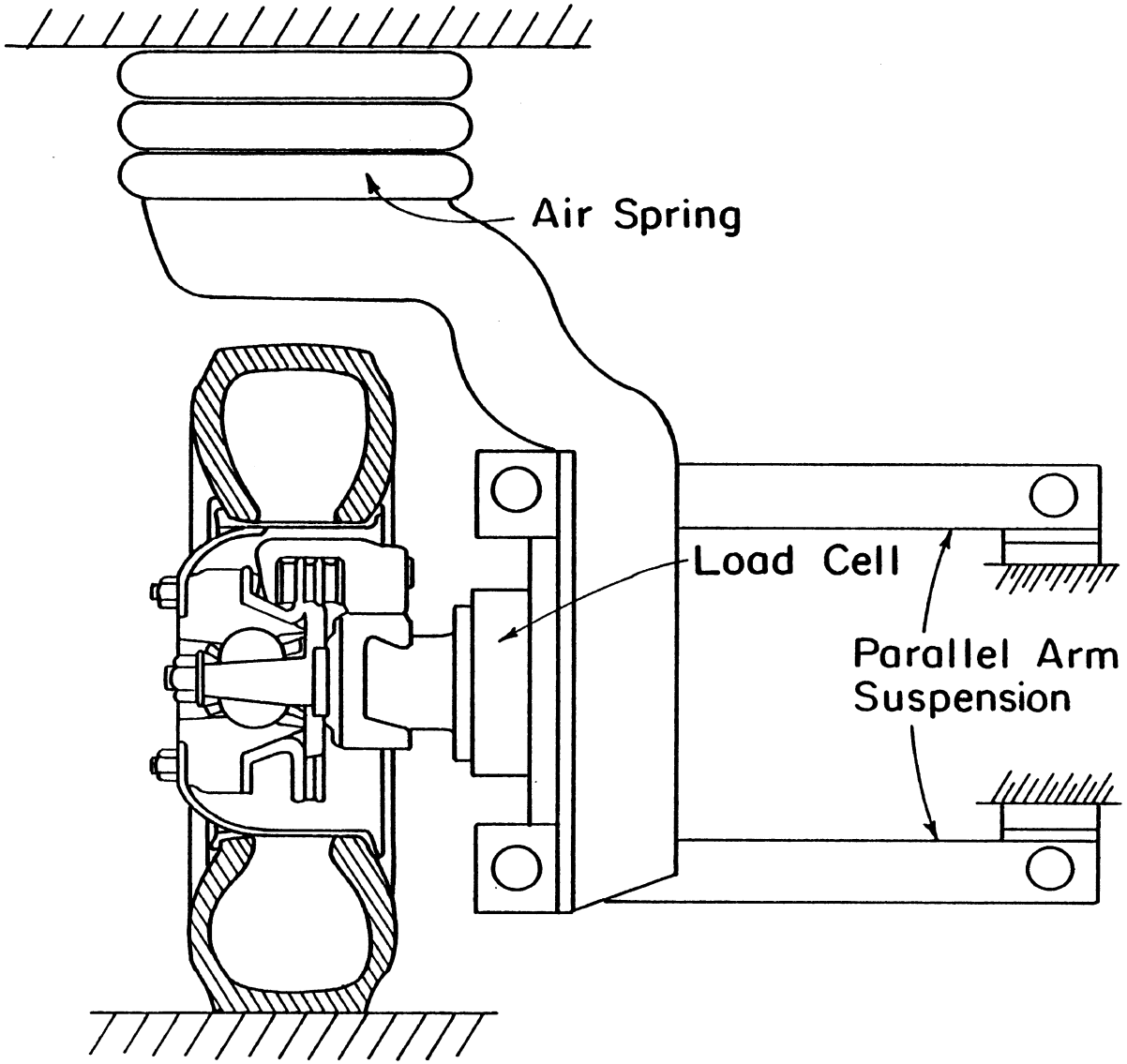

Figure 21. Test wheel structure.

Basic Tractor Configuration

(The tractor vehicle was a gift to The University of Michigan from the International Harvester Corp.)

International Harvester Model C04070A (cab-over) tractor with 213-inch wheel base and an IH air-tandem rear suspension. GVW is 50,000 lbs. The engine is a GM diesel #8V-71N (338 Hp. at 2400 rpm). The vehicle's transmission is a Fuller "Road Ranger" w/overdrive (13 speeds). The extra-long truck frame is stiffened with a nestled C-beam, consisting of 3 elements, and is outfitted with a Holland extra-heavy-duty fifth-wheel hitch.

Hydraulic Power -	5 gallons/minute flow rate at 2000 psi from a pressure-compensated piston pump
Hydraulic Accumulator -	1 gallon nominal volume
Pneumatic Power -	delivery rate of 40 ft^3/min at 120 psi from a single-stage compressor
Air Storage Tank -	6 cubic feet nominal volume
Electrical Power -	diesel-driven 30-kilowatt generator, supplying 110 VAC, single phase and 208 VAC, three-phase power
Electrical Distribution -	all electrical power switching is done through a single panel providing:

	1) the selection of either on-board power generation or a shunt connection to available garage power source for setup and indoor calibration 2) main current circuit breakers 3) motor start circuits 4) remote generator start circuit 5) instrument power circuit switching 6) generator voltage monitoring
Water Delivery - (for pavement wetting)	200 gallons/minute discharge from an impeller-type pump (provides .040-inch water film thickness over an 18-inch-wide swath at a test speed of 60 mph)
Water Storage Tank -	720-gallon capacity

In addition to carrying the equipment needed to provide the services listed above, the tractor supports a special module containing the operator's station (see Figure 20). This module contains a data-acquisition laboratory with five channels of signal conditioning for strain-gauge transducers, two channels of thermocouple conditioning, and five additional channels for recording signals from potentiometers or tachometers (see Figure 22). The test data are recorded in analog form on FM magnetic tape. A six-channel pen-chart recorder is used to monitor the data as they are being gathered.

The data are collected under realistic operating conditions, simulating an actual time history of wheel lockup. A typical test takes less than 1.0 second as illustrated in Figure 23. A special circuit controls the lockup cycle and

releases the brake quickly once lockup has occurred. This procedure provides meaningful data without flat-spotting or overheating the tire.

A typical recording of raw data from a single lockup cycle is presented in Figure 24. A standard procedure has been to apply the basic lockup cycle five or six times in succession at each condition of velocity and vertical load. These data are then digitally processed and averaged to make tables and graphs of normalized longitudinal force (F_x/F_z) versus slip. In these data, slip is calculated from the wheel angular velocity signal, ω, using the following relationship:

$$s_i = \left(\frac{\omega_o - \omega_i}{\omega_o}\right) 100$$

where

s_i = longitudinal slip for the i^{th} digital increment after the brake torque is applied

ω_o = the wheel speed just prior to brake application

ω_i = the instantaneous value of wheel speed at the i^{th} increment

A sample output from the data-processing procedure is presented in Figure 25.

The longitudinal force characteristics of truck tires are dependent upon vertical load and velocity in addition to longitudinal slip. In order to "map out" a tire's braking traction, results similar to those in Figure 25 are obtained at various loads and velocities. To describe the characteristics of a particular tire, data at various loads and velocities may be

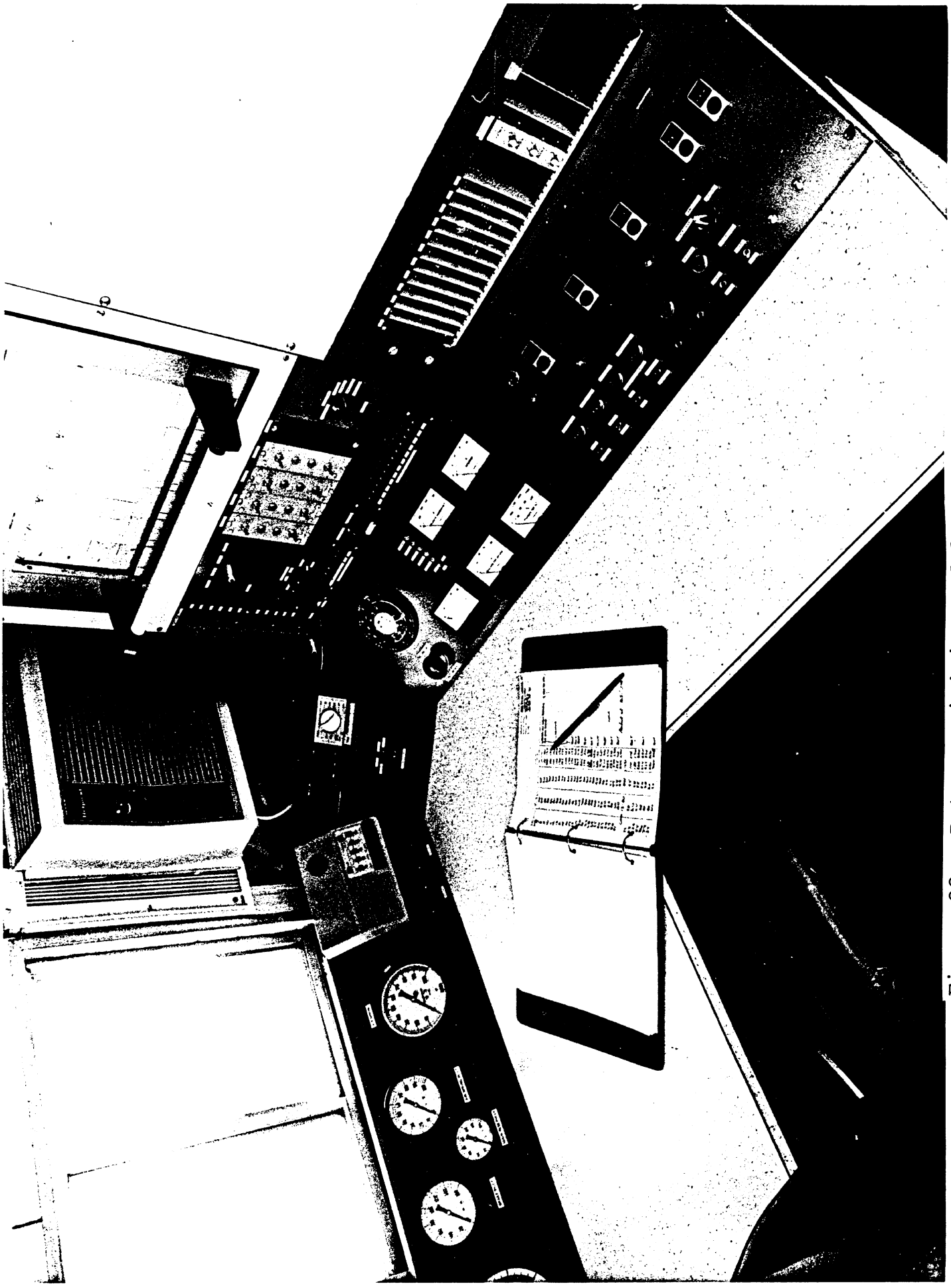

Figure 22. Data acquisition module on tractor.

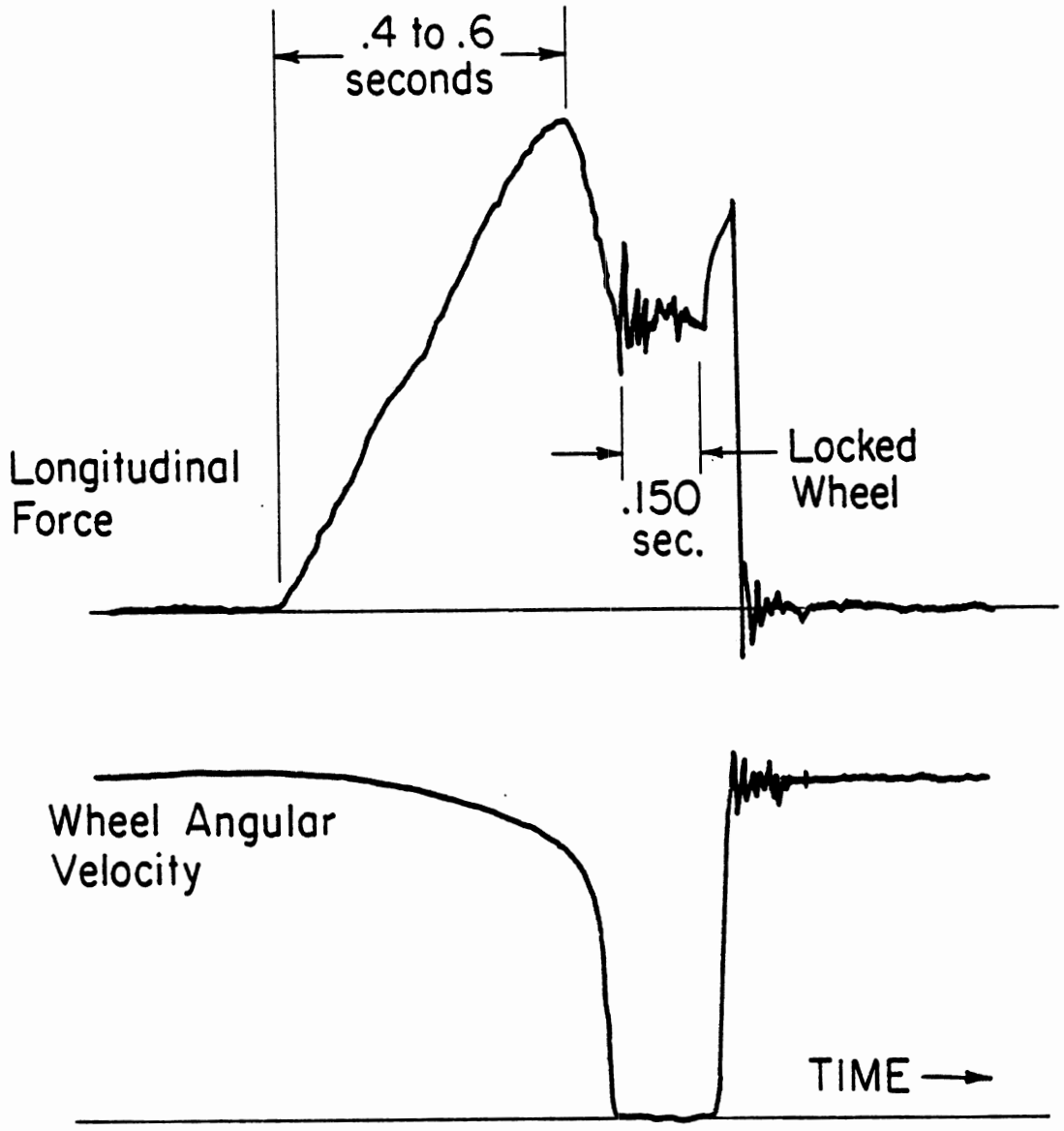

Figure 23. Approximate time scale of the basic "lockup cycle."

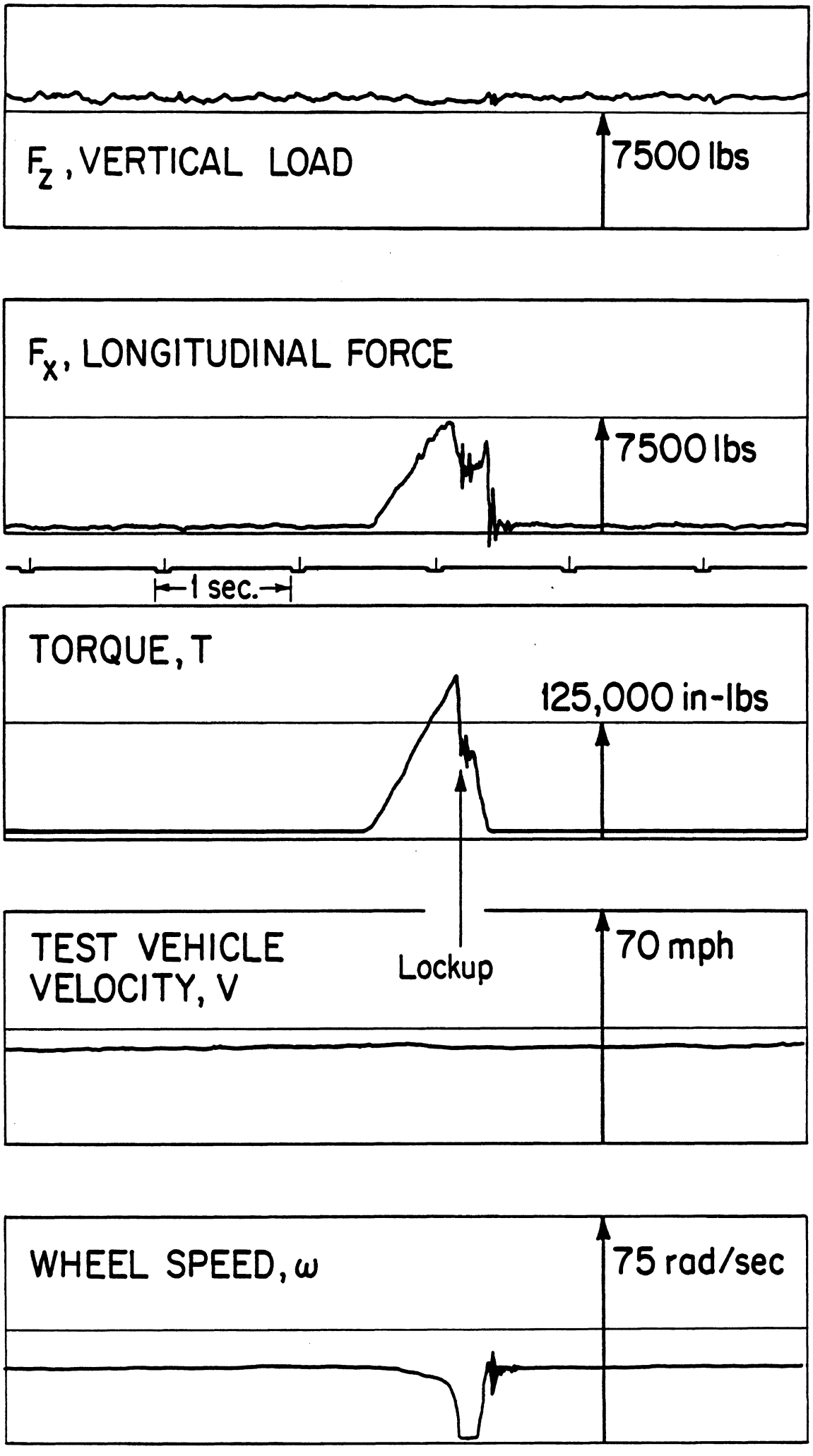

Figure 24. Time histories describing a "lockup cycle."

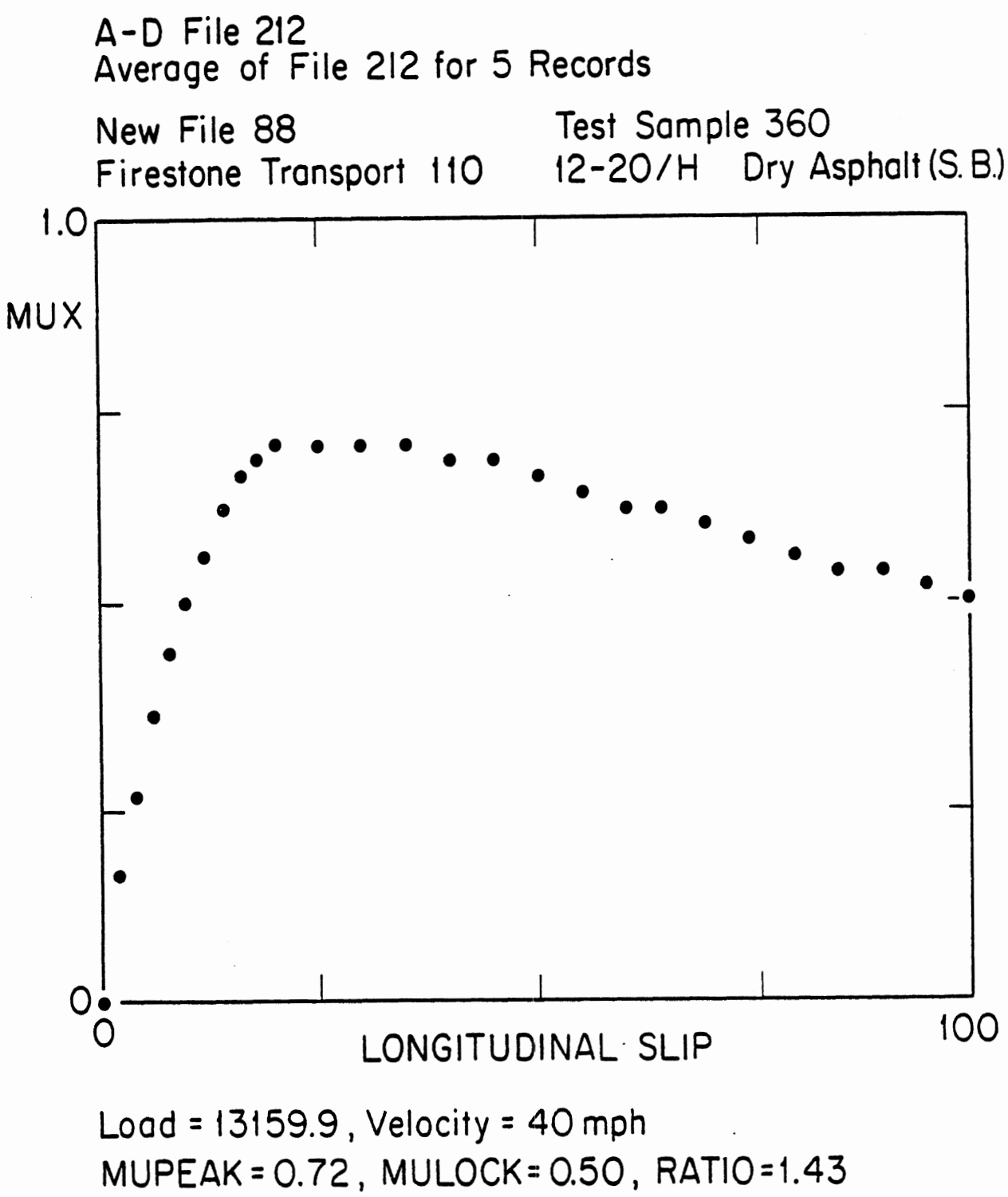

Figure 25. Processed Data, F_x/F_z vs. slip (MUX = F_x/F_z)

combined to make families of curves, as illustrated in Figure 26.

To date, numerous studies of truck-tire braking traction have been made.[22, 23, 24, 27, 28, 29] Tires of differing sizes have been tested. Tests have been performed on a variety of road surfaces. The influences of tire construction (radial or bias ply) and tread type (highway rib or lug) have been examined on wet and dry pavements. Results from longitudinal force tests have been used in comparative studies supported by both industry and government.

In summary, the mobile dynamometer is an elegant device that is available for making sophisticated studies of the shear force properties of truck tires. The machine has the following characteristics and specifications with respect to longitudinal force measurements:

Vertical Load Range:

1850 lbs (approximate tare weight) to 15,500 lbs (with provision to go to 20,000 lbs)

Velocity Range:

3 mph to 70 mph (maximum speed may be limited by the distance provided at the test area)

Longitudinal Force Range:

0 to 20,000 lbs

Slip Range:

0 to 100% (free-rolling to locked wheel)

Figure 26. Typical load and velocity influences on the F_x/F_z versus slip behavior of a 10.00x20/F tire.

Transducer Accuracy Tolerances:

	Accuracy in Percent of Reading	Applicable Range
Longitudinal force	± 2%	to 20,00 lbs
Vertical load	± 1%	to 20,000 lbs
Brake torque	± 1%	to 250,000 in/lbs

Slip Measurement Estimated Maximum Error:

-less than ± 2% slip at the peak of the -slip curve for velocities above 25 mph

-below 25 mph the maximum error in slip at the peak normalized force increases from ± 2% to approximately ± 6.5% at 3 mph

Repeatability of Test Results:

(The standard deviations given here depend on the homogeneity of the test surface in addition to properties of the test device and the test procedures. The results quoted are from tire tests at three different test areas.)[22]

The maximum standard deviation of the maximum normalized force: less than 0.02 for peak normalized forces in the range from 0.85 to 0.95.

The maximum standard deviation of the locked-wheel normalized force: less than 0.02 for locked-wheel (100% slip) forces in the range from 0.55 to 0.65.

3.2 Brake-Testing Devices

Special load cells called "torque-wheels" have been installed on heavy trucks making braking tests.[13] These devices provide direct measurement of the torque being applied to the wheel during test conditions defined by brake-line

pressure and the rotational velocity of the drum. In using a simulation to study and analyze the details of the performance of a particular vehicle in a specific test, the data obtained from torque wheels are invaluable in characterizing the hysteresis, fade, and effectiveness of individual brakes during a given test. However, torque-wheel data are not usually available for predictive studies and, furthermore, that data may represent the idiosyncrasies of a particular brake installation rather than the generic properties of a given type of brake.

Usually, data from tests using an inertia dynamometer[16] are available from the brake manufacturer. Quite often inertia dynamometer data are presented in the form of the average torque for "spin-down" stops from specified initial rotational velocities of the flywheel. In the past, these data have served to define average torque versus pressure characteristics and to verify that a brake can absorb a given amount of energy without fading excessively.

For purposes of conducting simulations of vehicle stopping performance, the averaged results from inertia dynamometer tests hide the instantaneous information desired, but the time histories of torque, pressure, and wheel speed generated during inertia dynamometer testing can be processed to yield an empirical function describing the effectiveness of the brake (see the discussions associated with Figures 5 and 6 in Chapter 2).

The development of efficient, programmable digital equipment suitable for handling the raw data from inertia dynamometers makes it reasonable to consider empirically based representations of individual brakes. Although an initial research project, directed toward developing an empirical model of the brake, has been completed,[16] the proposed methodology has not been sufficiently exercised for a variety of different types of brakes over wide ranges of operating conditions. Until sufficient research is performed to develop a generally useful form for representing brake data, much of the information included in data from inertia dynamometers cannot be used in predicting, analyzing, and understanding vehicle braking performance.

In addition to acquiring and studying brake test results from torque wheels and inertia dynamometers, an approximately constant-speed brake dynamometer has been developed at HSRI.[30] This device was created through a relatively simple extension of the capabilities of the mobile truck-tire dynamometer. Specifically, the spindle supporting the test wheel mounted on the semitrailer of the mobile dynamometer has been designed to accommodate the installation of virtually all heavy truck air brakes (and some heavy-vehicle hydraulic brakes).[31]

All of the needed instrumentation for measuring torque, wheel speed, temperature, and air pressure is available on the mobile dynamometer. To prepare for testing a particular brake, an adapter (spacer) is fabricated to fit the brake into the existing wheel and hub assembly, thereby converting the truck-tire dynamometer into a mobile brake dynamometer.

The mobile brake dynamometer provides a different type of testing capability from that provided by a conventional inertia dynamometer. First, the mobile dynamometer can be used to study the amount of hysteresis present when the brake pressure is run through a cycle typical of antilock braking. On an inertia dynamometer, wheel speed cannot change rapidly due to the large inertia of the flywheel. Obviously, the brake cannot lock up rapidly. However, a brake being tested on the mobile dynamometer can lock up or approach lockup, and hysteretic lags between brake torque and brake-line pressure can be studied.[30] For example, the results presented in Chapter 2 (Figure 7) were obtained using the mobile dynamometer.

The primary operational difference between the mobile and inertia dynamometers is that the mobile dynamometer is a constant rotational speed device rather than a spin-down tester. If the tire-road interface can supply the necessary force to prevent wheel lock, wheel speed quickly adjusts to the applied brake torque so that the longitudinal slip of the tire is appropriate for generating the force necessary for a torque balance on the test wheel. The time histories presented in Figure 27 illustrate the nature of the pressure, torque, and wheel speed (spin velocity) waveforms obtained during a typical test using the mobile dynamometer. (The waveforms shown in Figure 27 may be compared with corresponding waveforms shown in Figure 5 of Chapter 2 to provide a graphic idea of the differences between tests performed with inertia and mobile dynamometers.) As indicated in

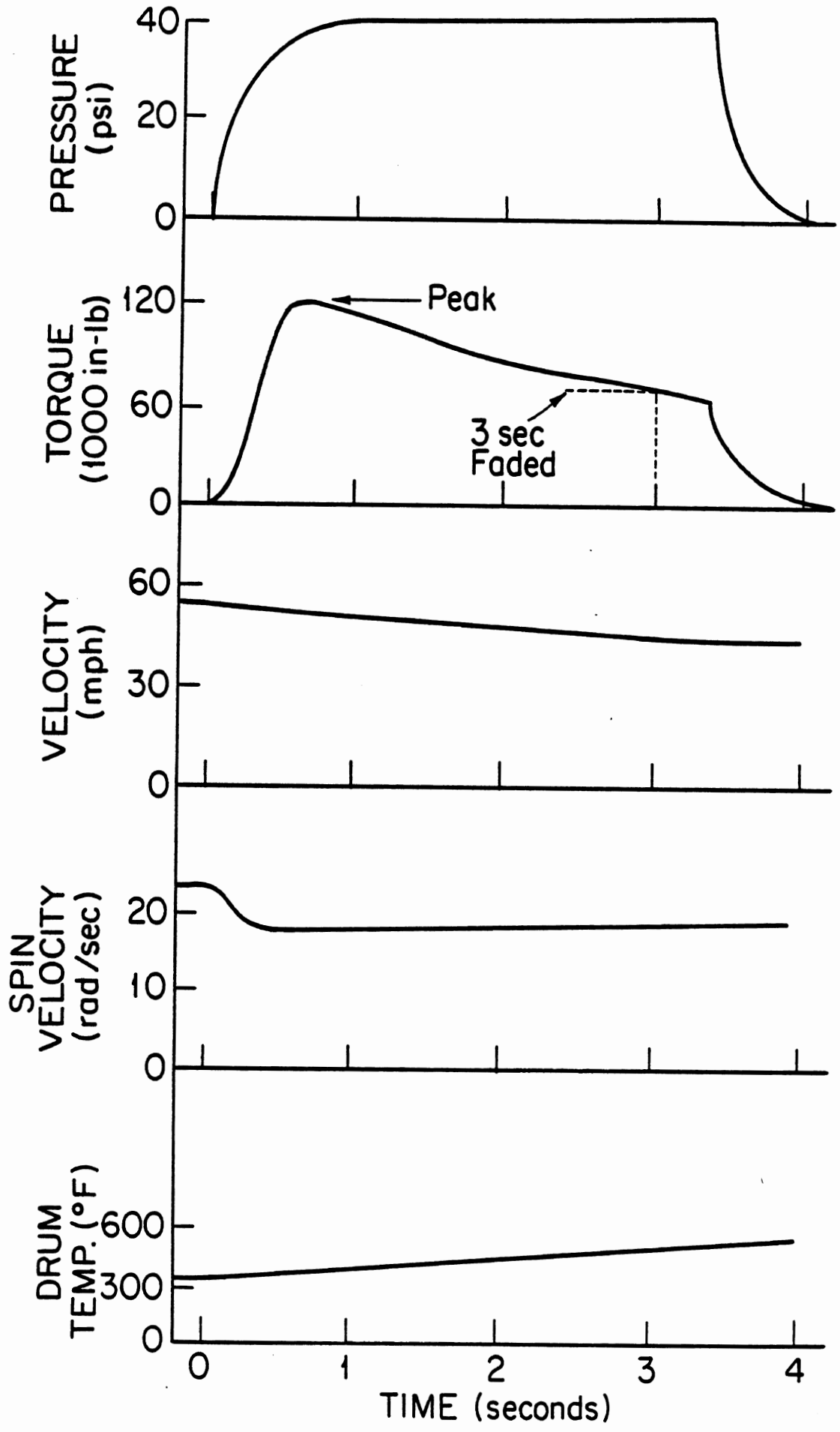

Figure 27. Typical Waveforms from the Mobile Brake Dynamometer.

Figure 27, wheel speed is nearly constant after an initial transient. Hence, the mobile dynamometer can be used in studies in which the influences of changes in velocity are not present during an individual test.

The mobile dynamometer has been employed in examining the phenomenon of brake fade in heavy vehicles.[30] Burnishing procedures suitable for conditioning brake linings and drums have been developed. The machine has been applied in studies of the torque effectiveness of dual-wedge and S-cam brakes. For example, Figure 28 is a carpet plot showing the influence of pressure and test velocity on the maximum torque and the torque three seconds after the initiation of braking for a standard dual-wedge brake (15 in. diameter, 7 in.-wide linings, 12 deg. wedge angles, type-12 air chambers, cast-iron drum, ABB-693-551D linings). Although data of the type shown in Figure 28 have received a significant amount of attention in research on motortruck braking, a fundamental understanding of the phenomenon of in-stop fade and recovery has not been acquired. Apparently, the model development cycle consisting of component measurement, model refinement, and additional computer simulation should be reiterated using new hypotheses concerning the important variables involved in determining in-stop fade.

An additional piece of laboratory equipment used in the study of the air chambers installed in brake systems is shown in Figure 29. This apparatus is used to measure actuation force as a function of chamber pressure and push-rod stroke.

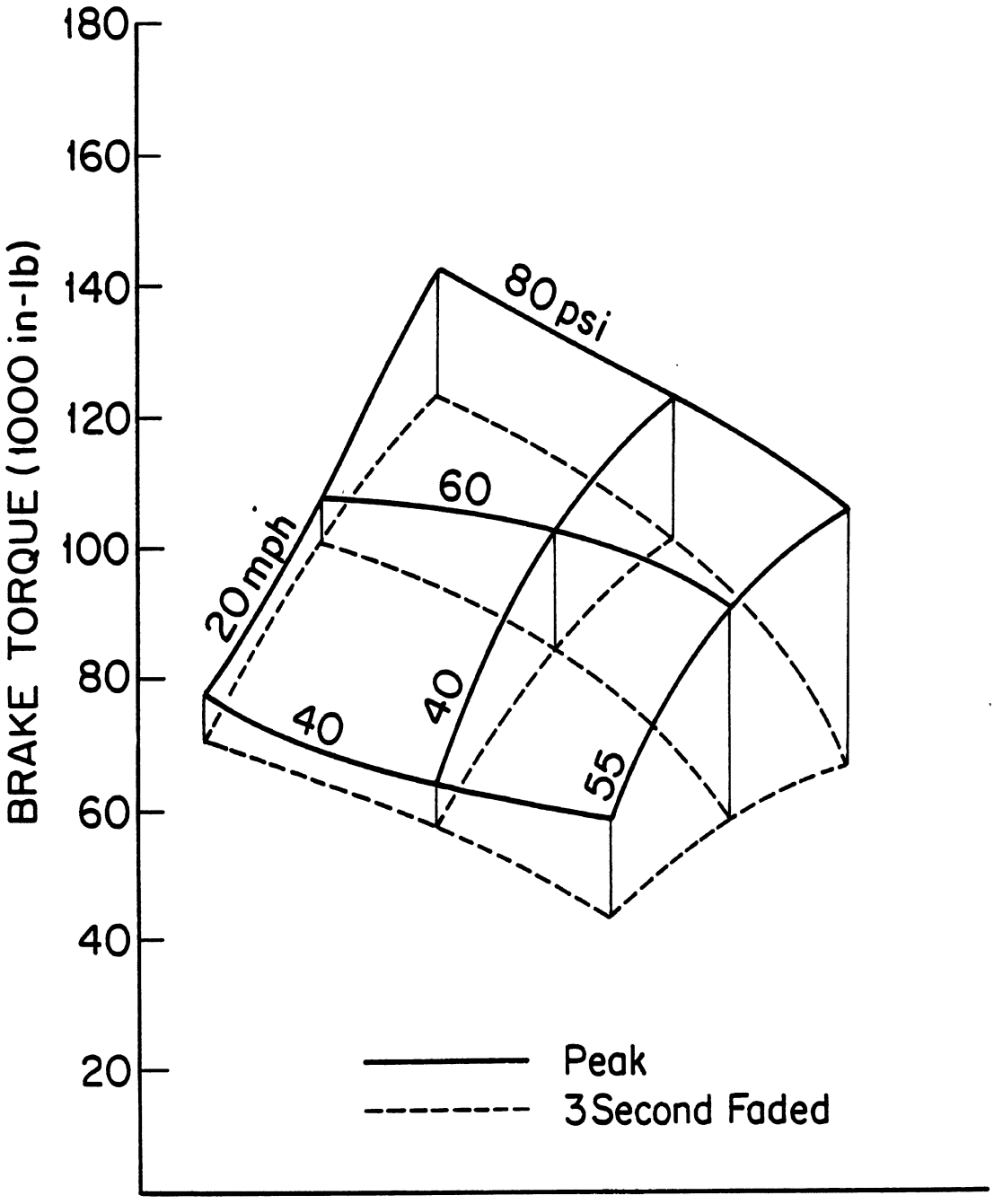

Figure 28. Peak and Faded Torque for a Dual-Wedge Brake.

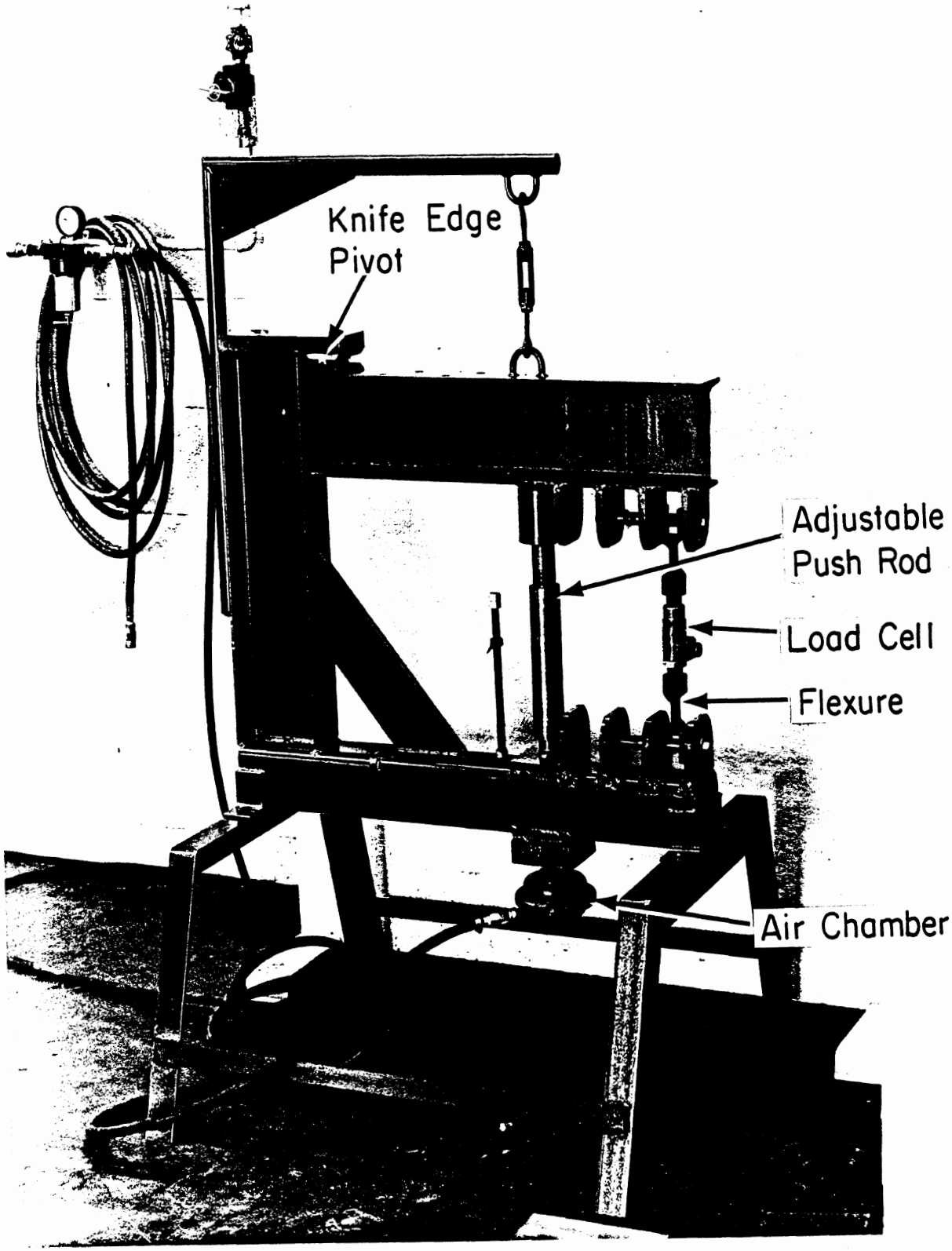

Figure 29. Air Chamber Test Machine.

The length of the vertical push rod is adjusted to obtain different amounts of stroke. As illustrated by the test results shown in Figure 30, the actuation force falls off rapidly at large stroke (above 1.7 in. in this case). Typically, a brake using this air chamber would be adjusted for about 1 in. of stroke at 100 psi. However, careful attention must be paid to the stroke involved in brake testing[15, 16] (and, of course, in vehicle braking).

The net conclusion to be drawn from this discussion of brake-testing devices and from the discussion of brake modeling presented in Chapter 2 is that the data representing brake performance should be carefully examined as to accuracy, generality, and relevance to the vehicle conditions to be studied. Since the performance of a particular brake depends upon esoteric factors such as its work history, lining friction variability, and installation or maintenance variables (e.g., stroke), evalutions of predictions of vehicle braking performance should be tempered with an appreciation of the influence of esoteric factors on the brake data used in the computerized model.

3.3 Measurement of the Properties of Air Control Systems

The measurement of antilock system properties has been the emphasis of the air system research performed at HSRI. The measurement of antilock system properties is necessary because (1) descriptions of antilock systems in terms suitable for computer simulation are not generally available,

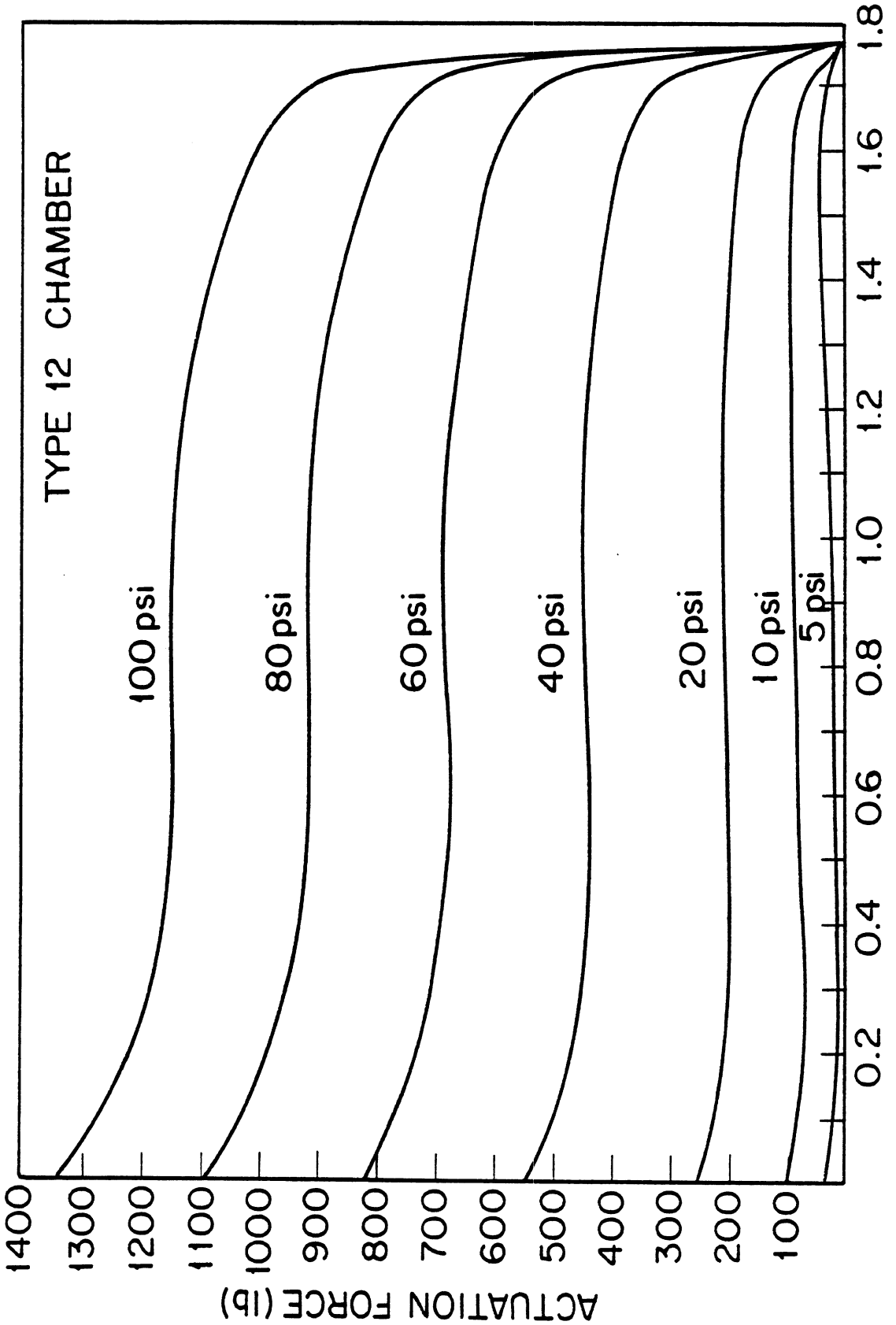

Figure 30. Brake Chamber Characteristics.

and (2) detailed data concerning the function of particular systems are proprietary.

HSRI employs a unique analog computation technique for determining the parameters defining antilock systems. In this technique, the air system and antilock modules of a vehicle are operated in real time using an analog computer model of the vehicle. By examining the "braking performance" of the simulated system, antilock and air system parameters are derived. This section discusses details of this method for developing a model of a given antilock system.

Although the logical rules describing how a particular system operates are to be measured in the laboratory, it helps considerably to have an idea of the basic principles used in the system under study. Almost all currently available systems generate a special ramp function (or its equivalent) when an impending wheel lockup is detected (i.e., when the wheel angular acceleration times the tire radius exceeds approximately one "g" of deceleration). The form of this "reference ramp" is shown in Figure 31. A new reference ramp is started at the initiation of each cycle of antilock braking. The reference ramp is used in deciding upon the times to release and reapply the brakes during antilock braking.

Current antilock designs differ primarily in the methods of pressure modulation employed. Significantly different wheel-speed cycling behavior is obtained from systems using single/double solenoid air valves, pneumatic logic, or high-frequency pulse rate solenoid modulation.[32] In addition, the rate of pressure increase is controlled in some systems.

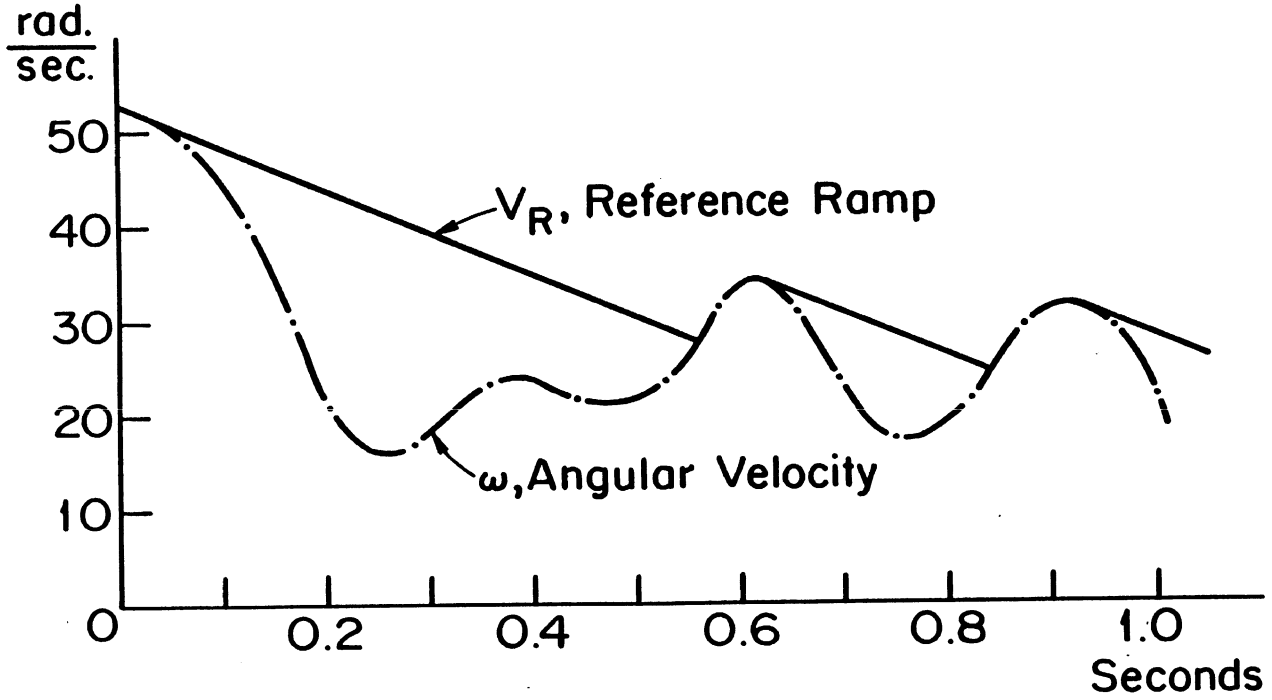

Figure 31. A typical Reference Ramp.

The pressure level sought by the modulator is adjusted in certain systems. Even though the pressure rise-and-fall characteristics are recognizable from measured wave forms, it obviously helps to know what features to look for.

The form of a basic test arrangement, including a truck and an analog circuit, is illustrated in the upper part of Figure 32. In this arrangement a frequency-modulated pulse train simulating the output of the wheel-speed sensor is wired to the input of the antilock control (computer) module. A pressure transducer is installed in a brake chamber on the axle whose braking is being studied. The output of the pressure transducer is fed into the analog computer. The analog computer simulates the brake, wheel dynamics, tire shear force characteristics, the deceleration of the vehicle, and the wheel-speed sensor. A variety of vehicles and tire-road friction conditions is simulated by changing potentiometer settings in the analog computer circuit.

Time histories of braking conditions during a simulated stop are obtained from the analog computer (see Figures 33 and 34 for examples of measured time histories). Parameters and characteristics related to the antilock logic scheme are deduced from the measured time histories. A set of rules (control laws) for predicting wheel lock and reselection of brake pressure is assumed, exercised, and compared with laboratory results. The synthesized rules are adjusted until reasonable agreement between measured and simulated results is obtained.

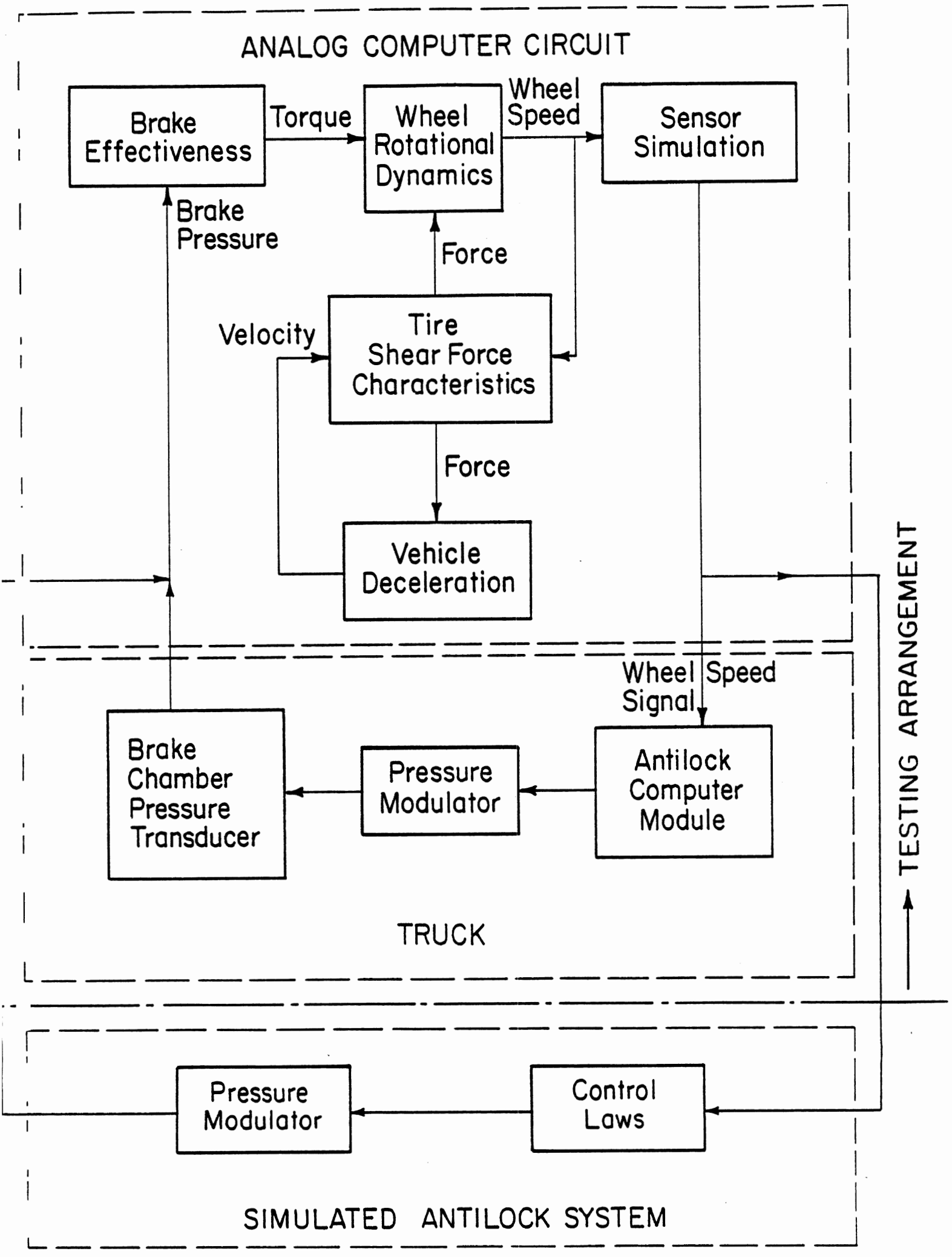

Figure 32. Setup For Deducing Antilock System Properties.

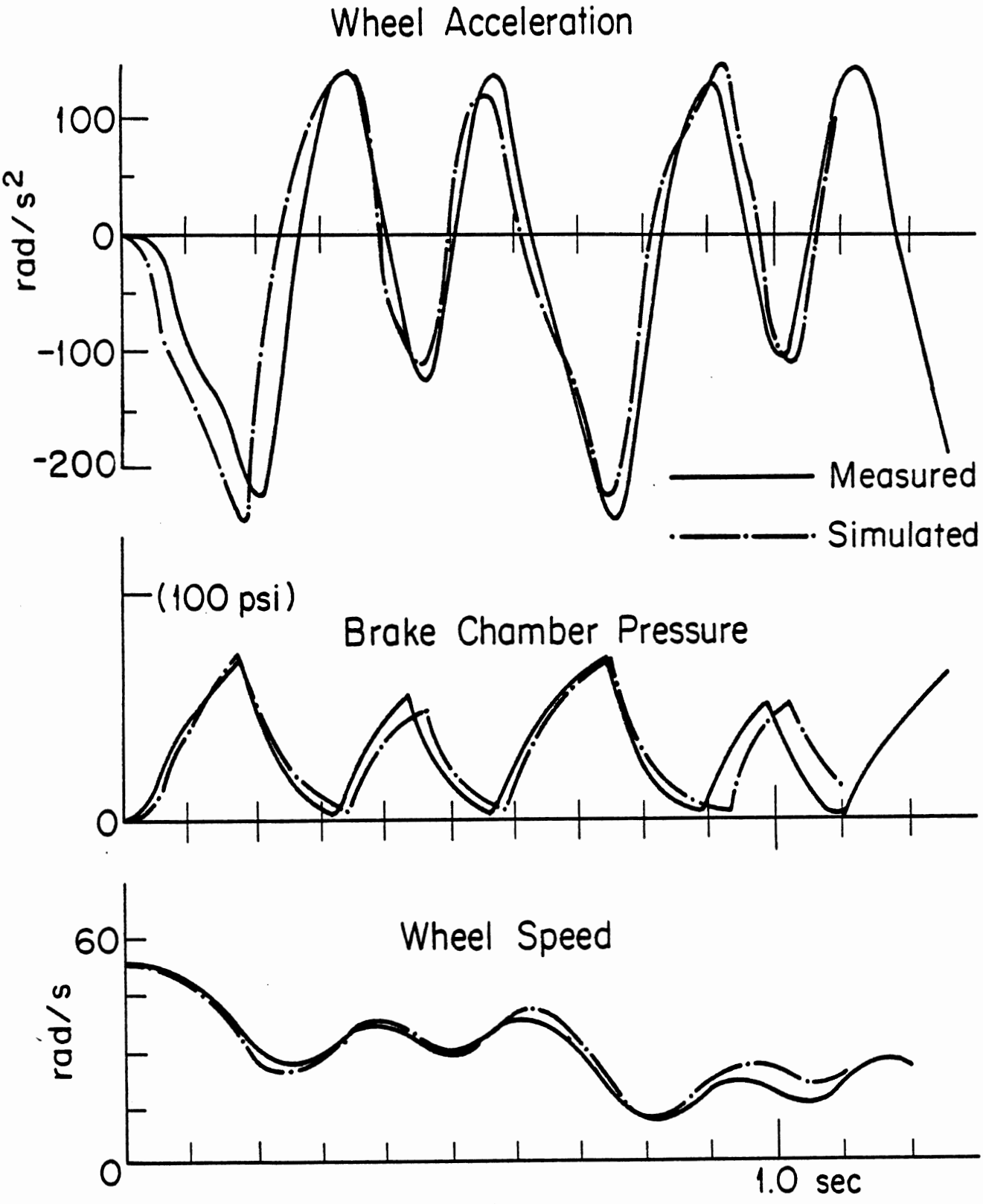

Figure 33. Laboratory measurement and simulated performance of braking of a lightly loaded axle.

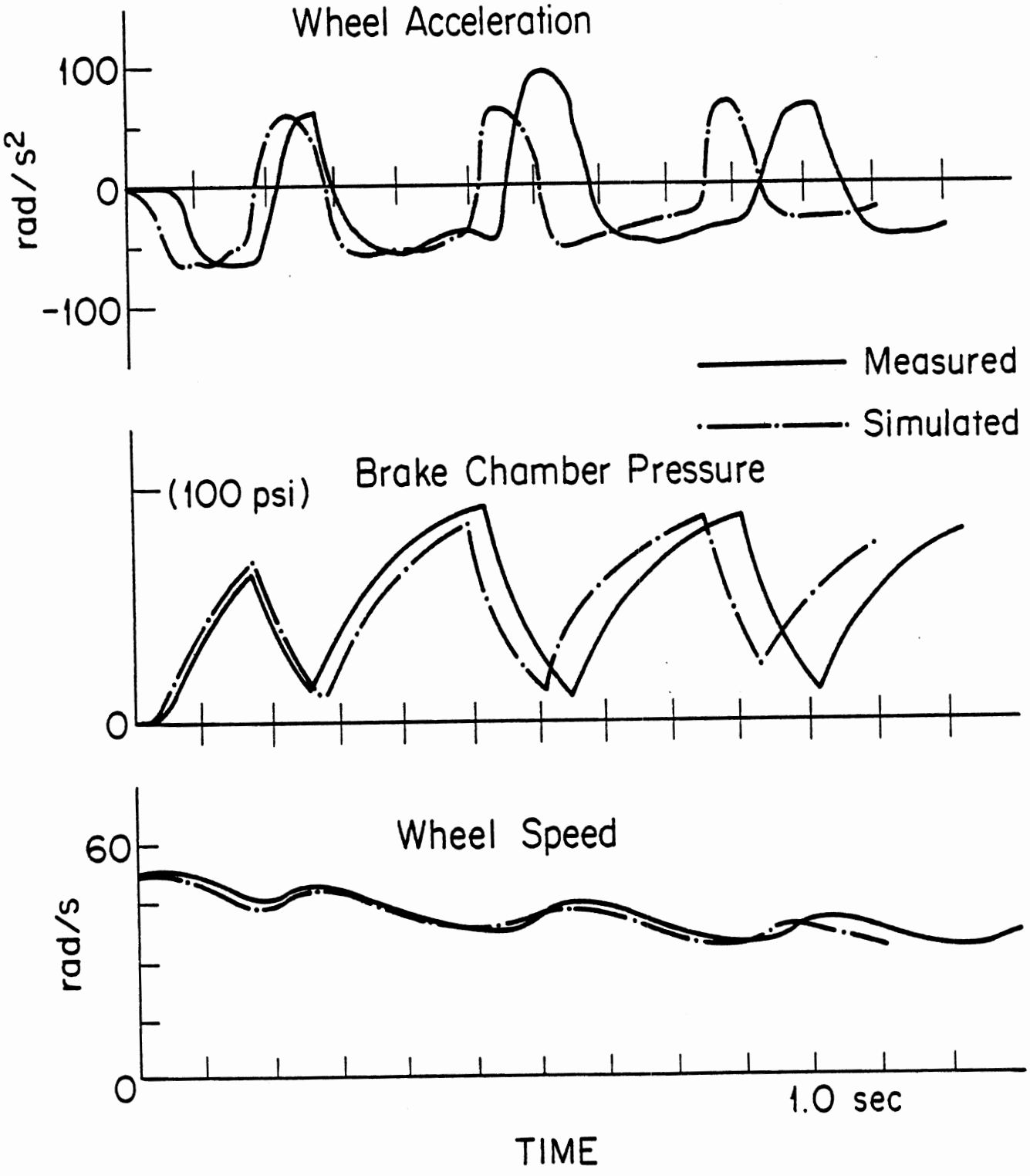

Figure 34. Laboratory measurement and simulated performance of braking of a heavily loaded axle.

For example, the antilock system used in obtaining the results shown in Figures 33 and 34 may be represented by a set of control laws of the following form:

(1) A pressure reduction command is generated if

$$\dot{\omega} < -a \quad \text{and} \quad bV_r - \omega + c\dot{\omega} + d > 0$$

or if $\omega = 0$ (wheel lockup)

where

a, b, c, and d are positive constants,

$\dot{\omega}$ = wheel acceleration,

ω = wheel speed,

and V_r = a reference ramp

(2) A pressure increase command is generated if

$$\dot{\omega} > e \quad \text{and} \quad \omega - V_r + f > 0$$

or if $\dot{\omega} > g$,

or if $t - t_o > h$ (the brake has been off too long)

where

e, f, g, and h are positive constants,

t is time, and

t_o is the last time a pressure reduction command was generated.

In summary, Figure 32 provides the basis for a conceptual idea of the scheme used for finding a model suitable for simulating a particular antilock system. First, the antilock

hardware is tested. Then, a synthesized model of the system is exercised and adjusted to match results from hardware tests. Evidence of the success of this approach is contained in the agreement between simulated and measured results presented in Figures 33 and 34 for lightly and heavily loaded axles.

The procedures just described have been refined and organized into a more orderly process.[32] The control module and pressure modulator are set up in the laboratory. A hybrid computer system is used for making a prescribed set of tests. The digital part of the hybrid system controls the sequence of tests and the storage and processing of test results. The analog computer is used in simulating the vehicle (as before). The results of antilock system tests with different axle loads, road surface conditions, wheel inertias, and initial velocities are analyzed to produce switching curves which define the form of the "reference ramp" and the influence of other variables on the "ON-OFF" cycling of the antilock system. The regression procedures used to fit the test data indicate that linear functions of initial wheel velocity, wheel acceleration, and time since the last change in solenoid state provide inequalities that do an excellent job of matching test data, yielding coefficients of determination greater than 0.9 and often close to 0.99.

3.4 Devices for Measuring Suspension Properties

At the beginning of this research, improvised temporary setups were devised for measuring heavy-vehicle

suspension properties.[33] Arrangements of load cells, hydraulic jacks, and supporting structures were used to obtain spring rates and coulomb friction levels for single-axle and tandem-axle suspensions. Intricate rigs using cables and hydraulic cylinders were developed for measuring the parameters needed for simulating the interaxle load transfer occurring in tandem suspensions.[34]

Based on the experience gained with improvised devices, an automated facility was constructed for measuring the properties of heavy-vehicle suspensions. Interest in the results from the initial facility led to the development of a revised and improved parameter-measurement facility. Hence, the current facility is a "third-generation device."

In general terms, the present facility is capable of measuring the compliance, kinematic, and coulomb friction properties of heavy-vehicle suspensions and steering systems as they react to vertical force, roll moment, lateral force, brake force, and aligning moment.[35] The facility can accept single-axle and tandem-axle suspensions of all on-highway track widths. The maximum allowable tandem spread is 70 inches. Suspensions may be tested on either a vehicle or an abbreviated frame section.

The facility shown in Figure 35 comprises (1) a static structure for holding the frame rails in a fixed position, (2) a table that can be moved vertically and/or rolled through the action of four large hydraulic cylinders (mounted in a pit below the table), (3) four wheel-pad assemblies which (a) apply

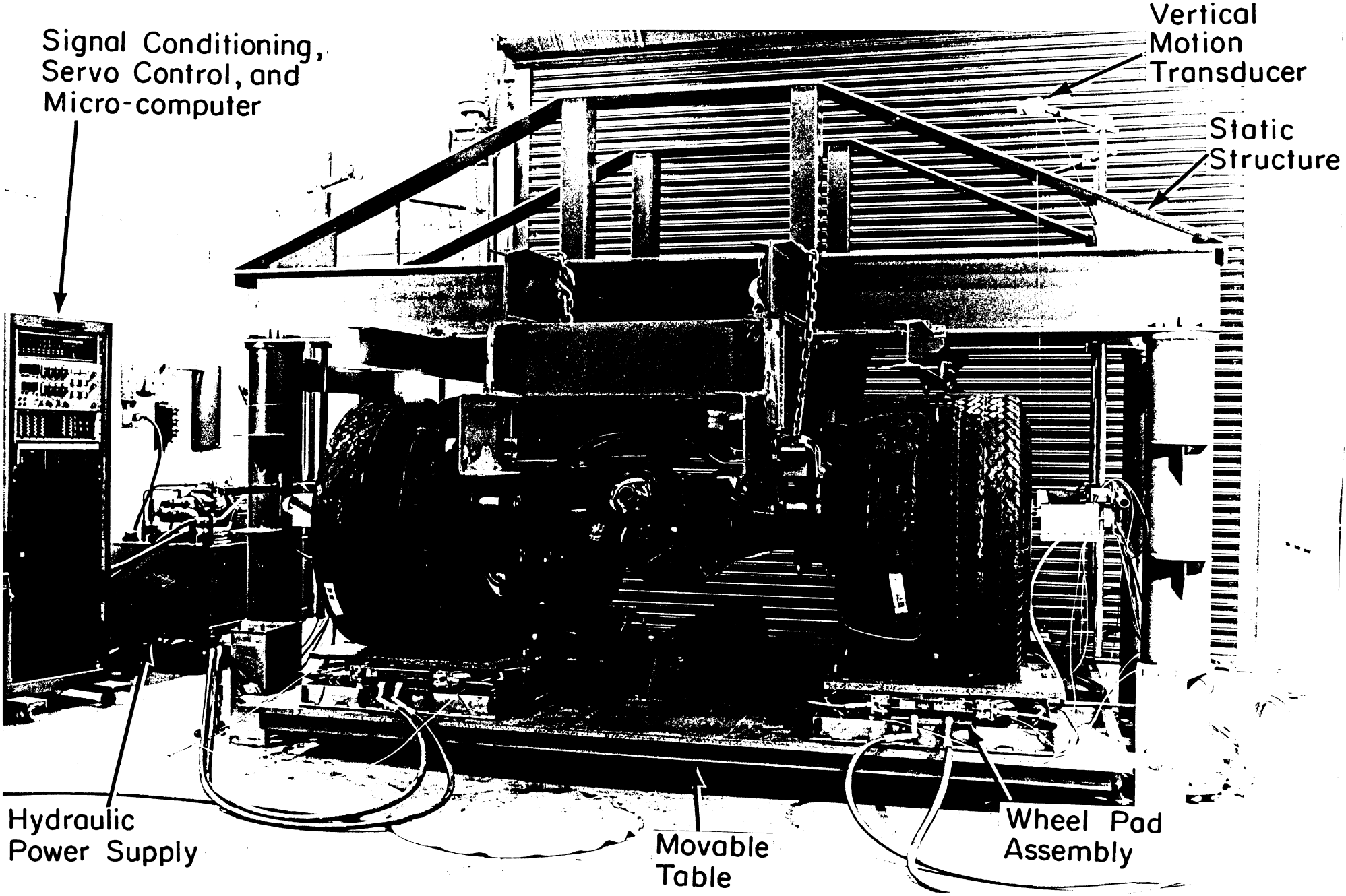

Figure 35. The HSRI Heavy Vehicle Suspension Test Facility.

shear forces to the tires, (b) contain load cells for measuring horizontal and vertical forces,and (c) allow the tires to move parallel to the table as needed when the suspension deflects, (4) motion transducers for measuring pertinent deflections, and (5) an electronic unit for controlling the tests and gathering and storing data.

With regard to braking-related measurements (i.e., spring characteristics and interaxle load transfer due to brake torque), the facility has the following capabilities:

vertical deflection:	10 inches
vertical load:	80,000 lbs (20,000 lbs per wheel pad)
longitudinal (braking) force:	24,000 lbs (6,000 lbs per wheel pad)

(A complete discussion of the capabilities of this device with regard to steering- and braking-related parameters occurs in [35].)

Figure 36 contains an illustrative example set of spring force data for the four-spring tandem suspension shown mounted on the test facility in Figure 35. The area enclosed in the small and large hysteresis loops shown in Figure 36 is a measure of the energy dissipated in a cycle of spring deflection. The average slope of the force-versus-deflection characteristics is an indication of the apparent spring rate. Note that "small" amplitude cycles have an apparent spring rate that is higher than the apparent spring rate of a large amplitude cycle. The computer representation of this type of spring data was discussed in Chapter 2 in connection with Figure 16.

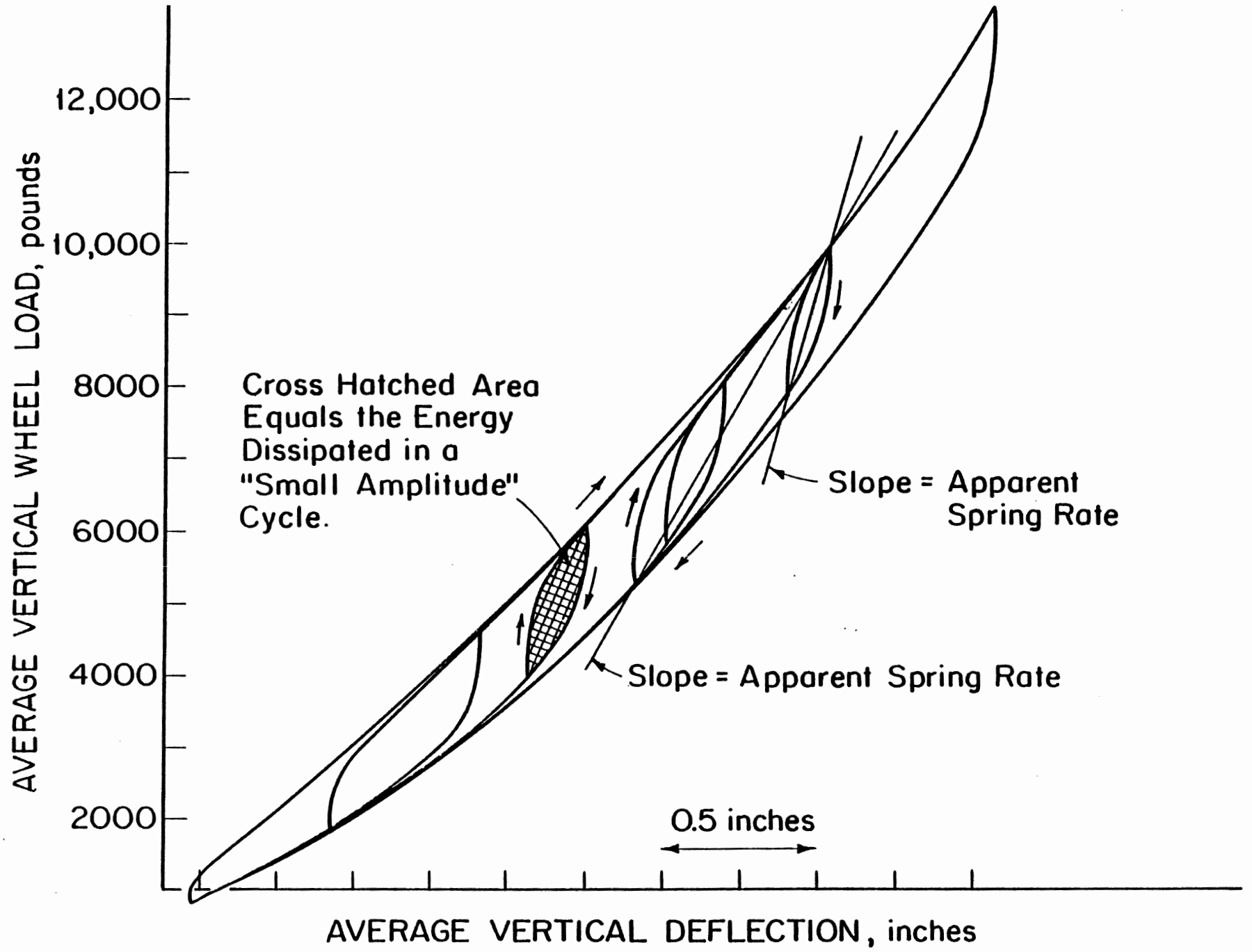

Figure 36. Four Spring Suspension Characteristics.

The spring data obtained from the suspension test facility have been shown to be useful for studying dynamic phenomena that occur at much higher frequencies than the capabilities of the suspension test facility. (The suspension test facility can operate at approximately 2 Hz, but it is intended for making quasi-steady-state measurements.)

Figure 37 shows a device which was constructed to exercise leaf springs at frequencies up to 15 Hz. The air spring (see Figure 37) applies a preload to the spring, and the hydraulic cylinder exercises the spring about the preloaded condition.

Figure 38 presents typical test results for one of the springs from the four-spring suspension used in the measurements given in Figure 36. The "smoother" curves in Figures 38a, b, and c were obtained at a cycling frequency of 0.5 Hz. They correspond approximately to the small amplitude cycle shown in the neighborhood of 7,000 lbs of vertical load in Figure 36. The more variable cycles shown in Figure 38 were made at 6, 10, and 15 Hz. The superimposed high-frequency oscillations on the 15 Hz data are due to resonances in the test fixture rather than to spring characteristics. (Note that the data presented in Figure 38 include the force due to spring rate and nonlinear damping, but do not include the force due to the mass of the spring.)[36] The spring characteristics obtained at 6, 10, and 15 Hz agree rather closely with the data obtained at 0.5 Hz.

In summary, the heavy-vehicle suspension test facility provides accurate measurements of the force-versus-deflection characteristics of heavy-vehicle springs. These measurements

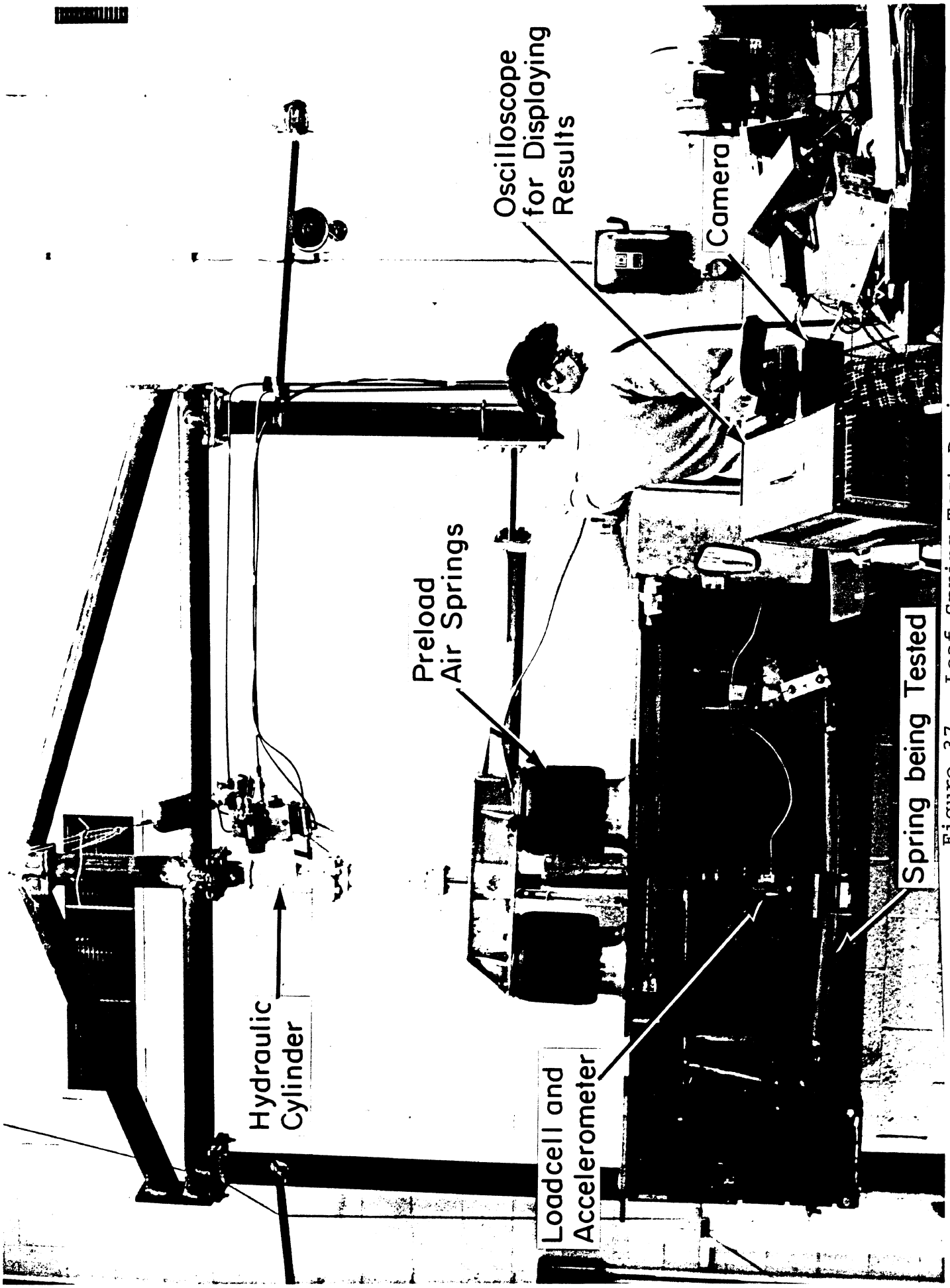

Figure 37. Leaf Spring Test Device.

Preload: 6000 lbs

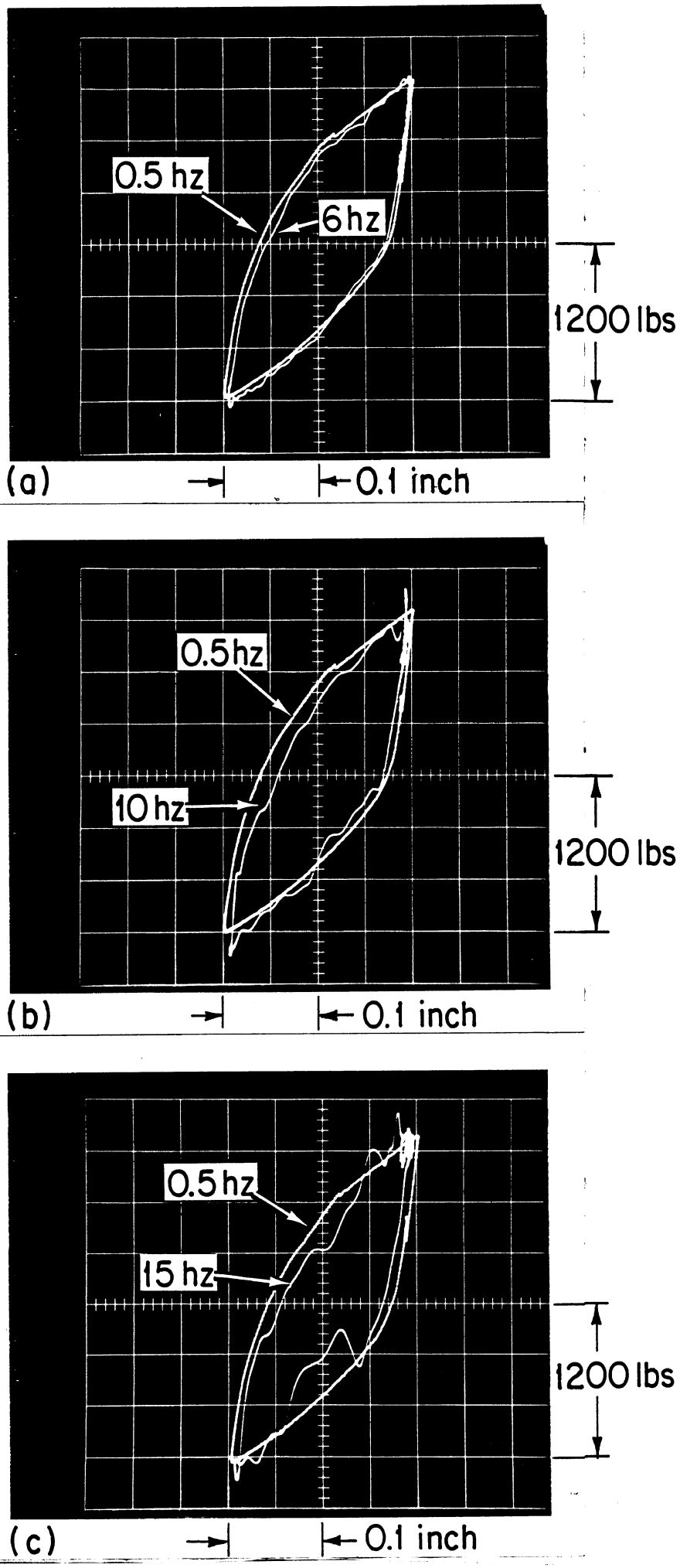

Figure 38. Leaf Spring Test Results.

are useful for characterizing spring performance up to at least 15 Hz, covering more than the frequencies of interest in braking studies and an important band of frequencies for ride studies. In addition, since the test facility is arranged to apply braking forces to the suspension, sophisticated studies of interaxle load-transfer can be made readily in the laboratory.

3.5 A Pitch-Plane Inertial Properties Facility

With respect to braking of highway vehicles, important inertial properties are center-of-gravity (c.g.) height and pitch moment of inertia. Figure 39 shows a test facility specifically developed for measuring the pertinent inertial characteristics of trucks, highway tractors, and commercial trailers. Using this device, the measurement of the inertial properties of vehicles weighing up to 35,000 lbs may be accomplished in approximately four hours.

The primary features of the facility are (1) relative ease in lifting and swinging heavy vehicles, (2) means for careful selection of the location of the swing's pivot points in order to optimize the accuracy of the measurements, and (3) adjustable supports for handling two- and three-axle vehicles with differing wheelbases.

Although it might seem that c.g. height and pitch moment of inertia could be calculated from layout drawings and component weights, experience has shown a theoretical approach

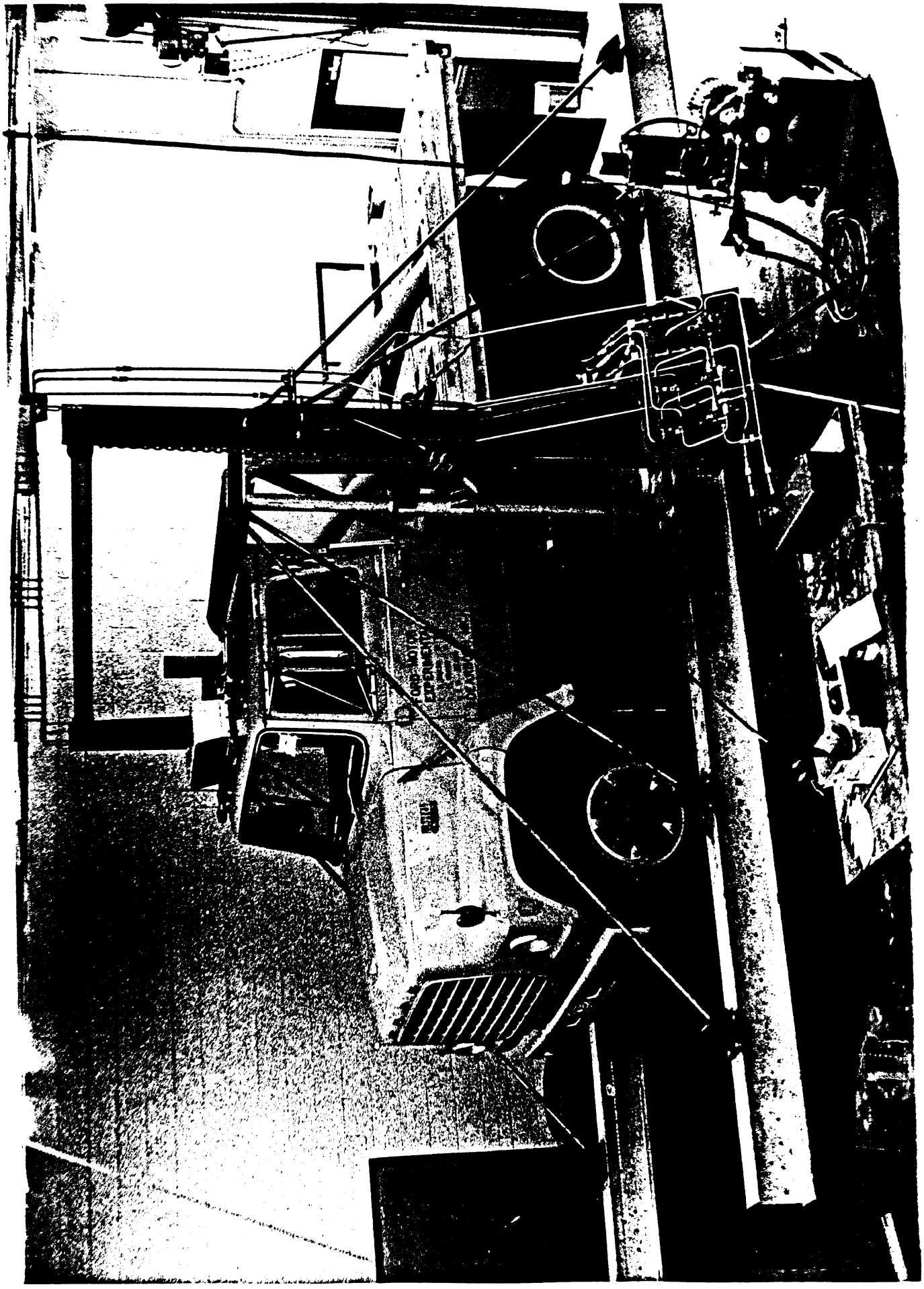

Figure 39. Pitch plane inertial properties test facility.

to be troublesome, requiring information that is difficult to obtain. If the vehicle of interest (or a comparable vehicle) exists in hardware (as was the case when the federal braking standards were initiated), then direct measurement of inertial properties is a practical, accurate approach. The popularity of the experimental approach is demonstrated by the fact that the inertial properties of more than 50 heavy vehicles have been measured using the pitch-plane inertial properties facility.

CHAPTER 4

PREDICTING BRAKING PERFORMANCE

This chapter addresses the analysis of braking performance for situations in which measured stopping distance might be longer than that anticipated by the vehicle manufacturer. After some preliminary remarks, a specific example, involving the antilock braking of a heavily loaded three-axle truck, is presented to illustrate the utility of a simulation approach in analyzing a difficult problem in understanding causes of substandard performance.

The simulation methodology described in this monograph is both comprehensive and complex. The initial use of the computerized model can be a major undertaking. After the parameters of a baseline vehicle have been measured and the simulation has been exercised to provide a detailed understanding of the performance of the selected vehicle, the user of the simulation methodology is in a favorable position to make comparative studies of various vehicles (or the influence of changes in the design of a vehicle).

Since the methodology may involve a major commitment of technical resources, judgment must be exercised regarding when it is reasonable to consider using a complex computerized model. Two situations in which the application of a complex model appears to be justified are (1) when simpler models

have failed or (2) when new approaches are being tried in a complex system in which important interactions are not readily apparent.

For example, a manufacturer might consider applying the computerized model to the types of vehicles commonly supplied to customers. Since the buyer of a commercial vehicle is allowed a multitude of choices regarding the types of brakes, suspensions, tires, etc., the manufacturer could conceivably perform simulations to predict the braking performance of any combination of components selected by a customer. A pragmatic means for evaluting the results predicted in a particular case would be to compare them with results for a vehicle which has both state-of-the-art braking capability and a wide base of customer acceptance.

From a slightly different point of view, a vehicle manufacturer might wish to evaluate the braking performance of current and proposed designs to see if any unanticipated difficulties are predicted. In this regard, component suppliers might be interested in assessing the influence of changes in component properties on the braking performance of particular types of vehicles to see what benefits may accrue and to convince vehicle manufacturers of the viability of a proposed change in component performance.

The analysis of a "problem vehicle" is yet another situation in which a manufacturer might want to use the computerized model. If customer complaints or test results indicate an undesirable or unacceptable braking situation, a

combination of simulation and testing can be used to identify the cause of the problem. After the problem is defined, the simulation can be used to screen proposed solutions if expensive hardware changes or testing requirements are foreseen.

Throughout any discussion of simulation activity it is well to keep in mind that simulation is experimenting with models. The computerized model is no more accurate than the parametric data put into it. Even though the model may be complex, an important feature of a particular vehicle may not be included in the model. The engineer investigating a particular phenomenon may need to add to the model in order to examine a specific aspect of a given problem. Successful application of the simulation methodology requires (1) an adequate computerized model, (2) accurate parametric measurements, and (3) as many carefully controlled vehicle tests as time, money, and equipment availability afford. A deficiency in any of these three areas may lead to uncertainties concerning the validity of the conclusions derived from the simulation activity.

Often a major effort goes into developing the model, but the model developers have little opportunity to exercise their model. They are considered to be "tool builders." The main opportunity for the model developer to try the model is usually in a validation activity that is performed to show that the model "works."

As a consequence of the tool-building approach, the simulation may not be exercised to any great extent. Sometimes

the simulation is not exercised because the solution to a current problem is found through the process of developing the model (i.e., carefully defining the system) and/or measuring component characteristics. Other times, prospective users do not know how to operate the model or evaluate results. In any event, a major difficulty seems to lie in communicating to users of the simulation what the model builders have done and learned.

Fortunately, the developers of the computerized model that was discussed in Chapter 2 have had an opportunity to apply their model in the following practical situation. After the addition of antilock systems to heavy trucks, vehicle manufacturers discovered that certain vehicles required unexpectedly long distances to reach a stop. Given these circumstances, what might have been straightforward computer validation activities were transformed into analyses of vehicle performance.

Two vehicle analysis studies have been conducted. The first study examined and explained the influence of tire, brake, suspension, and antilock system properties on the braking performance of a three-axle truck.[7] The second study examined factors influencing the efficiency of antilock systems.[8, 13] The following discussion is extracted from the second study.

The analysis concerned a three-axle truck that had been tested by White Motors, Inc., at the Bendix Automotive Proving Grounds (BAPG). Preliminary calculations predicted an estimated stopping distance of approximately 250 feet from 60 mph.

However, vehicle test results varied from 280 to 340 feet for repeated 60-mph stops. The majority of the tests produced stopping distances between 285 and 310 feet, with an average of about 300 feet. The stopping performance of this experimental vehicle not only was longer than expected, but also was very marginal with respect to the prevailing federal requirement of 293 feet in at least one of six tries. The experimental vehicle was a straight truck equipped with a beam axle, leaf-spring front suspension, rear "walking-beam" tandem suspension, and an axle-by-axle antilock brake control system. The antilock system employed "worst-wheel" control for each axle and pneumatic logic to control the rate of pressure build-up during each cycle. The front axle was equipped with dual-wedge brakes, and each rear axle had S-cam brakes.

The vehicle was heavily loaded to a gross vehicle weight of 50,700 lbs with a center of gravity height of 64 in. The location and size of the payload were selected to represent a "worst-case" situation for this type of vehicle.

The test vehicle was extensively instrumented, including measurements of (1) wheel speeds for all six wheels, (2) air pressures at the front, middle, and rear axles, (3) air pressure at the treadle valve, and (4) stopping distance, velocity, and deceleration. In addition, torque wheels were installed to measure brake torque at the front and rearmost wheels on the right side of the vehicle, and the vertical deflections of the front and rearmost axles were measured with respect to the frame rails.

Following the series of stopping distance tests, the vehicle's inertial properties and component characteristics were measured at HSRI. The "second-generation" suspension measurement facility was used to obtain force-deflection characteristics for the front and rear suspensions (see Section 3.4). The antilock systems were tested in the laboratory using the analog computer setup (Section 3.3).

The mobile dynamometer was employed to make tire force measurements on the surface used for the vehicle tests (i.e., at BAPG). Tire data were collected at 20,40, and 60 mph at three vertical loads (specifically, 0.5, 1.0, and 1.5 times rated load).

The combination of (1) detailed measurements made during full-scale vehicle tests, and (2) laboratory measurements of component properties provided the foundation for refining the computerized model and, ultimately, for using the simulation to deduce the mechanisms contributing to increased stopping distance. A review of the vehicle and component test results suggested the need for refinements in the representation of (1) the brake pressure versus torque hysteresis of the rear S-cam brakes, (2) air system lags that occur if chamber pressures fall below pushout pressure, and (3) rear tandem suspension force-deflection characteristics.

Examination of the brake-pressure, torque-wheel, and wheel-speed data from the vehicle tests revealed a total hysteresis of 27,000 in-lb between the boundaries in a torque-pressure loop of the form illustrated in the right-hand graph

of Figure 7 in Chapter 2. In addition, as illustrated in Figure 40, a "lag" in the increase in brake torque and a slow rise in pressure were observed if the brake pressure fell below the pushout pressure. The computerized model was modified to more accurately represent the hysteresis-torque relationship at low pressure and the air supply transport delay effect.

Furthermore, the tandem suspension measurements indicated a complex relationship between vertical load and suspension deflection. The leaf-spring model defined by equations 24 and 25 was developed to fit these test data. The use of the refined spring model was instrumental in explaining and examining the pitching and bouncing dynamics of this vehicle.[8]

A previous study[7] demonstrated the importance of imbalance between the brakes installed on an axle, and information from lining manufacturers[14] indicated that significant differences in torque capability are likely to occur between brakes of the same design. Accordingly, the vehicle test data were used to infer the amount of brake imbalance from side to side on each axle.

After gathering parametric data and modifying the computerized model, several simulation runs were made to determine a baseline set of parameters representative of a typical stop from 60 mph. Due to the variability between the results measured in various tests, a certain amount of judgment was exercised in selecting a representative test run to be compared with simulation results. The test run selected was for the

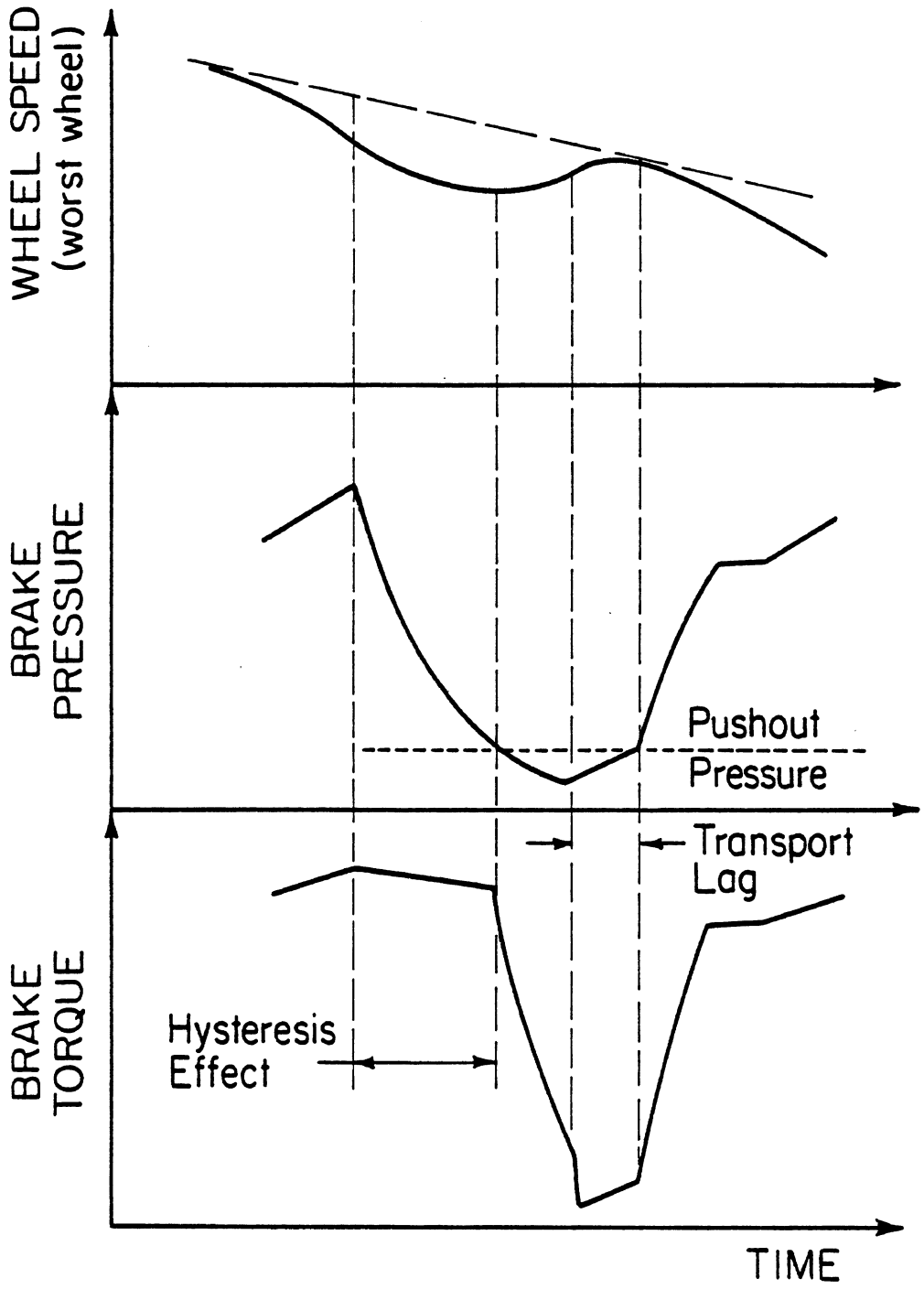

Figure 40. Effects of Brake Hysteresis and Air Supply Transport Lag.

majority of tests with stopping distances from 285 to 310 feet and similar cycling of wheel speed. Figure 41 shows a comparison of the simulated and measured vehicle responses chosen to represent the baseline performance of the vehicle. In view of the variability of the test results and the known sensitivity of wheel cycling to small differences in operating conditions, the level of agreement between measured and simulated vehicle response is good. Furthermore, the baseline computer representation predicted a stopping distance of 295 feet, while the vehicle stopped in 296 feet in the actual test.

A detailed understanding of the process through which rear-brake hysteresis, air-supply delays, and side-to-side imbalance combine to produce degraded stopping performance was developed during the efforts applied in verifying the computerized model. The sequence and timing of events taking place during a cycle of antilock braking are illustrated in Figure 40. During a pressure application, the "worst wheel" on an axle approaches the speed for maximum tire shear force while the other wheel is at a higher speed and less tire force because of the side-to-side imbalance in the brakes. When the antilock system reduces brake pressure, the worst wheel is operating at nearly maximum force. However, hysteresis in the brakes prevents the brake torque from rapidly falling off when the pressure is first reduced. This delay in the reduction of brake torque causes the worst wheel to tend toward locking up and thereby causes the antilock system to lower the pressure below the pushout pressure of the

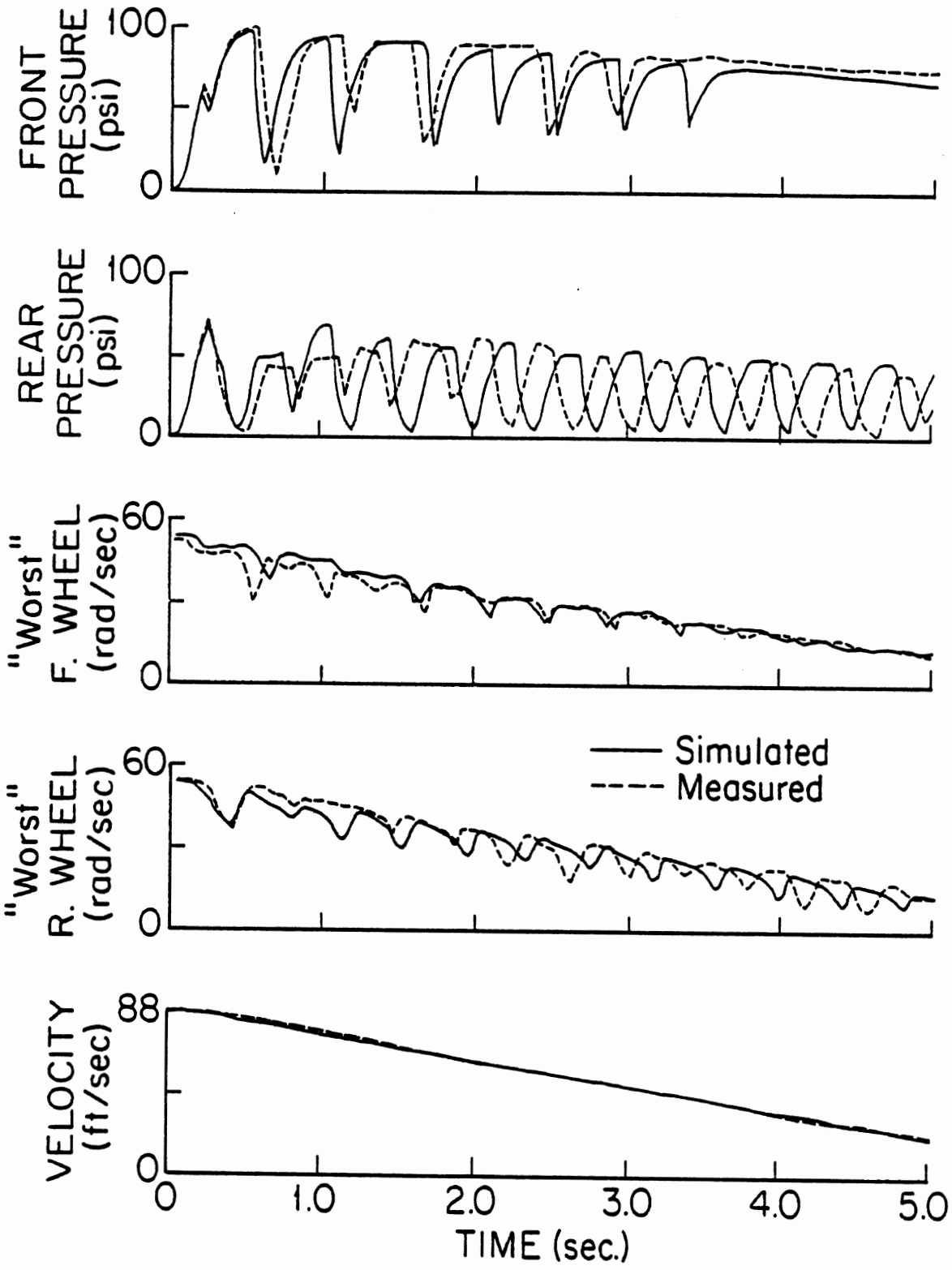

Figure 41. Simulated vs. Measured Vehicle Response.

brake. During this time, the other wheel (the "best" wheel) is approaching free-rolling conditions and is providing very little brake torque. Once the brake torque decreases to a low level, the worst wheel accelerates back to nearly a free-rolling condition, causing the antilock system to re-apply air pressure to the brake chamber. However, the pressure in the brake chamber rises slowly at first due to the air volume increase required to push the brake shoes out to the drum. For this vehicle the time required to push the brake shoes back out resulted in a maximum time lag of approximately 40 milliseconds. The net effect of the time lags caused by brake hysteresis and air pressure delay is to permit the tires to operate at nearly free-rolling (low-braking) conditions for extended periods of time.

Subsequent parametric studies indicated that the dynamic interaction between hysteresis, side-to-side imbalance, and air system transport lags caused significantly diminished braking performance. The calculations predicted a 230-foot stopping distance for a vehicle equipped with ideal brakes, that is, no imbalance, hysteresis, or air system lags. Without hysteresis, the predicted stopping distance was 253 feet, and without imbalance the stopping distance was 252 feet. The combination of hysteresis and brake imbalance along with the air system lag was needed to achieve extraordinary stopping distances of approximately 295 feet.

The adverse effects of rear brake imbalance and hysteresis were amply demonstrated using the computerized model. Although

the discussion presented here has centered on brake system imperfections, the computerized model has been used to study the influence of changes in loading, tire characteristics, suspension properties, and antilock system logic on the stopping performance of the vehicle.[8, 13] In addition to improving the brakes, it was found that stopping distance performance could be improved by (1) reducing the effectiveness of the rear brakes or using load-sensitive proportioning valves, (2) modifying the operation of the antilock system, or (3) modifying the properties of the rear suspension.

The analysis presented in this chapter illustrates a situation in which a complex model is needed to represent detailed mechanisms that combine to degrade stopping performance during antilock braking.

CHAPTER 5

CONCLUDING STATEMENTS

This monograph has presented a description of a computerized model designed for predicting the braking performance of commercial vehicles. Versions of this computerized model have been delivered to administrations of the federal government for their use in studying highway safety. Vehicle manufacturers have applied this model in the process of developing vehicle designs, including antilock braking systems. The originators of the model have made detailed studies of the braking performance of heavy trucks equipped with antilock systems. The computerized model is an available analytical tool with demonstrated capabilities for studying braking performance.

The so-called "simulation" methodology employed in improving and refining the computerized model has led to major advances in the equipment available for measuring the pertinent properties of heavy vehicles. New devices now available include (1) a mobile truck-tire and brake dynamometer, (2) a tandem and single-axle suspension test facility, (3) a laboratory setup for deducing antilock system parameters, and (4) a pitch-plane inertial properties test facility. All of these devices have been used in making extensive studies of the performance of vehicle

components having an important influence on braking performance. The use of these devices has led to a better understanding of the shear force properties of truck tires; the fade, hysteresis, and variability of brake torque characteristics; the force-deflection characteristics of leaf springs, including their inherent damping properties; the control laws and pressure modulation characteristics of currently available antilock systems; and parameters describing the mass distribution characteristics of heavy vehicles.

At present, a major goal is to document the research upon which this monograph is based. A series of volumes presenting research results for tires, brakes, suspensions, antilock systems, and inertial properties will be prepared during the coming year. These volumes should enhance the use of the computerized model, since a major hurdle obstructing the use of the model is the availability of suitable parametric information on vehicle and component properties.

Future studies aimed at improving stopping capability would benefit from the development of a better understanding of (1) the factors influencing the effectiveness of truck brakes, (2) the interaxle load transfer occurring in tandem suspensions, (3) the influences of pressure modulation characteristics on the performance of antilock systems, and (4) the capabilities of brake proportioning devices. The simulation methodology for studying the factors listed above has been developed, and the necessary elements of this methodology are ready to be applied.

In closing, it should be observed that the braking research described herein has been incorporated to a large extent into similar research on combined braking and steering maneuvers. The combined braking and steering problem is clearly much more complicated than the problem of straight-line braking. Future progress in analyzing vehicle performance in braking in a turn or in accident-avoidance maneuvers involving braking and turning depends upon developing (1) means for measuring the combined lateral and longitudinal force-producing properties of truck tires and (2) models of the steering system, including the influences of braking torques and forces as well as side forces and aligning moments on front-wheel angle. The simulation methodology used for developing an understanding of braking phenomena appears to be an appropriate approach for unraveling the complex interactions occurring during combined braking and turning maneuvers.

REFERENCES

[1] Transcript of public meeting (FMVSS 121) National Highway Safety Administration, Washington, DC, October 29-31, 1975.

[2] Federal Motor Vehicle Safety Standard No. 121. U.S. Motor Vehicle Code 49CFR571.121; 5121-1 to 5121-10.

[3] Paccor, Inc. vs. National Highway Traffic Safety Administration [Decision]. Court of Appeals, Ninth Circuit, San Francisco, California, April 17, 1978.

[4] Fancher, P. S. "Braking Performance of Commercial Vehicles Equipped with Anti-lock Systems." An Overview of Simulation in Highway Transportation 7:2, Part 2 (December 1977).

[5] Rasmussen, R. E., Hill, F. W., and Riede, P. M. "Typical Vehicle Parameters for Dynamic Studies." Report A-2542. Ann Arbor: University of Michigan, Highway Safety Research Institute, 1970.

[6] Winkler, C. B., Bernard, J., Fancher, P., MacAdams, C., and Post, T. "Predicting the Braking Performance of Trucks and Tractor-Trailers." (Phase III Technical Report). Ann Arbor: University of Michigan, Highway Safety Research Institute, 1976. (Available from National Technical Information Service, Springfield, VA 22151, Reports: PB-263216 and PB-266706.

[7] Fancher, P. S., and MacAdams, C. C. "Computer Analysis of Antilock System Performance in the Braking of

Commercial Vehicles," in Proceedings of a Conference on the Braking of Road Vehicles (Sponsored by the Automobile Division of the Institution of Mechanical Engineers in association with the Institute of Road Transport Engineers, Loughborough University of Technology (Loughborough, England, March 23-25, 1976).

[8] Fancher, P. "Pitching and Bouncing Dynamics Excited During Antilock Braking of a Heavy Truck." Proceedings of the 5th VSD-2nd IUTAM Symposium on Dynamics of Vehicles on Roads and Tracks, Vienna, Austria, September 1977.

[9] Tielking, J. T. Tire Analysis Program Package: Computer Program Manual, Final Report, Volume II (contract No. DOT-FH-11-8268; Catalog No. PB 29158) Springfield, VA: NTIS, [DATE?].

[10] Koch, B. "Computer Simulation of Steady State and Transient Tire Traction Performance." Vehicle System Dynamics 4 (July 1975): 121-125.

[11] Bernard, J. E., Winkler, C. B., and Fancher, P. S. "Computer-Based Mathematical Method for Predicting the Braking Performance of Trucks and Tractor-Trailers" (Phase II Technical Report), Ann Arbor: University of Michigan, Highway Safety Research Institute, 1973. (Available from National Technical Information Service, Springfield, VA 22151; Report PB-221-630.)

[12] Federal Register 44:33 (February 15, 1979): 9783-9786. (Docket No. 79-03; Notice 01; NHTSA 4910-59.)

[13] MacAdams, C. C. "Computer Simulation and Parameter Sensitivity Study of a Commercial Vehicle During Antiskid Braking." Proceedings of the 6th VSD-2nd IUTAM Symposium on Dynamics of Vehicles on Roads and Tracks. Berlin, Germany, September 1979.

[14] Federal Register 39:221 (November 14, 1974): 4016-4019.

[15] Steis, D. E. "Inertia Brake Dynamometer Testing Techniques for FMVSS 121" (SAE paper no. 751010), November 1975.

[16] Johnson, L. K., Fancher, P. S., and Gillespie, T. D. "An Empirical Model for the Prediction of the Torque Output of Commercial Vehicle Air Brakes" (HSRI Report No. UM-HSRI-78-53). Ann Arbor: University of Michigan, Highway Safety Research Institute, 1978.

[17] Newcomb, C. P., and Spurr, R. T. The Braking of Road Vehicles. London: Chapman and Hall, 1967.

[18] Bernard, J. E. "A Digital Computer Method for the Prediction of Braking Performance of Trucks and Tractor-Trailers (SAE Paper No. 730181), presented at the International Automotive Engineering Conference, Detroit, Michigan, January 1973.

[19] Mitchell, B., Abrams, R., and Scott, R. A. "Improvement of Mathematical Models for Simulation of Vehicle Handling," Programmer's Guide for the Five Degrees of Freedom Models (Volume II). (Final Report to NHTSA, contract number DOT-HS-7-01715) Ann Arbor: University of Michigan, Highway Safety Research Institute, 1979.

[20] Dugoff, H., Fancher, P. S., and Segel, L. "An Analysis of Tire Traction Properties and Their Influence on Vehicle Dynamic Performance." (SAE Paper No. 700377). 1970 International Automobile Safety Conference Compendium. New York: Society of Automotive Engineers, 1970.

[21] Fancher, P. S. and Grote, P. "Development of a Hybrid Simulation for Extreme Automobile Maneuvers." Proceedings of the 1971 Summer Computer Simulation Conference. Boston, 1971.

[22] Ervin, R. D., McAdam, C. C., and Fancher, P. S. "The Longitudinal Traction Characteristics of Truck Tires As Measured on Dry Pavements." (HSRI Report No. UM-HSRI-PF-75-3). Ann Arbor: University of Michigan, Highway Safety Research Institute, 1975.

[23] Ervin, R. D. "The Noise and Traction Characteristics of Bias-Ply Truck Tires" (HSRI Final Report No. UM-HSRI-PF-76-2-1). Ann Arbor: University of Michigan, Highway Safety Institute, 1976.

[24] Ervin, R. D. "Effects of Tire Properties on Truck and Bus Handling." (HSRI Final Report No. UM-HAEI-76-11 for National Highway Traffic Safety Administration, Contract No. DOT-HS-4-00943). Ann Arbor: University of Michigan, Highway Safety Research Institute, 1976.

[25] Sharp, R. S. "The Nature and Prevention of Axle Tramp." Proceedings 1969-1970 of the Institution of Mechanical Engineers Automobile Division. Vol. 184, Part 2A, No. 3. London, England: The Institution of Mechanical Engineers, 1970.

[26] Gillespie, Thomas D., MacAdam, Charles C., and Hu, Garrick T. "Truck and Tractor-Trailer Dynamic Response Simulation, T3DRS:VI: User's Manual" (HSRI Report No. UM-HSRI-79-38-1 for Federal Highway Administration, Contract No. DOT-FH-11-9330). Ann Arbor: University of Michigan, Highway Safety Research Institute, 1979.

[27] Ervin, R. D. "Measurement of the Longitudinal and Lateral Traction Properties of Truck Tires," Proceedings of a Conference on the Braking of Road Vehicles. (Sponsored by the Automobile Division of The Institution of Mechanical Engineers in association with the Institute of Road Transport Engineers, Loughborough University of Technology, Loughborough, England, March 23-25, 1976).

[28] Ervin, R. D. "Mobile Measurements of Truck Tire Traction," Proceedings of a Symposium on Commercial Vehicle Braking and Handling. Ann Arbor: University of Michigan, Highway Safety Research Institute, 1975.

[29] Ervin, R. D. and Fancher, P. S. "Preliminary Measurements of the Longitudinal Traction Properties of Truck Tires" (SAE Paper No. 741139). Presented at the Truck Meeting, Troy, Michigan, November 4-7, 1974.

[30] Post, T. M., Fancher, P. S., and Bernard, J. E. "Torque Characteristics of Commercial Vehicle Brakes" (SAE Paper No. 750210) Presented at the Automotive Congress and Exposition, Detroit, Michigan, February 24-28, 1975.

[31] Gillespie, T., Johnson, L, and Fancher, P. "Modeling the In-Stop Torque Performance of Hydraulically-

Actuated Truck Brakes: (HSRI Report No. UM-HSRI-78-58). Ann Arbor: University of Michigan, Highway Safety Research Institute, 1978.

[32] MacAdam, C. C., and Fancher, P. S. "Survey of Antilock System Properties (Final Technical Report No. UM-HSRI-78-47 to Motor Vehicle Manufacturers Association, Contract No. MVMA Proj. # 1.37). Ann Arbor: University of Michigan, Highway Safety Research Institute, 1978.

[33] Murphy, R. W., Bernard, J. E., and Winkler, C. B. "A Computer-Based Mathematical Method for Predicting the Braking Performance of Trucks and Tractor-Trailers" (Phase I Report of Motor Truck Braking and Handling Performance Study). Ann Arbor: University of Michigan, Highway Safety Research Institute, 1972. (Available from the National Technical Information Service, Springfield, VA 22151, Report PB-212-805).

[34] Winkler, C. B. "Analysis and Computer Simulation of the Four Elliptical Leaf Spring Tandem Suspension" (SAE Paper No. 740136). Presented at the Automotive Engineering Congress and Exposition, Detroit, Michigan, February 25-March 1, 1974.

[35] Winkler, C. B. and Hagan, M. "Heavy Vehicle Suspension Test Facility." To be presented at the Society of Automotive Engineers National Truck Meeting, King of Prussia, Pennsylvania, October 1980. (SAE Paper No. 800905)

[36] Fancher, P. S., Ervin, R. D., MacAdam, C. C., and Winkler, C. B. "Measurement and Representation of the Mechanical Properties of Truck Leaf Springs."

To be presented at Society of Automotive Engineers National Truck Meeting, King of Prussia, Pennsylvania, October, 1980. (SAE Paper No. 800906)